Universidade de Aveiro
Ano 2022

ANA FILIPA PEREIRA FERREIRA

MODULATION OF SPERM MOVEMENT BY PROTEIN PHOSPHATASE INHIBITORS

MODULAÇÃO DO MOVIMENTO DOS ESPERMATOZOIDES POR INIBIDORES DAS PROTEÍNAS FOSFATASES

2022

Universidade de Aveiro
Ano 2022

ANA FILIPA PEREIRA FERREIRA

MODULAÇÃO DO MOVIMENTO DOS ESPERMATOZOIDES POR INIBIDORES DAS PROTEÍNAS FOSFATASES

Dissertação apresentada à Universidade de Aveiro para cumprimento dos requisitos necessários à obtenção do grau de Mestre em Bioquímica, realizada sob a orientação científica da Professora Doutora Margarida Sâncio da Cruz Fardilha, Professora Auxiliar com Agregação ao Departamento de Ciências Médicas, Universidade de Aveiro e da Professor Doutor Carlos Pedro Fontes Oliveira, Professor Auxiliar do Departamento de Química, Universidade de Aveiro

This study was supported by the Institute for Biomedicine—iBiMED (UIDB/04501/2020, UIDP/04501/2020) and by the project EXPL/CVT-CVT/1112/2021, both financed by the Portuguese Foundation for Science and Technology (FCT) of the Portuguese Ministry of Science and Higher Education and by the European Union (QREN, FEDER and COMPETE frameworks).

o júri

Presidente	Prof. Doutor Brian James Goodfellow Professor auxiliar da Universidade de Aveiro
Vogal	Prof. Doutor Marco Aurélio Gouveia Alves Investigador auxiliar da Universidade do Porto
Vogal	Prof. Doutora Margarida Sâncio da Cruz Fardilha Professora auxiliar com agregação à Universidade de Aveiro

agradecimentos

Á minha orientadora Dra. Margarida Fardilha, por toda a ajuda e disponibilidade ao longo deste ano, não só a nível científico, como também pela coragem que me deu para ir além do que me achava capaz. Ao meu orientador Pedro Oliveira também pela disponibilidade e apoio prestado.

Aos meus colegas do grupo pela boa disposição e contribuições ao meu trabalho, principalmente à Joana e ao Pedro, pela infinita paciência e disponibilidade para me ajudarem.

Ao Dr. Paolo Netti que prontamente me recebeu no seu laboratório em Nápoles, assim como ao David, Claudia e Luigi por toda ajuda e amizade durante esta experiência. Em especial, agradeço à Isabella que, além do apoio incondicional ao longo do meu estágio, me fez sentir em casa num país estrangeiro. Foi um privilégio ter trabalhado convosco.

Aos amigos que tornaram Aveiro o meu lugar favorito, em especial à Inês e à Rita que estiveram lá em todas as horas a dar-me a confiança que às vezes falhava, à Filipa e à Patrícia que mesmo longe estiveram sempre tão perto, e ao Miguel que além de grande amigo, zelou sempre pela estatística da minha tese. Aos habitantes legais e ilegais da Casa, um enorme obrigada por tudo. Também aos amigos que me esperavam na terra natal e que perdoaram todas as minhas ausências sem nunca deixarem de me motivar.

Agradeço em especial à minha família. Aos meus pais que me proporcionaram esta oportunidade e nunca duvidaram que eu conseguiria tudo a que me propus. Aos meus irmãos pela constante troça que se tornou em motivação. Por fim, à minha avó que garantiu que nunca me faltasse nada ao chegar a casa.

palavras-chave

Fertilidade masculina, motilidade, proteína fosfatase tipo 1, proteína fosfatase tipo 2A, proteína fosfatase tipo 2B, cantaridina, tautomicina, cipermetrina, análise de esperma assistida por computador

resumo

A fertilidade masculina depende da capacidade dos espermatozóides de fertilizar o ovócito no sistema reprodutivo feminino. Atualmente, sabe-se que três proteínas fosfatases (PFs) têm um papel crucial na aquisição e regulação da motilidade do espermatozoide, a isoforma espermática tipo 1 gama 2 (PF1γ2), proteína fosfatase tipo 2A (PF2A) e proteína fosfatase tipo 2B (PF2B). A interação entre estas PFs tem sido extensivamente investigada, graças à contribuição dos inibidores de PF, contudo, uma grande parte deles nunca foi testado em espermatozóides. Este estudo teve como objetivo avaliar as alterações do padrão de motilidade dos espermatozóides, após a incubação com cantaridina (CAN) e tautomicina (TAU), que inibem PF1 e PF2A, assim como a cipermetrina (CYP), um inibidor de PF2B. Além disso, foi utilizado um método de análise baseado em *machine-learning* (análise alternativa), além da análise do sistema *Computer-Aided Sperm Analysis (*CASA). Os resultados da análise CASA mostraram que os inibidores de PF causaram um aumento na imotilidade, aliado a uma diminuição da motilidade progressiva rápida (PR) e da velocidade dos parâmetros cinemáticos. A análise alternativa também revelou um aumento dos espermatozóides hiperativados e com trajetórias circulares, assim como, contrariamente, um aumento dos espermatozóides PR. CAN afetou mais significativamente os espermatozoides PR, enquanto que TAU afetou mais os espermatozoides progressivos lentos (PL). CYP causou um impacto significativo tanto nos PR, como nos PL, sendo este o inibidor que causou decréscimos mais significativos tanto na motilidade, como nos parâmetros cinemáticos. Os resultados das duas análises foram por vezes divergentes, o que pode ser explicado por diferenças entre os métodos, como por exemplo o *frame rate* dos vídeos e a altura das câmaras de análise. Concluindo, contrariamente ao descrito na literatura, os nossos resultados mostram que CAN, TAU e CYP diminuíram consistentemente a motilidade e os parâmetros cinemáticos dos espermatozoides, sem afetar a viabilidade celular. Assim, estudos adicionais são necessários de modo a entender melhor o papel dos PFs na regulação da motilidade ativada e hiperativada.

keywords

Male fertility, sperm motility, protein phosphatase type 1, protein phosphatase type 2A, protein phosphatase type 2B, cantharidin, tautomycin, cypermethrin, computer-aided sperm analysis

abstract

Male fertility relies on the ability of spermatozoa to fertilize the egg in the female reproductive tract. It is known that three protein phosphatases (PPs) are crucial in sperm motility acquisition and regulation, the sperm-specific PP type 1 isoform gamma 2 (PP1γ2), protein phosphatase type 2A (PP2A) and protein phosphatase type 2B (PP2B). An interplay between these PPs has been extensively investigated, with the contribution of some PP inhibitors, however, several were never reported to be tested in spermatozoa. This study aimed to assess the motility pattern alterations following incubation with cantharidin (CAN) and tautomycin (TAU), which inhibit PP1 and PP2A, as well as cypermethrin (CYP), a PP2B inhibitor. Besides, a machine learning-based method of analysis (alternative analysis) was used along with the Computer-Aided Sperm Analysis (CASA) system. CASA results showed that PP inhibitors caused an increase in immotility paired with decreased rapidly-progressive (RP) motility and velocity of the kinematic parameters. The alternative analysis also revealed an increase in hyperactivated spermatozoa and circular trajectories and, contrarily, an increase in RP spermatozoa. CAN affected more significantly RP spermatozoa, whereas TAU most impacted slowly-progressive (SP). CYP caused a significant impact in both RP and SP, being the inhibitor that caused more significant decreases in sperm motility and kinematic parameters. Results from both analyses, CASA and alternative analysis, were often divergent, which could be explained by the differences between the methods, such as video frame rate and height of the analysis chambers. In conclusion, contrarily to the literature, CAN, TAU and CYP consistently decreased spermatozoa motility and kinematic parameters, without affecting cell viability. Hence, additional studies are required to further understand PPs role in activated and hyperactivated motility regulation.

TABLE OF CONTENTS

List of Figures

List of Tables

List of Abbreviations

ALH: amplitude of the lateral displacement of the head

ATP: adenosine triphosphate

BCF: beat-cross frequency

CA: calyculin A

Ca^{2+}: calcium

cAMP: cyclic adenosine monophosphate

CAM: calmodulin

CAN: cantharidin

CASA: computer-aided sperm analysis

CCDC181: coiled-coil domain-containing protein 181

CIRC: circular trajectory

CsA: cyclosporin A

CYP: cypermethrin

DEL: deltamethrin

DNC: dance

E: endothall

Fe: iron

FR: frame rate

Fps: frames per second

FRT: female reproductive tract

GSK3: glycogen synthase kinase 3

GSK3α: glycogen synthase kinase 3 subunit alpha

GSK3β: glycogen synthase kinase 3 subunit beta

$HCO3^-$: bicarbonate

HYP: hyperactivated spermatozoa

IC_{50}: half maximal inhibitory concentration

kD: kilodalton

LIN: linearity of the curvilinear path

MAD: mean angular displacement

Mn: manganese

NP: non-progressive

OA: okadaic acid

PDE: phosphodiesterase

PDE11: phosphodiesterase 11

PDE4: phosphodiesterase 4

PIP: PP1 interacting protein

PK: protein kinase

PKA: protein kinase A

PP: protein phosphatase

PP1: protein phosphatase type 1

PP1α: protein phosphatase alpha

PP1β: protein phosphatase beta

PP1γ1: protein phosphatase 1 gamma 1

PP1γ2: protein phosphatase 1 gamma 2

PP2A: protein phosphatase type 2A

PP2A-A: protein phosphatase type 2A scaffolding

PP2A-B: protein phosphatase type 2A regulatory

PP2A-C: protein phosphatase type 2A catalytic subunit

PP2B: protein phosphatase type 2B

PP5: protein phosphatase 5

PPME1: protein phosphatase methylesterase 1

PPP1R11 (also known as I3): protein phosphatase 1 Regulatory Inhibitor Subunit 11

PPP1R2 (also known as I2): protein phosphatase 1 inhibitor 2

PPP1R2P3: protein phosphatase 1 Inhibitor 2 like

PPP1R7 (also known as SDS22): protein phosphatase 1 regulatory subunit 7

PPP2CA: protein Phosphatase 2 Catalytic Subunit Alpha

PPP3CA: protein phosphatase type 2B catalytic subunit A

PPP3CB: protein phosphatase type 2B catalytic subunit B

PPP3CC: protein phosphatase type 2B catalytic subunit C

PPP3R1: protein phosphatase type 2B regulatory subunit 1

PPP3R2: protein phosphatase type 2B regulatory subunit 2

RIPPO: regulatory interactors of protein phosphatase 1

RP: rapidly-progressive

sAC: soluble adenylyl cyclase

SD: standard deviation

Ser: serine

SFK: Src family kinase

SKI606: Src family kinase inhibitor

SP: slow-progressive

STR: straightness

Tau: tautomycin

Thr: threonine

VAP: velocity along the average path

VCL: velocity along the curvilinear path

VSL: velocity along the straight-line path

WHO: World Health Organization

WOB: wobble

Zn: Zinc

1. Introduction and Aims

1.1. Sperm physiology

1.1.1. Structure of the Mammalian Spermatozoon

The mammalian spermatozoon is a very specialized unique cell, characterized by a highly condensed nucleus, lack of most of the organelles, small size (50 to 60 µm), transcriptional inactivity and capability to move[1,2]. Structurally, it is constituted by the head and the flagellum, both covered by a plasma membrane[1]. The human spermatozoon is represented in Figure 1**A**, along with two cross-sections of the flagellum, from the midpiece and the principal piece **(**Figure 1**B).**

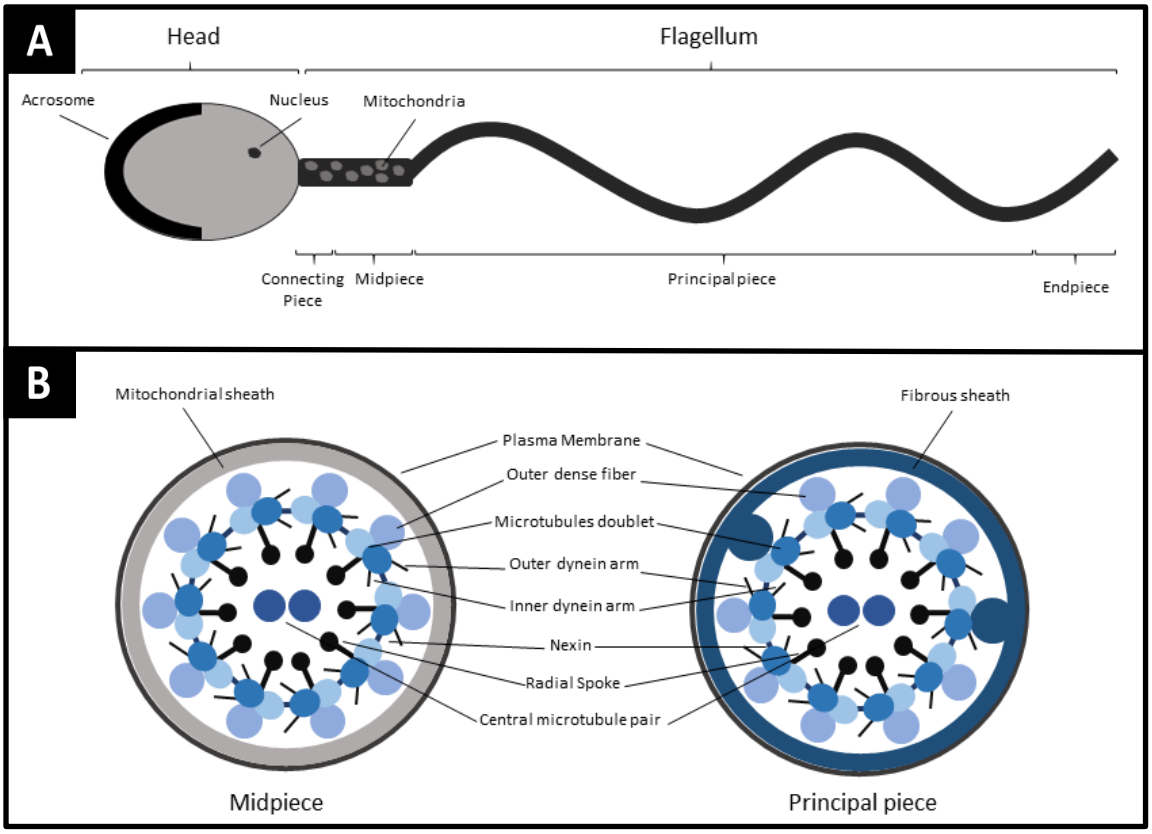

Figure 1*. Structure of the human spermatozoon and ultrastructure representation of the flagellum.* ***A:*** *Spermatozoa are divided into head (nucleus and acrosome) and flagellum (connecting piece, midpiece, principal piece, and endpiece).* ***B:*** *Two cross-sections of the flagellum showing the differences between the midpiece and principal piece are represented. Midpiece contains the*

mitochondrial sheath surrounding the outer dense fibers, along with the plasma membrane. Here the axoneme is composed of the radial spoke, the microtubule central pair, the microtubule doublets, associated with inner and outer dynein arms and with the adjacent pair by nexin. The principal piece contains a fibrous sheath and a plasma membrane surrounding the outer dense fibers, as well as, in two opposing microtubule doublets, the outer dense fibers are replaced by longitudinal columns of fibrous sheath. Adapted from Freitas et al.[3].

Concerning the spermatozoon head, it contains the nucleus, which carries the genetic information, and the acrosome, which encloses hydrolytic enzymes. Those play an essential role during the acrosome reaction by digesting the zona pellucida of the oocyte, prior to fertilization[1,4].

The flagellum is subdivided into four regions, the connecting piece, which links the flagellum to the head, the midpiece, the principal piece and the endpiece. All four comprise the axoneme which is the structure responsible for generating the motive force required for the flagellar pattern motility. The axoneme is composed by a ring of nine microtubule doublets, connected to each other by nexin links, surrounding a central pair, which in turn is connected to the doublets by radial spokes. From each of the doublets projects an inner and outer dynein arm, which are key structures to produce movement. In brief, the flagellar beat initiates, in the presence of ATP, with a phosphorylated dynein from one doublet interacting with the subsequent doublet, forcing it to slide down. This movement encounters resistance, because the microtubules are linked to the connecting piece at the base of the spermatozoon head, which leads to the bending of the flagellum. Thus, since this process is active on one side of the flagellum and inactive on the opposite site, the result is the waveform pattern movement[1,4–7].

The midpiece of the flagellum is also known to enclose the mitochondrial sheath and the outer dense fibers, both surrounding the axonemal complex, along with the plasma membrane. The mitochondria found in the mitochondrial sheath contribute to the ATP production that powers sperm movement, along with other sources of energy. In the principal piece, the axoneme is surrounded by fibrous sheath, in addition to the outer dense fibres; however, in two opposing microtubule doublets, the outer dense fibres are substituted by longitudinal columns of fibrous sheath. Lastly, the endpiece does not

present accessory structures besides the axoneme and surrounding plasma membrane[1,3,5,6].

1.1.2. Sperm motility

Male fertility relies on the ability of spermatozoa to fertilize the egg in the female reproductive tract (FRT), which requires the spermatozoon to be capable of movement after ejaculation. The root of some of the most prevalent male infertility disorders, such as asthenzoospermia (poor sperm motility), is usually unknown or difficult to find, due to a lack of understanding of the molecular pathways that regulate sperm motility[2,3,5]. After spermatogenesis, spermatozoa leave the testis as morphologically complete but functionally immature cells. Therefore, to acquire fertilization ability, the spermatozoon needs to undergo maturation in the epididymis and capacitation in the FRT, in which it acquires activated and hyperactivated motility, respectively[8,9]. In fact, a high percentage of motile spermatozoa is a crucial component of fertility, since it is considered a strong predictive marker of fertility potential[2].

According to Paoli *et al.*, sperm motility can be defined as a propagation of transverse waves along the flagellum in a proximal-distal direction, which produces an impulse that pushes the spermatozoon towards the female gamete[10]. This is achieved when spermatozoa own a morphologically complete flagellum, when they are able to produce energy to fuel the movement and present functional signalling pathways that efficiently regulate protein phosphorylation status[3,10].

Spermatozoa acquire motility across their passage throughout the epididymis, emerging with progressive motility after complete and successful maturation. The epididymis consists of three major regions, the caput which is the proximal end that succeeds the testis, followed by the corpus and the cauda, where sperm is stored until ejaculation[3,8]. Some authors consider an additional anatomical region in rodents, the initial segment, positioned between the testis and the caput region, however, its presence in other mammals was not clearly described[9]. Several studies confirm that spermatozoa enter the caput epididymis immotile and endure diverse morphologic, metabolic, and

biochemical changes until they reach the caudal end progressively motile. These alterations include changes in intracellular concentrations of calcium (Ca^{2+}) and cyclic adenosine monophosphate (cAMP), pH and phosphorylation status of critical amino acid residues[3,5,9,11–13]. The resulting activated motility is characterized by low-amplitude symmetrical tail movements that drive spermatozoa in a straight line in non-viscous media, as the seminal plasma[5,12].

Despite being progressively motile when ejaculated, spermatozoa are not capable of fertilization, they must acquire hyperactivated motility in the FRT, presumably in the fallopian tubes, through the capacitation process[2,5,14]. Capacitation is triggered by the unique environment of the FRT and causes spermatozoa to undergo a specific cascade of biochemical and physiological alterations, that ultimately allow them to reach and fertilize the oocyte[15–18]. Overall, capacitation involves the removal of the membrane cholesterol by albumin, which increases membrane permeability and hyperpolarization[19,20]. Consequently, there is a rise in sperm intracellular pH, associated with higher bicarbonate (HCO_3^-) concentration, that increases Ca^{2+} uptake[21–23]. This provokes the activation of the testis-specific soluble adenylyl cyclase (sAC), which produces the secondary messenger cAMP. This event activates protein kinase A (PKA) which subsequently initiates a protein tyrosine phosphorylation cascade[12,16,17,24]. Hyperactivated motility is characterized by asymmetric and high amplitude flagellar bends that allow the spermatozoon to move along the dense mucus of the FRT, in a circular or figure-8 trajectory[5,15]. *In vitro* hyperactivated motility induction requires Ca^{2+}, HCO_3^- and other metabolic substrates that mimic the female tract environment[17,25]. Capacitation and hyperactivation constitute distinct processes that can happen separately since they are regulated by different biochemical players. However, to some extent these mechanisms overlap, and the two processes are usually reported in association[5,18,26].

Although extensive research has been made concerning sperm motility, a large number of the signalling pathways that mediate it are yet to be unravelled. Further comprehension of the biochemical pathways subjacent to the acquisition of both activated and hyperactivated motility is indispensable to understand male fertility, as well as to look for novel solutions to motility-related infertility conditions.

1.2. Protein phosphatases and their role in sperm function

The equilibrium of protein phosphorylation systems, which results from the coordinated action of protein kinases (PKs) and protein phosphatases (PPs), is essential to maintain cellular viability and function. Moreover, reversible phosphorylation of structural and regulatory proteins consists in a major intracellular control mechanism, regulating, for instance, cell metabolism, signal transduction, gene expression, intracellular transport, and cell cycle progression[9,27–30]. Indeed, it is the most common post-translational type of modification in eukaryotes[31,32].

Since spermatozoa are virtually transcriptionally and translationally inactive, its specific functions are mediated mainly by protein phosphorylation[9,30,33]. Alongside with the extensively researched PKs, sperm-specific PPs are known to have critical roles in spermatozoa maturation, namely regarding motility acquisition and regulation[9,12,13,34,35]. According to Smith *et al.,* in bovine caput epididymis immotile spermatozoa have higher phosphatase activity, when compared to caudal motile sperm[36]. **Figure 2** portrays a representation of the PPs and PKs involved in the acquisition of activated motility during epididymal sperm maturation (**Figure 2A**) and hyperactivated motility acquisition in the FRT (**Figure 2B**).

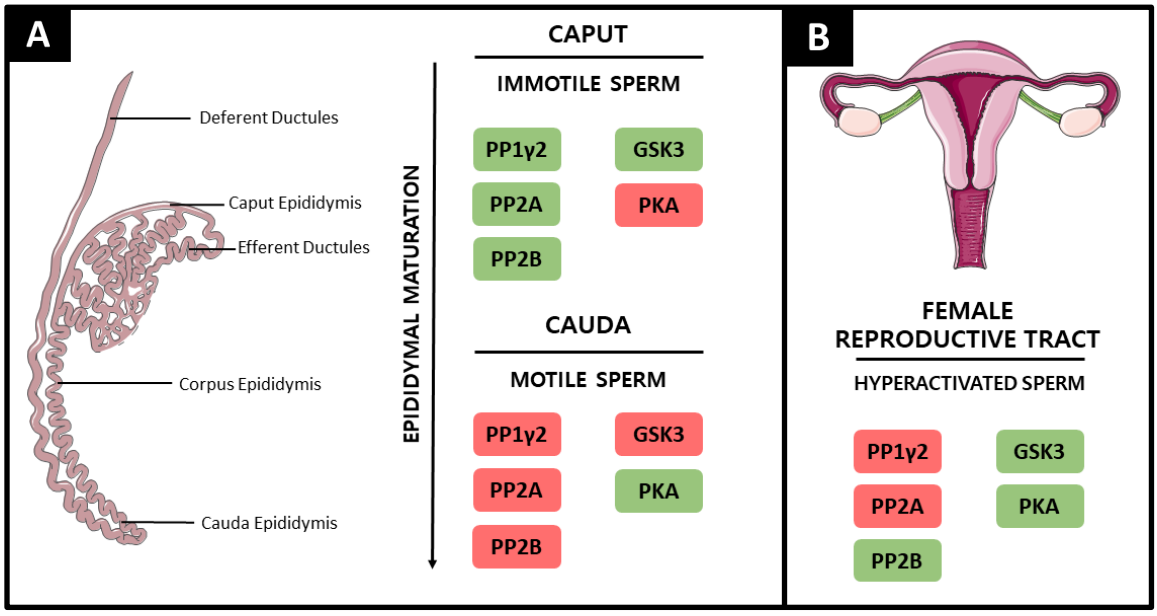

Figure 2. *Representation of the PPs and PKs involved in activated motility acquisition in the epididymis, as well as in hyperactivation in the female reproductive tract. The colour green represents catalytic activity, whereas red stands for enzymatic inactivity.* ***A:*** *Epididymis*

representation including its three epididymal subdivisions: caput, corpus and cauda, as well as deferent and efferent ducts. In caput epididymis, spermatozoa are immotile, the PPs PP1γ2, PP2A, PP2B and the PK GSK3 present catalytic activity, while PKA is inactive in sperm. In cauda, mature and motile spermatozoa are characterized by inactive PP1γ2, PP2A, PP2B and GSK3 and active PKA; ***B.*** *Female reproductive tract representation where hyperactivated spermatozoa present catalytically inactive PP1γ2 and PP2A, whereas PP2B, GSK3 and PKA present catalytic activity.* ***Abbreviations****: PPs: protein phosphatases; PKs: protein kinases; PP1γ2: protein phosphatase type 1 gamma 2; PP2A: protein phosphatase type 2A; PP2B; protein phosphatase type 2B; GSK3: glycogen synthase kinase 3; PKA: protein kinase A*

In this section, protein phosphatase type 1 (PP1), protein phosphatase type 2A (PP2A) and protein phosphatase type 2B (PP2B) will be characterized and the proposed interactions between them, concerning sperm motility acquisition and hyperactivation, will be discussed.

1.2.1. Phosphoprotein phosphatase type 1 (PP1)

PP1, also known as PPP1, is the predominant PP identified in the spermatozoon[36,37]. This Ser/Thr PP is expressed in all eukaryotic cells and is involved in various cellular processes, namely transcription, replication, pre-mRNA splicing, protein synthesis, muscle contraction, carbohydrate metabolism, neuronal signalling, cell survival, and cell cycle progression[38,39]. Since the first description of its association with sperm motility in 1996[13], PP1's role in the signalling events involved in sperm motility acquisition within the epididymis has long been investigated[3,12,37]. The catalytic subunit of PP1 is highly conserved among eukaryotes, it consists of a single domain of ~30 kDa that complexes with the regulatory subunits. PP1 catalytic activity is due to the channel formed by three β-sheets of the β-sandwich, along with two metal ions (Manganese (Mn) and Iron (Fe)) coordinated by six amino acid residues (one Asn, three His and two Asp) that form the active site[29,40]. In mammals, the catalytic subunit of PP1 presents four distinct isoforms - PP1α, PP1β, PP1γ1 and PP1γ2 - encoded in three different genes (*PPP1CA, PPP1CB, PPP1CC*). PP1γ1 and PP1γ2 result from alternative splicing of the same gene, *PPP1CC*, being the first ubiquitously expressed, along with PP1α and PP1β, and the latest the testis-enriched and sperm-specific isoform. The two isoforms' amino acid sequences are almost identical, differing only at the

C-termini [36,37,41,42]. The different isoforms of the catalytic subunit present different subcellular localization patterns and exist in the cell in association with regulatory subunits, the PP1 interacting proteins [PIPs; also known as regulatory interactors of protein phosphatase one (RIPPOs)][38,43,44]. More than 800 PIPs were identified so far, which guide PP1 action within the cell, specify PP1 substrates and regulate PP1 activity[39,45].

1.2.1.1 Phosphoprotein phosphatase 1 gamma 2 (PP1γ2)

Protein phosphatase 1 gamma 2 (PP1γ2) is the testis-enriched and sperm-specific PP1, which in mammals appears to be the principal isoform responsible for PP1 activity in spermatozoa[13,36,37]. It differs from the PP1γ1 on the C-terminal and is distributed throughout the flagellum, midpiece, and posterior region of the head of the spermatozoon[37,43]. Numerous studies showed that the decrease of PP1γ2 activity is associated with increased motility in the caudal epididymis sperm, whereas immotile caput spermatozoa present high levels of PP1γ2 activity. During capacitation, the downregulation of this PP activity was also evident in the spermatozoon. Phosphatase activity inhibition in caput epididymis, by both PP1 inhibitors calyculin A (CA) and okadaic acid (OA), was also able to induce motility[13,25,36,46]. Additionally, *Ppp1cc* gene knockout in mice, which causes the loss of both PP1γ1 and PP1γ2, resulted in impaired spermatogenesis and subsequent male infertility[47,48]. Conditional knockout of only PP1γ2 resulted in the same phenotype, strongly suggesting that *Ppp1cc* knockout mice infertility is likely due to loss of this isoform[49]. Besides, PP1γ2 transgenic expression in *Ppp1cc* null mice was able to restore sperm function and fertility[50]. Hence, it is thought that PP1γ2 is responsible for the role of PP1 in motility acquisition in the epididymis, hyperactivation and acrosome reaction of spermatozoa[3].

In the spermatozoon, PP1γ2 activity is mainly regulated by three specific inhibitors, protein phosphatase inhibitor 2 (PPP1R2, also known as I2), protein phosphatase 1 regulatory subunit 7 (PPP1R7, also known as SDS22) and protein phosphatase 1 regulatory subunit 11 (PPP1R11, also known as I3), whose association with PP1γ2 varies during epididymal sperm maturation[30,51,52]. In brief, PP1γ2 is solely bound to I3 in immotile spermatozoa of the caput epididymis, while in caudal spermatozoa it is bound to all three

inhibitors. These alterations play an important role in motility development because they are able to modulate PP1γ2 activity[51]. In 2013, a PPP1R2 isoform was identified in human spermatozoa, the protein phosphatase inhibitor 2-like (PPP1R2P3), which appears to be present only in caudal spermatozoa, inhibiting PP1γ2 and therefore contributing to motility acquisition. Due to Thr73 being substituted by Pro, PPP1R2P3 cannot be phosphorylated by glycogen synthase kinase 3 (GSK3)[53]. Furthermore, recently Schwartz *et al.* identified another possible PP1γ2 binding protein, which is CCDC181. Despite little is known about their interaction, the authors hypothesize that CCDC181 has a relevant role in generating and regulating flagellar and ciliary motility[54].

GSK3 was discovered to interact with PP1γ2 in spermatozoa, playing an essential role in its activation[13,55]. In mammals, this PK has two isoforms, GSK3α and GSK3β, which are both present in sperm[55]. Although in most cell types GSK3α and GSK3β functions are interchangeable, Bhattacharjee *et al.* found that GSK3α has an isoform-specific function in spermatozoa, that could not be overtaken by the GSK3β isoform[56]. Additionally, data from Freitas *et al.* revealed that the GSK3α isoform is specifically involved in human spermatozoa progressive motility[57]. Similar to PP1γ2, GSK3 presents six times more catalytic activity in immotile caput spermatozoa, when compared to motile caudal sperm[55,58]. Currently, it is known that GSK3 regulates I2 binding to PP1γ2, however, it is only speculated that the other PP1γ2 inhibitors referred (SDS22 and I3) are also regulated by phosphorylation[13,51].

1.2.2. Phosphoprotein phosphatase type 2A (PP2A)

PP2A activity was first documented in mammalian spermatozoa in 1996 by Vijayaraghavan et *al.*[13]. This Ser/Thr PP consists of a catalytic subunit (PP2A-C), which has two isoforms (α and β), a scaffolding subunit (PP2A-A, also with two isoforms) and a regulatory subunit (PP2A-B)[59,60]. The catalytic subunit of PP2A (36 kDa), which is one of the most conserved in eukaryotes, and the scaffolding subunit (65 kDa) form the enzyme core that can associate with different regulatory subunits to form the PP2A holoenzyme. The catalytic subunit consists of a typical α/β fold and contains two Mn ions at the enzyme's active site[28,61]. It can be covalently modified by either Tyr phosphorylation or carboxymethylation[28,60]. It was reported that PP2A plays a role in both bovine and human

sperm motility acquisition. Like PP1γ2, higher levels of this PP activity were identified in immotile caput spermatozoa, and a downregulation of its activity was evident in both caudal motile and hyperactivated spermatozoa. Changes in methylation of PP2A also modify sperm movement, as methylated PP2A is catalytically inactive in caudal spematozoa[25,60,62]. GSK3 is a known target of PP2A, since its phosphorylation was increased following PP2A inhibition. Hence, PP2A is thought to be involved in sperm motility mainly by regulating GSK3 activity[60].

1.2.3. Phosphoprotein phosphatase type 2B (PP2B)

PP2B, also known as calcineurin, is a Ser/Thr PP regulated by Ca^{2+}, which was also found in human and other mammalian spermatozoa[34,63]. This PP is Ca^{2+}/calmodulin(CAM)-dependent, meaning that it is inactive when it is not associated with Ca^{2+}-CAM[63]. PP2B is composed by two subunits, catalytic and regulatory. There are three isoforms of the catalytic subunit (PPP3CA, PPP3CB, and PPP3CC), being PPP3CC the sperm-specific catalytic isoform. The regulatory subunit also presents two isoforms PPP3R1 and PPP3R2, being the latest present in spermatozoa. Absence of either sperm-specific isoforms due to gene knockout results in male infertility[34,35,64,65]. PPP3CC contains four regions, the catalytic domain, a regulatory subunit binding segment, a CAM-binding segment and an autoinhibitory helix[66,67]. Like the other PPs, the active site of PP2B contains two metal ions, Fe and Zn, and six amino acid residues (three His, two Asn and one Asp)[65,66].

Upon the elevation of intracellular Ca^{2+}, CAM binds to the PPP3CC subunit, through the CAM binding region, which causes the activation of the enzyme, by allowing it to access its substrates[12,65]. Since it was shown in 1990 that immature caput spermatozoa present higher levels of Ca^{2+}, when compared to the cauda, a decline in PP2B activity throughout the epididymis journey was expected and further verified by Dey *et al.* in 2019[34]. Besides, it was recently demonstrated that PP2B increases its activity during capacitation, contrarily to what was previously thought[34,35]. PP2B regulates GSK3 phosphorylation, preferentially dephosphorylating the GSK3α isoform, contrarily to PP1γ2 and PP2A which target both isoforms[12,34].

1.2.4. PP1γ2, PP2A and PP2B interplay in the regulation of sperm motility

Taken together, the data exposed in the previous sections postulates that PP1γ2, PP2A and PP2B are strongly implicated in sperm motility regulation. In the last decades, the signalling pathways in which these PPs are involved have been deeply investigated. Indeed, apart from their individual role, an interplay between the three PPs has been proposed[3,9,12]. Notably, these PPs play distinct roles in motility on the different stages of spermatozoa maturation throughout the epididymis, as well as in hyperactivated motility. PP1γ2, PP2A and PP2B were collectively found to have consistently higher activity in the caput region, where spermatozoa are immature and immotile, whereas demonstrated low catalytic activity levels in the caudal, where spermatozoa have acquired activated motility[3,12]. This suggests that the decrease of their catalytic activity is a requirement for motility acquisition and, when these PPs remain activated in caudal spermatozoa, motility acquisition is not achieved[30,36]. Concerning hyperactivated motility, PP1γ2 and PP2A were found still catalytically inactive, while paradoxically PP2B presented phosphatase activity during capacitation[12,34.]

Considering the current state of the art, an interplay between both the PPs (PP1γ2, PP2A and PP2B) and PKs (GSK3 and PKA) can be proposed. This intricate interplay is schematically exposed in **Figure 3**, in relation to the different stages of maturation and type of motility, caput sperm (**Figure 3A**) and caudal sperm (**Figure 3B**), as well as hyperactivated FRT spermatozoa (**Figure 3C**).

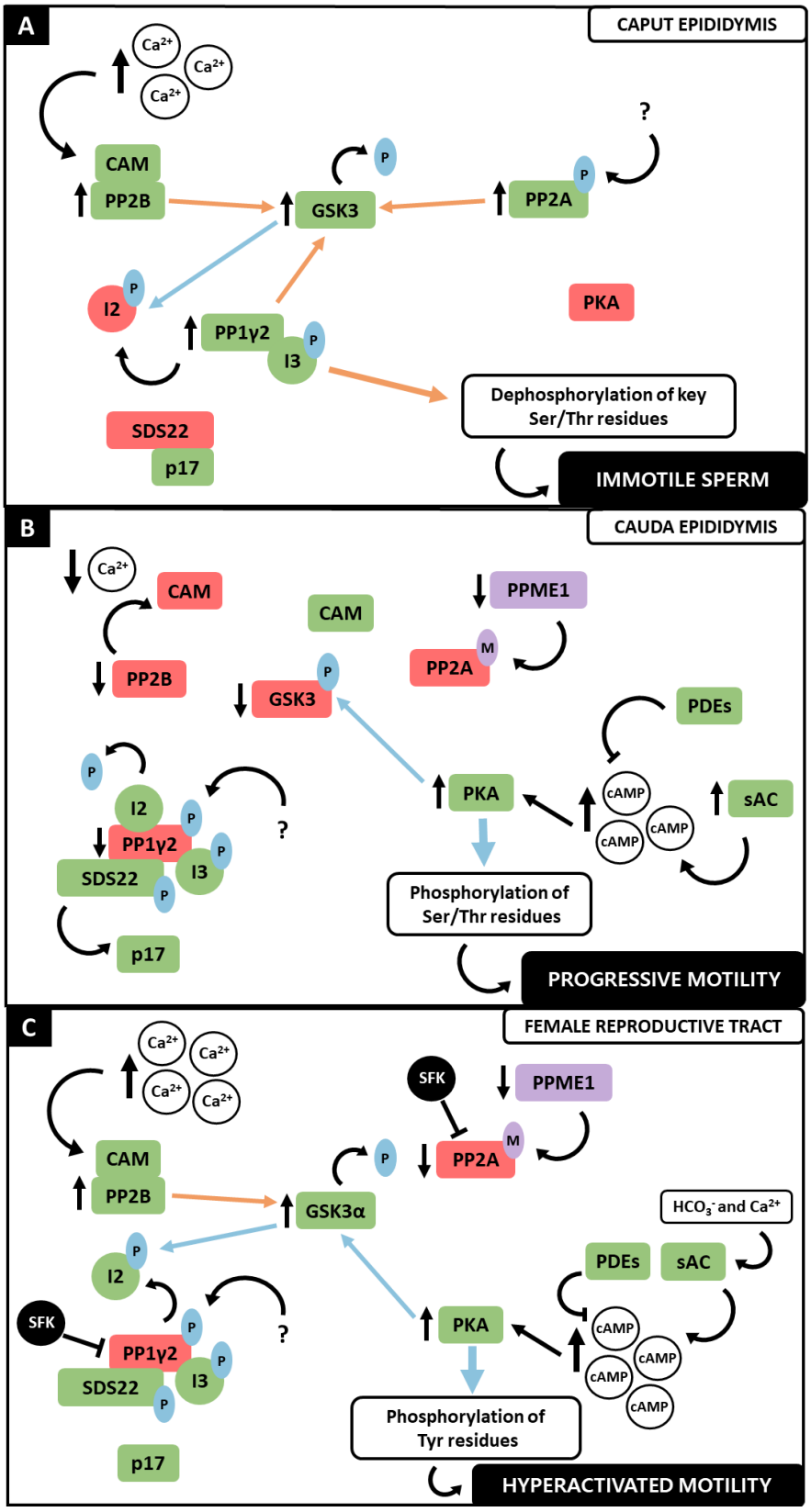

Figure 3. *Interplay between the PPs, PP1γ2, PP2A and PP2B, and PKs, GSK3 and PKA, regarding sperm motility regulation. The colour green represents catalytic activity, whereas red stands for enzymatic inactivity. Blue arrows define phosphorylation reactions, while orange represents*

dephosphorylation processes. A: In caput immotile sperm, Ca2+ increase promotes PP2B interaction with Ca2+-CAM complex that activates it. PP2B dephosphorylates GSK3α increasing its activity. Phosphorylated PP2A also contributes to the phosphorylation of both GSK3 isoforms. GSK3 phosphorylates the I2 that disassociates from PP1γ2, rendering it active, solely in a complex with I3. The inhibitor SDS22 is bound to p17. PP1γ2 dephosphorylates GSK3 and Ser/Thr residues, resulting in immotile sperm. PKA presents no significant catalytic activity. B: In cauda epididymis, Ca2+ concentration is lower, causing CAM dissociation from PP2B and its subsequent inactivity. PPME1 decreases allowing PP2A methylation and inactivity. Simultaneously, sAC is activated and produces cAMP, which in turn activates PKA. cAMP degradation is due to PDE activity. PKA phosphorylates PP1γ2 and GSK3 which decreases its activity and is no longer able to phosphorylate I2, which complexes with PP1γ2, alongside SDS22 that also dissociates from p17. Lastly, PKA's increased activity causes the phosphorylation of Ser/Thr residues that are a requirement for activated motility acquisition. C: The increase in Ca2+ once again activates PP2B that dephosphorylates GSK3α rendering it active and able to phosphorylate I2. Due to sAC activation by HCO3- and Ca2+, cAMP further increases and stimulates PKA activity. PKA phosphorylates GSK3. PP1γ2 is phosphorylated and in a complex with SDS22 and I3. SFK also contributes to decreasing PP1γ2 activity along with PP2A, which remains methylated. The increase in phosphorylation of Tyr residues contributes to achieve hyperactivated motility. Abbreviations: Ca2+: calcium; CAM: calmodulin; GSK3: glycogen synthase kinase 3; I2: Protein phosphatase 1 inhibitor 2; I3: Protein phosphatase 1 regulatory inhibitor subunit 11; M: methyl group; P: phosphate; PDE: phosphodiesterase; PK: protein kinases; PKA: protein kinase A; PP: protein phosphatases; PP1γ2: phosphoprotein phosphatase type 1 gamma 2; PP2A: phosphoprotein phosphatase type 2A; PP2B; phosphoprotein phosphatase type 2B; PPME1: protein phosphatase methylesterase 1; sAC: soluble adenylyl cyclase; SDSS2: Protein phosphatase 1 regulatory subunit 7; Ser: serine; SFK: Src family kinase; Thr: threonine.

In caput spermatozoa the increase in intracellular Ca^{2+} activates PP2B by promoting its interaction with the Ca^{2+}-CAM complex. Consequently, PP2B preferentially dephosphorylates GSK3α at its inhibitory residue Ser21, activating it[34]. Synergistically, at this stage active PP2A is demethylated and phosphorylated, therefore being able to also dephosphorylate both GSK3 isoforms[60]. The PK that phosphorylates PP2A is still unknown. Active GSK3 phosphorylates the PP1γ2 inhibitor I2 at Thr73, which results in active PP1γ2, in a complex with only I3, since SDS22 is bound to p17[52,60]. PP1γ2 not only contributes to dephosphorylate GSK3, but also to dephosphorylate key Ser and Thr residues that leave immature spermatozoa immotile[3,60]. In caput spermatozoa, PKA presents no significant catalytic activity[12].

During spermatozoa journey through the epididymis, the Ca^{2+} influx decreases, along with PP2B activity, rendering it inactive at caudal level and therefore unable to dephosphorylate the GSK3α isoform[34]. GSK3 dephosphorylation is further affected by the decrease in protein phosphatase methylesterase 1 (PPME1) activity in caudal spermatozoa,

which increases PP2A methylation causing its inactivity. Highly phosphorylated GSK3 at Ser residues is inactive and incapable of phosphorylating I2, which can inhibit PP1γ2[60]. Simultaneously, SDS22 is free from its interaction with p17, being in a complex with PP1γ2 as well[52]. The decrease in the activity of the Ser/Thr PPs which causes a notable decrease in dephosphorylation, and an increase in the number of phosphorylated residues, due to PKA activity was observed in caudal spermatozoa[8,12,68]. The sAC, whose activity is regulated by HCO_3^- and Ca^{2+} concentration, is activated and produces cAMP, activating PKA[68]. The concentration of cAMP in spermatozoa is also regulated by phosphodiesterases (PDEs) that are able to degrade it. There are eleven PDEs, of which PDE1, PDE4, PDE8, PDE10 and PDE11 are present in spermatozoa. Collectively, the equilibrium of sAC and PDE activity regulates cAMP levels in spermatozoa[12]. In fact, PKA itself has been thought to regulate PDE activity, in particular phosphodiesterase 4 (PDE4) and phosphodiesterase 11 (PDE11), whose catalytic activities were found increased following PKA phosphorylation, suggesting a feedback regulation of cAMP (interaction not shown in **Figure 3**)[69]. In 2018, Dey *et al*[70] proposed that GSK3 indirectly regulates cAMP concentration, since it modulates PDE4 function, decreasing it and presumably increasing cAMP levels. On the other hand, when GSK3 is catalytically inactive, lower levels of cAMP were expected. In caudal sperm that is not the case, as cAMP levels are increased and GSK3 activity decreases. Additionally, in caput epididymis when GSK3 is active, PDE4 inhibition should result in higher cAMP levels and subsequent PKA activity, which is also not verified (interaction not shown in **Figure 3**). These contradictive results suggest that more complex molecular interactions are involved, concerning GSK3/PDE4/sAC interaction, that may require additional research[70]. Overall, active PKA in caudal spermatozoa not only phosphorylates both GSK3 isoforms (Ser21/9), but also other proteins, which seems to be a requirement for motility acquisition in the mature spermatozoon[9,12,51]. PP1γ2 was found phosphorylated in caudal spermatozoa at its Thr320. The underlining mechanism is still unknown, but it is speculated that a cyclin-dependent kinase (CDK) is responsible for this residue's phosphorylation[12,30,71].

At the FRT, hyperactivated motility is required for successful fertilization and both PP and PK play important roles[17,34]. Ca^{2+} influx increases again inducing PP2B activity, which in turn dephosphorylates GSK3α, being both enzymes active during capacitation[34]. GSK3α

is now able to phosphorylate I2 that disassociates from PP1γ2 however, the other two inhibitors remain in a complex with this PP, rendering it still inactive. PP2A also remains inactive since it is methylated[3]. It was proposed by Battistone and colleagues that these PPs downregulation during capacitation is also mediated by a Src family kinase (SFK). They showed that spermatozoa capacitating in the presence of a SFK inhibitor (SKI606) presented a decrease in phosphorylation levels, which was overcome by exposure to a PP inhibitor (OA). Besides, incubation with SKI606 also affected motility parameters which were similar to those of non-capacitated spermatozoa[25]. Concomitantly, the high concentrations of Ca^{2+} and HCO_3^- stimulate cAMP production and a subsequent increase in PKA activity, which increases phosphorylation in Tyr residues among several known substrates within the spermatozoon, that seem to be required to achieve hyperactivated motility[25,72,73]. Remarkably, both PP2B and the GSK3α isoform present increased activity in hyperactivated spermatozoa, similarly to their activity in caput immotile spermatozoa. Although many authors have been suggesting that the decrease in PP catalytic activity and concomitant increase in PK's is a requirement for sperm motility, more recently, PP2B catalytic activity appeared to be essential for successful hyperactivation, accordingly to Dey *et al*.[25,34,35]. Comparing to activated motility, the mechanisms that underline hyperactivated motility acquisition are more complex and are affected by alterations other than protein phosphorylation, which could explain the disparity between the PPs activity during this process, as well as the difficulties to study this motility pattern[9,12,25,34,35,57].

Taking everything into account, the crosstalk between PP1γ2, PP2A and PP2B, as well as GSK3 and PKA, is essential during spermatozoa maturation along the epididymis and capacitation at the FRT, since they determine the phosphorylation status of spermatozoa proteins, which appears to be crucial to initiate and maintain activated and hyperactivated motility. Regardless of the countless studies made to understand the biochemical mechanisms underlining sperm motility, several inconsistencies are yet to be solved and many protein interactions unveiled.

1.3. PP1, PP2A and PP2B inhibition

The study of Ser/Thr PPs significantly advanced following the identification of several naturally occurring toxins that were powerful and specific PP inhibitors. This allowed further comprehension of PPs role in various cellular events and other phosphorylation-dependent processes[74–76]. To name a few, after the discovery of OA[36,77], the first compound that was found to be a potent inhibitor of both PP1 and PP2A, many other can be highlighted such as CA[36,78], Ciclosporin A (CsA)[79], cantharidin (CAN) and its analogues[80], cypermethrin (CYP)[81], tautomycin (TAU)[82], noludarin[83] and microcystins[83]. In fact, PPs are some of the most catalytically efficient enzymes, as they contain highly conserved active sites and do not possess high substrate specificity, which makes them very susceptible to inhibition by natural toxins[84,85]. Besides, although most PP inhibitors present distinct chemical identities, they usually interact with a similar set of amino acids, along with the two metal ions they coordinate, that collectively compose the PP's active site[74,86]. On the contrary, the different sensitivities the PPs present towards the inhibitors may be due to their very specific structural differences within the similarly folded catalytic core, despite their high degree of active site conservation[74].

Inhibition of PP1, PP2A and PP2B in spermatozoa was accomplished many times through the last century, which contributed to the comprehension of the signalling pathways discussed in the previous section. **Table 1** gathers the reports on the inhibition of the studied PPs in spermatozoa.

Table 1. *Reports on the inhibition of PP1, PP2A and PP2B by the PP inhibitors CA, OA, DEL, CsA and E in spermatozoa. For each report, the PP inhibitor, spermatozoa model, concentration required for inhibition and outcome achieved are presented.* ***Abbreviations:*** *PP1: phosphoprotein phosphatase type 1; PP2A: phosphoprotein phosphatase type 2A; PP2B; phosphoprotein phosphatase type 2B; PKA: protein kinase A; CA: Calyculin: OA: Okadaic Acid; DEL: Deltamethrin; CsA: Cyclosporin A; E: Endothal.*

PP Inhibitor	Model	[ ]	Outcome	Reference
Calyculin A	Fowl sperm	0.1µM	Loss of motility following the addition of $CaCl_2$ to demembranated spermatozoa, which was gradually restored by addition of EGTA.	Ashizawa *et al.* [87] 1994

		1.0 μM	Activation of intact sperm motility and stimulation of metabolic activity at 40 degrees.	Ashizawa *et al.* [88] 1995
		1) Maximal effect: 1000 nM 2) 100 nM	1) Induction of vigorous motility, stimulation of acrosome reaction in the presence of IPVL; 2) Significantly decreased ATP concentrations of spermatozoa.	Ashizawa *et al.* [89] 2006
	Mouse sperm	Maximal effects: 125 nM	Induced phosphorylation of several flagellar proteins, as well as PKA, inactivating it; Reduced progressive flagellar movement, inducing the hyperactivation-like motility pattern type.	Goto *et al.* [90] 2009
		0.1, 1, 3, 10, 100, 1000 nM	Overcome the block of capacitation-associated parameters by SKI606 and SU6656, such as PKA inhibition and tyrosine phosphorylation in a dose-dependent manner.	Krapf *et al.* [91] 2010
	Boar sperm	Maximal effect: 10 nM	Increased hypotonic volume, blocked the regulatory volume decrease (RVD) process, and increased relative cell volume.	Petrunkina *et al.* [92] 2007
		50 and 100 nM	Promotion of hyperactivation and cAMP-induced protein tyrosine phosphorylation identically at both concentrations.	Harayama *et al.* [93] 2012
	Bovine sperm	PP inhibition: 1.0 nM; Maximal effect: 3.4 nM	Activation of motility on caput and caudal spermatozoa; Demonstration of GSK3's presence in bovine sperm.	Vijayaraghavan *et al.* [13] 1996
		50 nM	Increase of phosphorylated PP1γ2 in both caput and caudal epididymal spermatozoa.	Huang *et al.* [94] 2004
	Monkey sperm	0.59 nM	Increase in %motility and an acceleration in mean path velocity;	Smith *et al.* [36] 1996
		100 nM	Increase in motile cells of the caput sperm, without any effect on their path velocity.	Smith *et al*[95] 1999
	Human sperm	IC_{50}: 0.75 nM	Increase in %motility and an acceleration in mean path velocity; Demonstration that sperm contains PP1 and its regulators.	Smith *et al.* [36] 1996
		100 nM	Increase in p105/81 phosphotyrosine levels and stimulation of sperm capacitation.	Leclerc *et al.* [96] 1996
Okadaic acid	Fowl sperm	1.0 μM	Loss of motility following the addition of $CaCl_2$ to demembranated sperm, which was gradually restored by addition of EGTA.	Ashizawa *et al.* [87]1994
		Maximal effect: 1000 nM	Less vigorous motility stimulation, induction of acrosome reaction in the presence of IPVL.	Ashizawa *et al.* [89] 2006
	Mouse sperm	0.1, 1, 3, 10, 100, 1000 nM	Overcome the block of capacitation-associated parameters by SKI606 and SU6656, such as PKA inhibition and tyrosine phosphorylation in a dose-dependent manner.	Krapf *et al.* [91] 2010
	Boar sperm	Maximal effect: 10 nM	Increased hypotonic volume, blocked the regulatory volume decrease (RVD) process, and increased relative cell volume.	Petrunkina *et al.* [92] 2007
	Bovine sperm	PP inhibition: 1 μM; Maximal effect: 5 μM	Activation of motility on caput and caudal sperm; Demonstration of GSK3's presence in bovine sperm.	Vijayaraghavan *et al.* [13] 1996

		5 nM	Increase of sperm motility parameters (%motility, velocity, and lateral head amplitude), as well as elevation of dimethyl PP2A and tyrosine phosphorylated PP2A.	Dudiki *et al.* [60] 2015
	Monkey sperm	37.2 nM	Increase in %motility and an acceleration in mean path velocity.	Smith *et al.* [36] 1996
	Human sperm	1.0 µM	Alteration of velocity along the curvilinear path and amplitude of the lateral displacement of the head; Inhibition of Ca^{2+}-dependent dephosphorylation of cAMP-dependent phosphoproteins in capacitating sperm.	Ahmad *et al.* [63] 1995
		38.8 nM	Increase in %motility and an acceleration in mean path velocity; Demonstration that sperm contains PP1 and its regulators.	Smith *et al.* [36] 1996
		1) 1 µM 2) 100 nM	1) Increase in p105/81 phosphotyrosine levels; 2) Stimulation of sperm capacitation.	Leclerc *et al.* [96] 1996
		100 nM	Inhibited the Ca^{2+}-stimulated dephosphorylation of human sperm phosphotyrosine-containing proteins.	Carrera *et al.* [97] 1996
		(IC_{50}) PP1: 10 nM PP2A: 0.1 nM	Increased phosphorylation on threonine residues; Demonstration that the activity of this PP decreases during the capacitation process.	Signorelli *et al.* [35] 2013
Cyclosporin A	Human sperm	2 µM	Blocked acrosomal exocytosis, suggesting PP2B is required in the early steps of the secretory process of the acrosome reaction.	Bennet *et al.* [98] 2010
Deltamethrin	Fowl sperm	1-100 nM Maximal effect: 10 nM.	Did not permit the restoration of motility at 40ºC but stimulated the acrosome reaction in the presence of IPVL.	Ashizawa *et al.* [99] 2004
	Human sperm	10 nM;	Inhibited the Ca^{2+}-stimulated dephosphorylation of human sperm phosphotyrosine-containing proteins.	Carrera *et al.* [97] 1996
		(IC_{50}) PP2B: 0.1 nM	Increased phosphorylation on threonine residues; Demonstration that the activity of this PP decreases during the capacitation process.	Signorelli *et al.* [35] 2013
Endothall	Human sperm	(IC_{50}) PP2A: 90 nM	Increased phosphorylation on threonine residues; Demonstration that the activity of this PP decreases during the capacitation process.	Signorelli *et al.* [35] 2013

1.3.1. Cantharidin (CAN)

CAN is a cell membrane permeable terpenoid, whose molecular structure is presented in **Figure 4A**. CAN is the vesicant in blister beetles, being its toxic action due to inhibition of PP activity. Despite its severe toxic effects, it has been largely used in medicine, especially due to its anticancer activity[74,80,100]. It was reported to inhibit both PP1 and PP2A, being a more potent inhibitor of PP2A, since it binds to PP1 *in vivo* with an IC_{50} of 500 nM, whereas the IC_{50} for PP2A binding is 40 nM[80,101–103].

CAN is a very small molecule when compared to the other naturally occurring PP inhibitors, therefore it directly interacts with the active site of PPs, binding to the catalytic metals, instead of occupying the pocket on the enzyme's surface[74]. CAN binds to PP1 through a hydrogen bond at its active site. **Figure 4B** portrays a model of the PP1:CAN complex, inferred by the similarities of the PP1:TAU active site interaction, which was obtained experimentally by Kelker and colleagues[104].

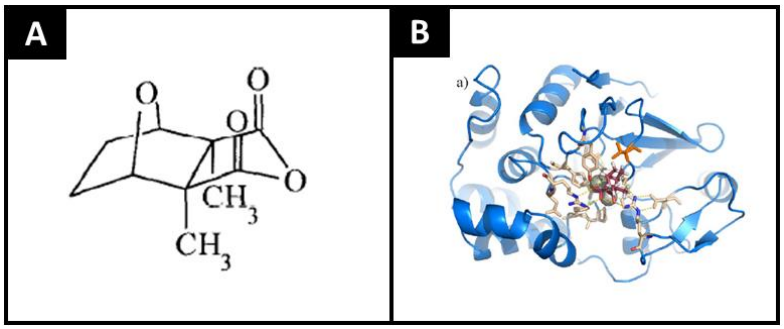

Figure 4. *Cantharidin (CAN).* ***A:*** *Chemical structure of CAN. Retrieved from*[101]*.* ***B****: PP1:CAN interaction model showing the hydrogen bond interaction network between CAN and the PP1 active site. Retrieved from*[104]*.*

Since PP2A catalytic subunit is one of the most conserved enzymes studied and its structure is in many aspects like other PPs, it might bind to the toxins in a similar way[61]. Notably, the interaction of PP2A to the inhibitors OA and microcystin-LR was experimentally reported to be through a similar set of amino acids, both occupying the same surface pocket of the active site[61]. Nonetheless, the structure of its interaction with CAN was not experimentally assessed so far. Concerning this inhibitor, to date only the structure of the complex PP5:CAN was studied[100]. CAN effects were never reported to be tested in spermatozoa.

1.3.2. Tautomycin (TAU)

TAU, chemically represented in **Figure 5A**, is also a PP1 and PP2A inhibitor. It is a polyketide isolated from *Streptomyces spiroverticillatus*[74,82]. Contrarily to CAN, TAU inhibits PP1 more potentially, with a IC_{50} of 0.4 nM, while for PP2A it is of 34 nM. It also weakly inhibits PP2B with a IC_{50} of 100 µM[82,105]. In fact, TAU is currently the most potent PP1 inhibitor available[86].

The structure of TAU-PP1 interaction was experimentally assessed and its schematic representation is shown in **Figure 5B**. TAU binds to PP1 at its active site by TAU hydrophilic moiety in the diacid form forming one water-mediated and six direct hydrogen bonds with the amino acid residues. The hydrophobic moiety contacts the hydrophobic groove of PP1, being its higher affinity to this enzyme due to this segment, as suggested by studies with structural analogues[74,76,104].

TAU was reported to be tested in spermatozoa in 2010 by Suzuki *et al.*. Suzuki and colleagues tested TAU in hamster spermatozoa (1 and 10 nM) and verified increased sperm hyperactivation after 2 hours and no effect on the percentage of motile sperm[106].

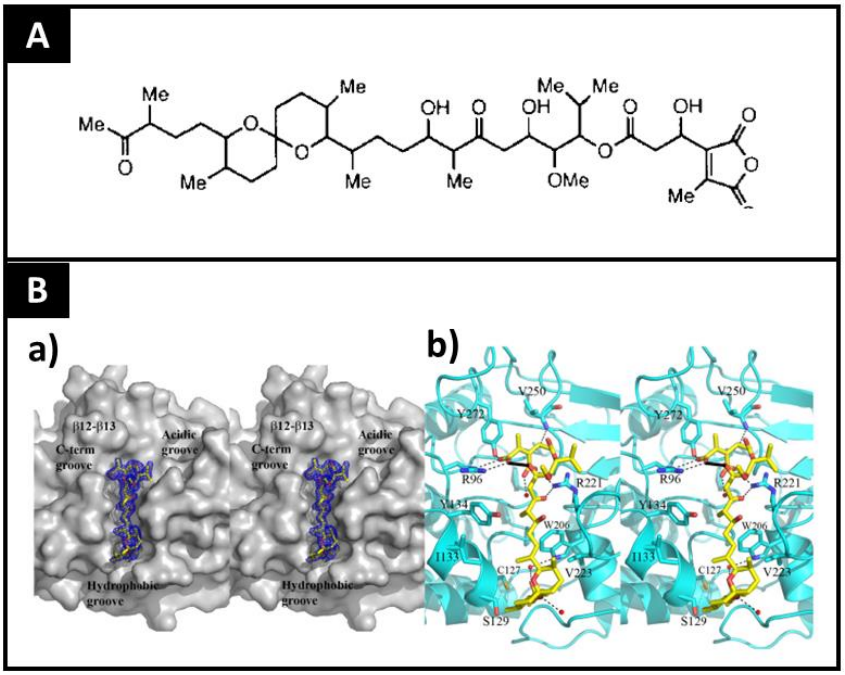

Figure 5. *Tautomycin (TAU).* ***A:*** *Chemical structure of TAU. Retrieved from*[82]. ***B:*** *Experimentally determined PP1:TAU complex. a) TAU bound to the surface of PP1; b) Detailed active site interactions, the intramolecular hydrogen bound is shown as a solid black line, while dotted lines represent potential hydrogen bonding interaction. Retrieved from*[104].

1.3.3. Cypermethrin (CYP)

CYP is a type 2 pyrethroid insecticide, produced by *Chrysanthemum Cinerariaefolium*, which modulates ion channel activity and was reported to inhibit PP2B at subnanomolar concentrations (40 pM)[81,107]. CYP chemical structure is represented in **Figure**

6. To date, the interaction of CYP and PP2B was not experimentally determined, however, since its active site architecture is similar to the other PPs, identical interactions should be expected.

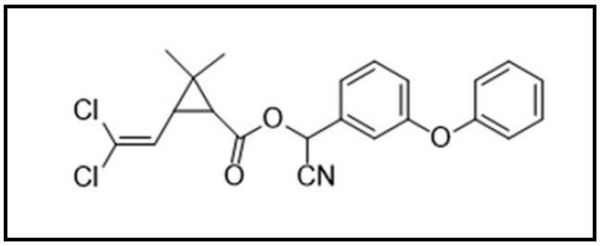

Figure 6. *Chemical structure of cypermethrin (CYP). Retrieved from*[107]*.*

CYP has been widely used to inhibit PP2B, following its first use in 1992 when Enan *et al.* tested it in bovine brain extract, with IC_{50} value of approximately 40 pM[81]. Regarding spermatozoa, high concentrations of CYP were tested in mammal and human spermatozoa to assess its toxic effects, since CYP is widely used as a pesticide and in the latest years its exposure among humans and animals has increased[108–110]. Zalata *et al.* verified a significant decrease in all human sperm motility parameters evaluated with 10 µM of CYP[108]. Previously, Yuan *et al.* obtained similar results with rat spermatozoa using concentrations of 1, 4, 16 and 64 µM. Besides, VCL, VSL, BCF, LIN and STR were reduced with increasing concentration and exposure time (1, 2 and 4h)[109]. Both studies tested concentrations much higher than the required to inhibit PP2B.

1.4. Evaluating sperm movement patterns with Computer-Aided Sperm Analysis (CASA) systems

It is of great value to evaluate sperm motility in semen samples because the total number of progressively motile spermatozoa presents biological significance regarding male fertility, as well as fertilization rates[111,112]. Currently, it is recommended a four-category system for grading sperm motility, accordingly to the World Health Organization (WHO) guidelines[113], which is summarized in **Table 2**.

Table 2. *Sperm motility grading system accordingly to WHO*[113]*.*

Sperm motility grading system accordingly to WHO		
Rapidly-progressive (RP)	25 µm/s	Spermatozoa moving actively (linearly or in large circle)
Slow-progressive (SP)	5 to 25 µm/s	Spermatozoa moving actively (linearly or in large circle)
Non-progressive (NP)	< 5 µm/s	Spermatozoa display all other patterns of active tail movements without progression
Immotile	-	Spermatozoa present no active tail movements

One of the most important tools that supported the study of sperm motility was the CASA system. CASA systems can detect and analyse motile cells with great accuracy and speed, making them suitable to evaluate sperm motility. To perform an analysis and obtain reliable movement parameters, at least 200 motile spermatozoa per specimen are needed. The CASA instrument consists of a light microscope equipped with a camera and a temperature-controlled object stage that maintains the sample at body temperature (around 37 °C), since both sperm movement and velocity are temperature-dependent and room temperature can result in inaccurate motility assessments. The CASA instrument is also linked to a computer software that enables data collection and organization[113–117]. According to several authors, the quality of the final results depends on three major factors, the counting chamber, dilution media and frame rate (FR) of the acquisition[118–120].

The development of CASA systems contributed to more objective and detailed assessments of sperm quality, since it overcomes the subjectivity of conventional semen analysis. Improved capabilities of CASA systems are consistently being developed over the years. Nonetheless, the estimation of percentage motility might still be unreliable, since debris can be confused with immotile spermatozoa. Besides, the software is rather expensive and requires species-specific calibration[121]. In fact, several factors can impact CASA performance, so the appropriate procedures should be rigorously followed, to obtain accurate and reproducible results[112–115,122,123].

1.4.1. CASA's variables and terminology

According to the sixth edition of WHO laboratory manual for the examination and processing of human semen[113], the CASA systems measure the motility standard variables shown in **Figure 7**.

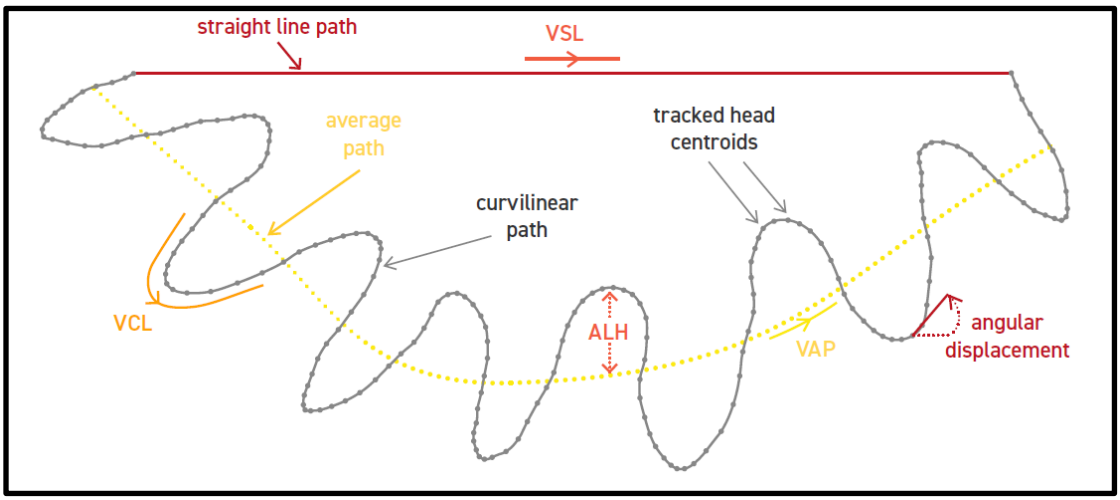

Figure 7. *Standard terminology for variables measured by CASA systems. Retrieved from*[113]*.* ***Abbreviations:*** *CASA: computer-aided sperm analysis; VCL: velocity along the curvilinear path; VSL: velocity along the straight-line path; VAP: velocity along the average path; ALH: amplitude of the lateral displacement of the head; VAP: velocity along the average path.*

Furthermore, a brief description of each type of movement is summarized in **Table 3**. Concerning these parameters, VSL, VAP, STR and LIN are indicators of sperm progression, being STR and LIN also used to describe the linearity of sperm swimming patterns. VCL, BCF and ALH relate to sperm viability and vigor[109,124]. It is important to note that the mathematical algorithms used to calculate some of these variables differ according to the CASA systems, making it often difficult to compare measurements between instruments[112,113]. VCL, VSL and VAP strongly correlate with each other, being VCL frequently used to more objectively measure sperm swimming speed, since it represents the actual velocity along the sperm trajectory[125,126]. STR usually correlates with LIN, being the second the most frequently chosen to describe the linearity of the trajectory, since it depends less on the CASA instrument and is, therefore, more convenient to compare between studies[109,124,127].

Table 3. *Variables measured by CASA systems. Adapted from*[113,126,128]*.* ***Abreviations:*** *CASA: computer-aided sperm analysis; VCL: velocity along the curvilinear path; VSL: velocity along the straight-line path; VAP: velocity along the average path; ALH: amplitude of the lateral displacement of the head; MAD: mean angular displacement; LIN: linearity of the curvilinear path; WOB: wobble; STR: straightness; BCF: beat-cross frequency; DNC: Dance*

Variables measured by CASA systems	
Velocity along the curvilinear path (VLC)	Time-averaged (μm/s) velocity of the sperm head moving along the path previously traced by the sperm in two dimensions under a microscope;
Velocity along the straight-line path (VSL)	Velocity (μm/s) along a straight line between the first and last points of the path;
Velocity along the average path (VAP)	Time-averaged velocity (μm/s) calculated along the average path, defined as a smooth curved path, calculated accordingly to the CASA algorithm;
Amplitude of the lateral displacement of the head (ALH)	Magnitude of the lateral displacement of the sperm head (μm), about the average path, linked to active sperm motility;
Mean angular displacement (MAD)	The time-averaged absolute values of the instantaneous angle of rotation (degrees) of the curvilinear path;
Linearity of the curvilinear path (LIN)	Derived from the calculation of VSL/VLC;
Wobble (WOB)	Oscillation of the curvilinear path about the average path (VAP/VLC);
Straightness (STR)	Linearity of the average path (VSL/VAP);
Beat-cross frequency, Hz (BCF)	Average frequency at which the curvilinear path crosses the average path, is correlated to the frequency of the flagellar beating;
Dance (DNC)	Measure of the pattern of sperm motion, representing the estimated space covered by sperm per second (VCL*ALH).

1.4.2. Conventional CASA systems limitations and alternative analyses

Hyperactivated motility differs from activated motility, as described in previous sections, originating a more complex flagellar movement. This altered pattern of motility is rather difficult to identify manually in a larger scale with great accuracy, therefore, diverse algorithms and computer-based systems were proposed to assess this type of motility, usually based on derived quantities by tracking head movement[113,129].

Currently, there is no consensus regarding how to objectively define the hyperactivated motility pattern, using the parameters evaluated by CASA. In general, it is considered an increased ALH and VCL, along with a decreased LIN, however, the cut-points are not well defined and differ between studies[129,130]. Recently Dey *et al.* also considered

that a substantial increase in VAP (> 100 µm/s) is indicative of hyperactivated motility, alongside an increased VCL (> 150 µm/s) and increased ALH[34]. Further, 2021 WHO manual considers that a decrease in BCF is also representative of hyperactivated spermatozoa[113].

In attempting to solve this problem, as well as other limitations referred above, some variations of CASA are being developed. For instance, novel computational capabilities, such as CASAnova[131], allow both the assessment of kinetic parameters and the classification of thousands of spermatozoa simultaneously. In fact, it provides an accurate, quantitative and high-throughput automated method for monitoring alterations in motility during *in vitro* capacitation[131]. This enables the study of hyperactivation at an almost instantaneous change in individual flagellar beating, instead of an average of the sperm population[132]. Another example is OpenCASA[133], which was developed in response to the lack of an open source to perform an integrated analysis of several parameters of seminal quality, including sperm motility[133].

Despite being the most used tool due to its undeniable advantages, the existing CASA systems are still not currently recommended for routine clinical use[113,129]. Therefore, the need to improve semen analysis methodology persists. Machine learning-based analysis, though still in preliminary development, constitute promising automatic tools to analyze large amounts of data, with respect to infertility research, as well as to use in the clinical field[134–136]. One method of machine-learning based automatic sperm quality assessment currently being developed was used in our study. **Table 4** summarizes the differences and similarities between the Sperm Class Analyzer CASA System with SCA® analysis and the machine learning-based analysis used in our study, which will henceforward be referred to as CASA system analysis and alternative analysis, respectively.

Table 4. *Comparison between CASA System with SCA® analysis and an alternative analysis.*

	Sperm Class Analyzer CASA System v6.6.18 software	**Alternative analysis**
Microscope	Light microscope equipped with a temperature-controlled object stage (37°C)	Light microscope with a lateral camera (ORCA-flash 4.0)
Objective	10x	20x
Mode of analysis	Automatic report of the SCA software (according to WHO)	Visual classification of single sperm trajectories + Posterior machine learning-based analysis in the recorded videos (according to WHO)
Chamber for analysis	Leja20 slides	Glass capillary 200x2000µm
Video frame rate (FPS)	25	100
Hyperactivation analysis	No	Yes
Motility classes	Immotile, non-progressive, slow-progressive, and rapid-progressive	Immotile, non-progressive, slow-progressive, rapid-progressive, **hyperactivated, circular trajectory and others**
Kinematic parameters retrieved	VCL, VSL, VAP, LIN, STR, WOB, ALH and BCF	VCL, VSL, VAP, LIN, STR, WOB, ALH, BCF, **MAD** and **DNC and others**

The FR is the frequency at that consecutive frames are captured by a video camera and is expressed as frames per second (fps). The difference in FR is notable between methods, which has an impact on the results, since a higher FR, such as the one of the alternative analyses, makes the analysis more accurate and the distinction between motility parameters more precise. Besides, the chambers used to load the samples can substantially impact the results, since it was shown that low width can limit natural sperm velocity, and the glass capillaries used in the alternative analysis have 10x more height than those from the CASA analysis[137,138].

One of the greatest advantages of machine learning-based methods resides on the recognition of the motility classes and kinematic parameters, which is unalterable in the CASA systems but can be personalized in any machine learning-based analysis, to retrieve the desired information, particularly information regarding circular trajectories and hyperactivated spermatozoa.

1.5. Aims

Infertility affects around 15% of couples in reproductive age worldwide and this number is expected to increase. With male infertility cases still attaining alarming numbers, the need of further investigation persists. Not only to better understand, identify, and treat sperm motility-related infertility cases, but also to provide additional knowledge on the research for male contraceptives targeting motility[113,139,140].

Many advances have been made concerning the understanding of sperm motility regulation. Notwithstanding, since the PP interplay is more complex than previously thought, many specific interactions and inconsistencies are yet to be elucidated. The discovery and use of naturally occurring toxins, which presented as powerful and specific PP inhibitors, significantly contributed to the great advance of PP studies. However, to date, only a small portion of the inhibitors identified was reported to be tested in sperm.

As such, the main goal of this study was to test the effects of three PP inhibitors, cantharidin, tautomycin and cypermethrin, on bovine and human spermatozoa. To achieve that we proposed the following tasks:

1. Test distinct concentrations and incubation times of the PP inhibitors (CAN, TAU and CYP) to differentially inhibit the three PPs (PP1, PP2A and PP2B), in bovine sperm and assess its effects on both motility and kinematic parameters;
2. Test the effect of TAU in human sperm motility and kinematic parameters;
3. Compare the results using two methods of semen analysis: the CASA system analysis and machine learning-based analysis (alternative analysis).

2. Methodology

Experimental procedures took place both in the Signal Transducing Laboratory, at the Institute of Biomedicine (IBiMED) at the University of Aveiro, as well as in University of Naples Federico II (Naples, Italy) at the Center for Advanced Biomaterials for Healthcare (CRIB) facilities. **Figure 8** and **Figure 9** schematically summarize the methodology of the present study.

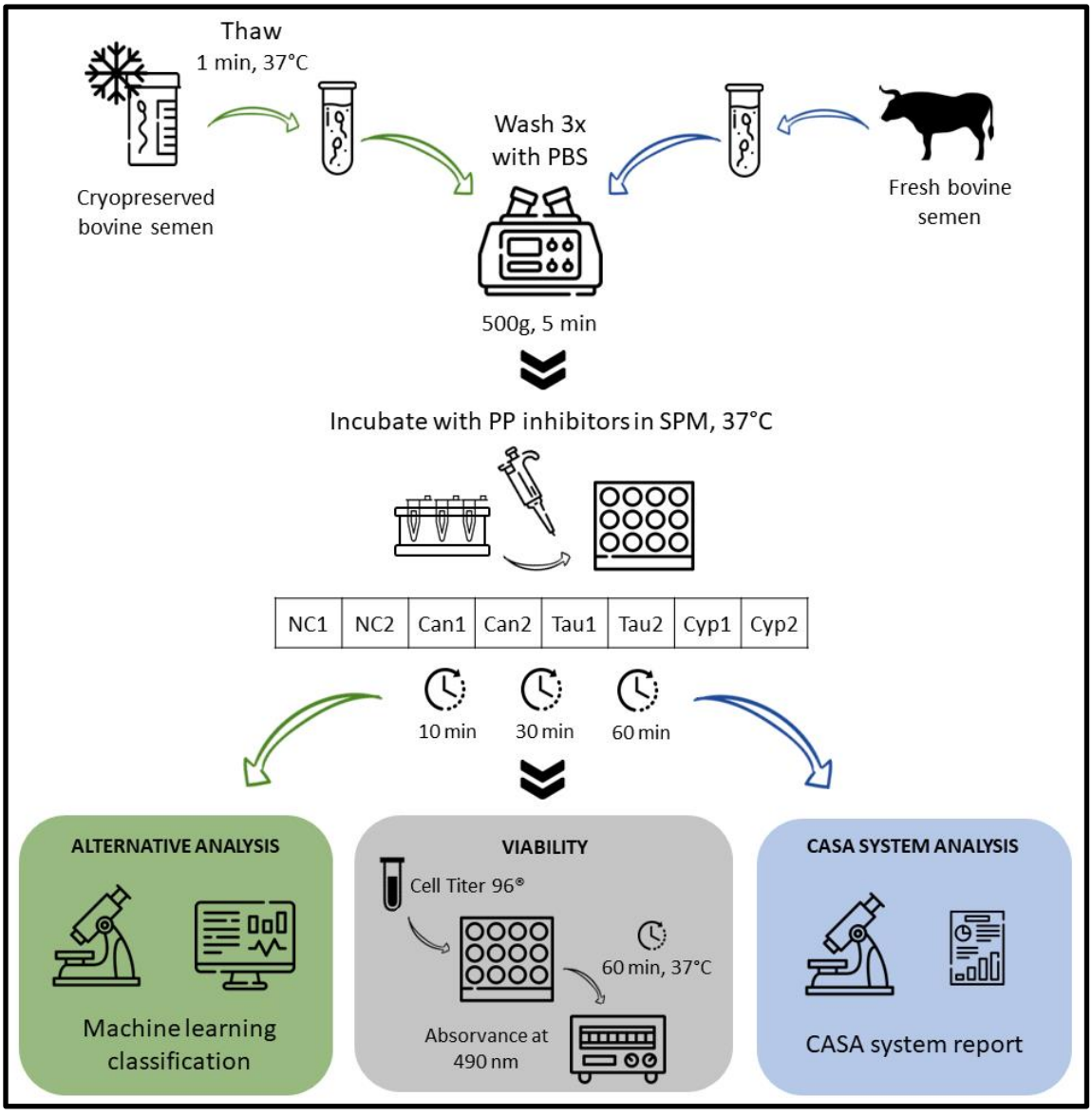

Figure 8. *Experimental procedure performed in bovine spermatozoa including sample preparation, viability assessment and motility analysis performed after the incubation with CAN, TAU and CYP.*

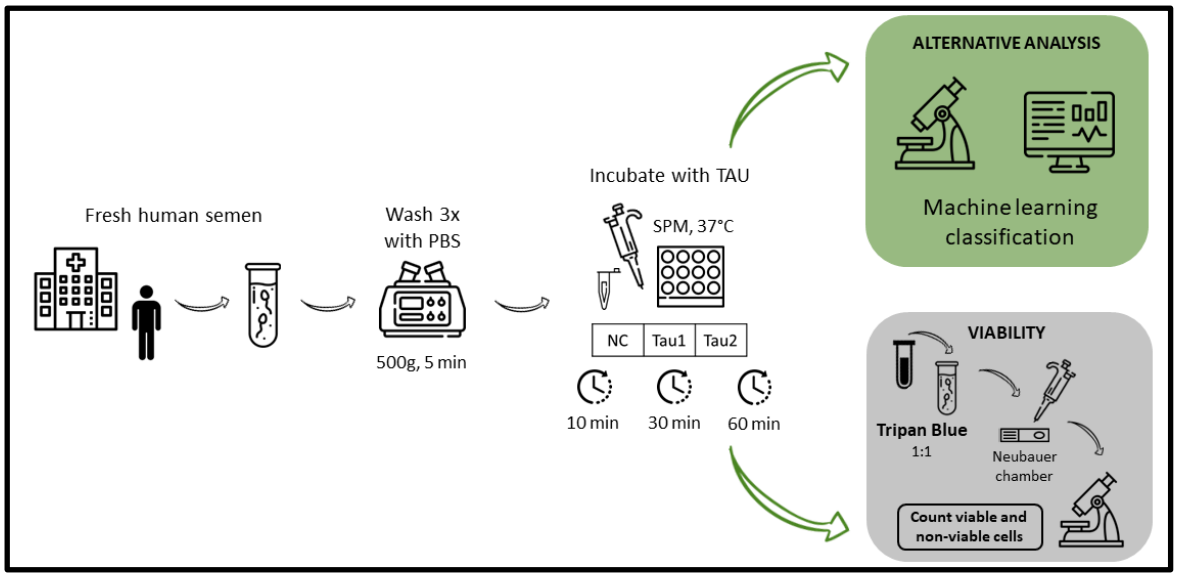

Figure 9. *Experimental procedure performed in human spermatozoa, including sample preparation, viability assessment and analysis performed after incubation with TAU.*

2.1. Sample processing

2.1.1. Fresh bovine samples

Fresh bovine semen samples were obtained from LusoGenes, Lda (Aveiro, Portugal). Spermatozoa were then washed 3 times and isolated from seminal plasma by centrifugation (500g for 5 min at 21ºC), using pre-heated phosphate buffered saline (PBS). A first sample analysis was performed to assess sperm motility and determine concentration using Sperm Class Analyzer CASA System with SCA® v6.6.18 software (Microptic S L, Barcelona, Spain). Spermatozoa were then re-suspended in pre-heated sperm preparation medium (SPM) (Origio, Copenhagen, Denmark) at the defined final concentration.

2.1.2. Cryopreserved bovine samples

Cryopreserved bovine semen samples were purchased in frozen straws from ABC Genetix s.r.l. (Milan, Italy) and stored in liquid nitrogen until the experiment. The straws contained 250 µL of volume and a concentration of 30 x10^6 sperm/mL. The procedures

were performed in sterile conditions. At the beginning of the experiment, the straws were retrieved from the liquid nitrogen container and left in the oven in a water bath for 1 min to thaw, at 37 ºC. Spermatozoa were washed 3 times and isolated from seminal plasma by centrifugation (500g for 5 min at 21ºC) using pre-heated PBS. The pellet was then re-suspended in pre-heated SPM (Origio, Copenhagen, Denmark).

2.1.3. Fresh human samples

Fresh human normozoospermic samples were donated by the Frederico II University Hospital (Naples, Italy). The procedures were performed in sterile conditions. Spermatozoa were washed three times and isolated from seminal plasma by centrifugation (500g for 5 min at 21ºC) using pre-heated PBS. The pellet was then re-suspended in pre-heated SPM (Origio, Copenhagen, Denmark).

2.2. PP inhibitors assays

CAN (ALX-270-063-M025) and CYP (ML-PR100-0050) were purchased from Enzo Life Sciences Inc (Farmingdale, New York, USA) and TAU (BV-B1237-10) from Biovision Inc (Waltham, Massachusetts, EUA). The inhibitors were reconstituted in solution according to the instructions of the manufacturer. CAN and TAU were reconstituted in DMSO both at a final concentration of 100 µM, whereas CYP was dissolved in ethanol 100% in a final concentration of 25 mg/mL (60mM).

2.2.1. PP inhibitor assays in bovine spermatozoa

For the PP inhibitors assays, 7.5 x10^6 bovine spermatozoa were used per condition in a final medium volume of 100µL. Spermatozoa were incubated for 10, 30 and 60 min at 37ºC with distinct concentrations of the three inhibitors, according to **Table 5**. These concentrations were chosen attending to each PP inhibitor IC_{50}. Two control conditions were performed, the NC1 (negative control; without inhibitors), which consisted of

spermatozoa incubated only in SPM medium and NC2 (negative control; ethanol 100%), consisting of spermatozoa in medium and ethanol 100%.

Table 5. *Characterization of the experimental conditions, including the inhibitor and respective concentration, as well as NC1 and NC2 constitution.* ***Abbreviations:*** *PP: protein phosphatase; Can: cantharidin; Tau: tautomycin; Cyp: cypermethrin; NC: negative control.*

Condition characterization		PP inhibited
NC1	-	-
NC2	Ethanol 100%	-
Can1	Cantharidin at 100 nM	PP2A
Can2	Cantharidin at 1000 nM	PP2A and PP1
Tau1	Tautomycin at 10 nM	PP1
Tau2	Tautomycin at 100 nM	PP1 and PP2A
Cyp1	Cypermethrin at 0.1 nM	PP2B
Cyp2	Cypermethrin at 1 nM	PP2B

2.2.2. Tautomycin assay in human spermatozoa

For the TAU assay, 4.0 x10^6 human spermatozoa were used per condition in a final medium volume of 50µL. Spermatozoa were incubated for 10, 30 and 60 min at 37ºC with two distinct concentrations of TAU (Tau1: 10nM and Tau2: 100nM). The NC1 consisted in spermatozoa incubated only in SPM medium.

2.3. Viability assay

2.3.1. CellTiter 96® AQueous Non-Radioactive Cell Proliferation Assay

Viability was evaluated in fresh bovine spermatozoa using the CellTiter 96® AQueous Non-Radioactive Cell Proliferation Assay (Promega, Madison, Wisconsin, USA) according to the manufacturer's guidelines. In brief, 20 µL of CellTiter 96® were added to 7.5 x10^6 spermatozoa in a final volume of 100 µL per condition and incubated for 1h at 37

ºC. Absorbance was measured at 490 nm using the Infinite® 200 PRO (TECAN, Genius, Männedorf, Switzerland). The reduction of tetrazolium compounds has previously been used as a reliable and rigorous assessment of spermatozoa viability[141].

2.3.2. Tripan Blue assay

Viability was assessed in human spermatozoa with the Tripan Blue Solution 0.4% (Thermo Fisher Scientific Inc, Massachusetts, USA). After 10 and 60 min of incubation with TAU, 10µL of spermatozoa were incubated with 10µL of the Tripan Blue solution. Spermatozoa were observed at the microscope in a Neubauer chamber and both viable and non-viable cells were counted. The proportion of viable cells was then calculated.

2.4. Sperm motility evaluation

2.4.1. CASA System with SCA® v6.6.18 software analysis

Bovine sperm motility was assessed using CASA System with SCA® v6.6.18 software (Microptic S L, Barcelona, Spain) for all conditions after 10, 30 and 60 min of incubation. The samples (2 µl) were loaded in pre-heated individual chambers of Leja Standrat Count 8 chamber slide 20 µm depth (Leja Products B. V., The Netherlands). The analysis was performed five times (n=5) according to the sixth edition of WHO guidelines[113]. The percentage of each sperm motility class was determined: immotile, NP, SP and RP. Additionally, the following sperm motility parameters were assessed for each motility class: VCL (µm/s), VAP (µm/s), VSL (µm/s), LIN (%), STR (%), WOB (%), ALH (µm) and BCF (Hz).

2.4.2. Alternative analysis

Sperm motility was assessed using an Olympus IX81 microscope incorporated with an additional lateral camera (ORCA-flash 4.0) for all conditions after 10, 30 and 60 min of incubation. At each timepoint, 10 µL of the condition was diluted in 190 µL of medium and

analysed in glass capillaries with 200 x 2000 µm (HeightxWidth)**.** Samples were observed with the 20x objective of the microscope and several 5-second videos were recorded for each condition and time point. The procedure was done in triplicate for bovine samples (n=3) and duplicate for human spermatozoa (n=2). Machine learning-based analysis was then performed on the videos to classify spermatozoa in immotile, NP, SP, RP, hyperactivated (HYP) and circular trajectory (CIRC). Besides, kinematic parameters of spermatozoa motion were retrieved (VCL (µm/s), VAP (µm/s), VSL (µm/s), LIN (%), STR (%), WOB (%), ALH (µm), BCF (Hz), MAD (degrees) and DNC (degrees).

2.5. Statistical Analysis

All values were expressed as mean ± standard deviation (SD). Statistical analysis was performed using GraphPad Prism (version 8.0.1). Statistical significance was evaluated using a non-parametric approach, the Mann-Whitney test *($p < 0.05$)* or the Kruskall-Wallis *($p < 0.05$),* followed by Dunn's correction of the p-values.

3. Results

3.1. Bovine spermatozoa remain viable after incubation with PP inhibitors

Bovine spermatozoa were incubated with different concentrations of the inhibitors (**Table 5**) and cell viability was assessed in each condition and timepoint, using the CellTiter 96® AQueous Non-Radioactive Cell Proliferation Assay (Promega, Madison, Wisconsin, USA) according to the manufacturer's guidelines. The results are expressed as mean of three experiments (n=3) after normalization to the NC1. **Figure 10** shows the results of this assay for each inhibitor. Non-parametric Mann-Whitney tests were performed ($p<0.05$) between each condition and the NC1 (or NC2) for each timepoint. There were no statistically significant differences between the inhibitor treatments and the NC1, represented by the line drawn at 100%. There was also no significant difference between CYP conditions and NC2.

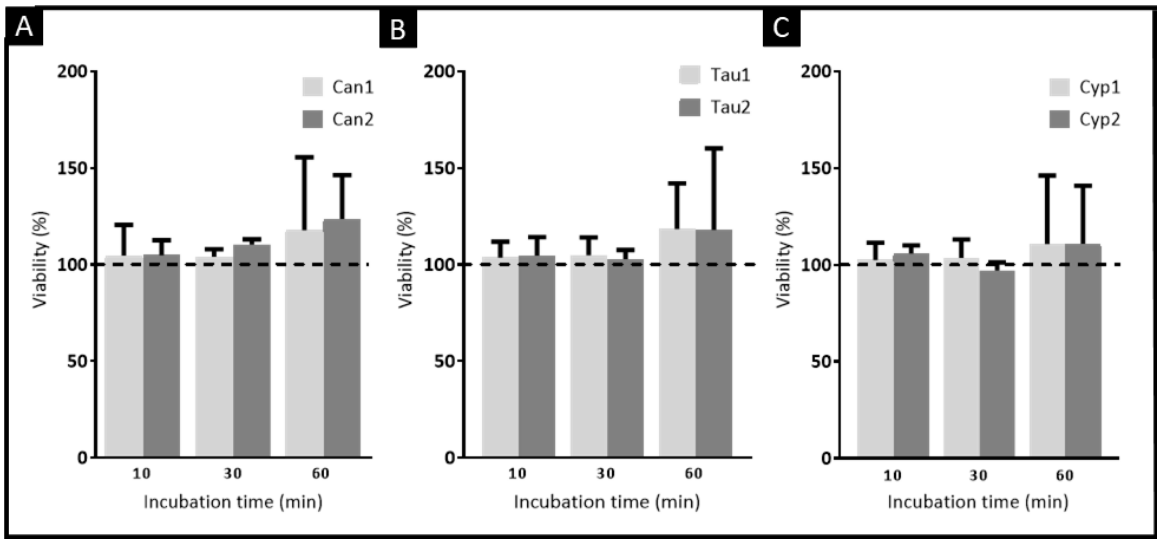

Figure 10. *Impact of PP inhibitors on sperm viability (%). 7.5 x10^6 spermatozoa were incubated with 100 or 1000 nM of CAN (Can1 and Can2, respectively), 10 or 100 of TAU (Tau1 and Tau2, respectively), and 0.1 and 1 nM of CYP (Cyp1 and Cyp2, respectively).* ***A.*** *CAN;* ***B.****TAU;* ***C.*** *CYP. Each bar represents the mean of three experiments (n=3) after normalization to the NC1 (or NC2) of the respective timepoint, represented by the line drawn at 100%.*

3.2. Incubation with PP inhibitors impacts bovine spermatozoa motility parameters

Bovine spermatozoa were incubated with different concentrations of the PP inhibitors (**Table 5**) and motility was assessed after 10, 30 and 60 min of incubation. Two analyses were performed: the Sperm Class Analyzer CASA System (Microptic S L, Barcelona, Spain) (CASA system analysis) and a machine learning-based analysis (alternative analysis). For each experimental condition the percentage of spermatozoa in each of the four motility classes was determined with the CASA system analysis (immotile, non-progressive (NP), slowly progressive (SP) and rapidly progressive (RP))[113]. The alternative analysis also allowed the assessment of the percentage of hyperactivated (HYP) and circular motion (CIRC) spermatozoa.

The motility results are shown as mean of five experiments (n=5) for the CASA analysis and 3 experiments (n=3) for the alternative analysis, after normalization to the NC1 (or NC2) at each timepoint, represented by a line drawn at 1.0 in all Figures. Non-parametric Kruskall-Wallis tests were performed ($p<0.05$) between the inhibitor conditions and the NC1 (or NC2) for each timepoint of analysis, followed by Dunn's correction of the *p-values.* In Supplementary Material can be found representative videos retrieved with both analysis for each condition of the experiment.

3.2.1. Cantharidin effects on bovine spermatozoa motility

Following incubation with both concentrations of CAN, with the CASA analysis, a tendency of increased immotile spermatozoa in all timepoints was observed, except for Can1 after 60 min of incubation (**Figure 11A**). Concerning NP and SP motility, a tendency of increase was observed for most conditions, particularly after 30 and 60 min of incubation (**Figure 11B** and **Figure 11C**). RP motility was the most affected, since it was decreased in all conditions and times of incubation, being statistically decreased with Can2 after 60 min of incubation (**Figure 11D**).

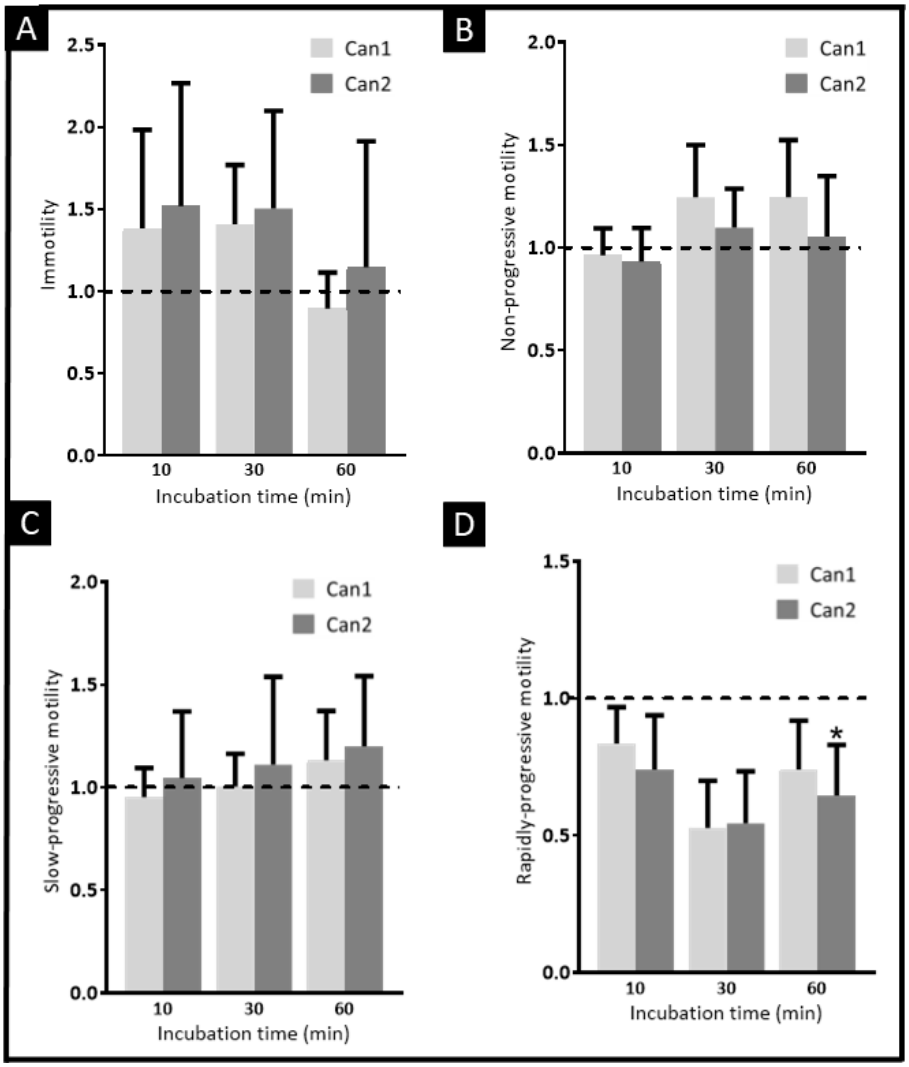

Figure 11. *Impact of CAN incubation in motility parameters of bovine spermatozoa. 7.5 x10^6 spermatozoa were incubated with 100 or 1000 nM (Can1 and Can2, respectively) and motility parameters were assessed with Sperm Class Analyzer CASA System, after 10, 30 and 60 min.* ***A.*** *Immotility;* ***B.*** *Non-progressive (NP) motility;* ***C.*** *Slow progressive (SP) motility;* ***D.*** *Rapidly progressive (RP) motility. Each bar represents the mean of five experiments (n=5), after normalization to the NC1 of the respective timepoint, represented as a line drawn at 1.0. Statistically significant findings are indicated with (*) representing a p-value inferior to 0.05*

Concerning the alternative analysis, statistically significant different differences were not found for any parameter. Immotile spermatozoa were also increased, except Can1 after 10 and 60 min of incubation (**Figure 12A**). Contrarily, RP cells were increased with both concentrations after 60 min of incubation (**Figure 12B**). Spermatozoa with both hyperactivated and circular motility were increased in all conditions when compared to the NC1 (**Figure 12C** and **Figure 12D**).

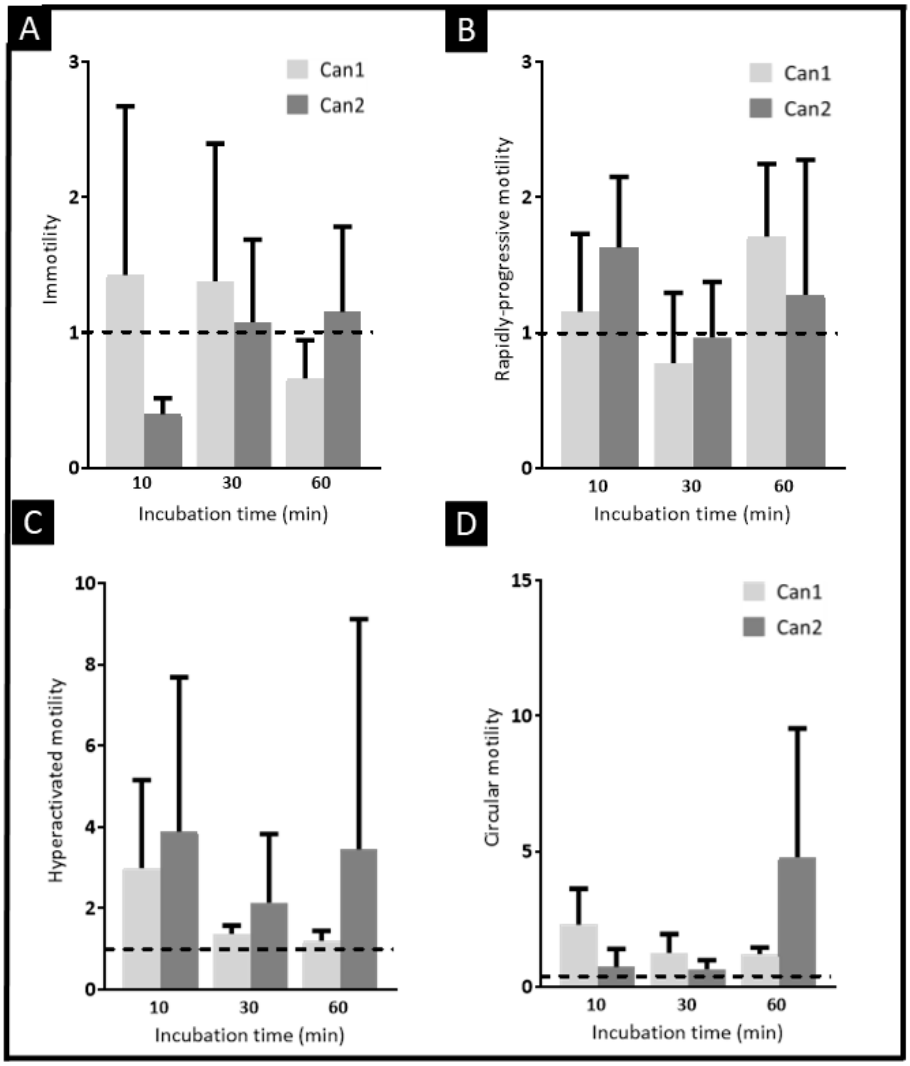

***Figure 12**. Impact of CAN incubation in motility parameters of bovine spermatozoa. 7.5 x10^6 spermatozoa were incubated with 100 or 1000 nM (Can1 and Can2, respectively) and motility parameters were assessed with the machine learning-based analysis (alternative analysis), after 10, 30 and 60 min. **A.** Immotility; **B.** RP motility **C.** Hyperactivated motility; **D.** Circular motility. Each bar represents the mean of three experiments (n=3), after normalization to the NC1 of the respective timepoint, represented as a line drawn at 1.0.*

3.2.2. Tautomycin effect on bovine spermatozoa motility

TAU incubation caused a non-statistically significant increase in immotile spermatozoa in all conditions and times of exposure (**Figure 13A**). NP motility was increased after 30 and 60 min of incubation (**Figure 13B**). Regarding RP motility, it was significantly decreased in Tau2 after 10 and 30 min of incubation and Tau1 after 60 (**Figure 13D**).

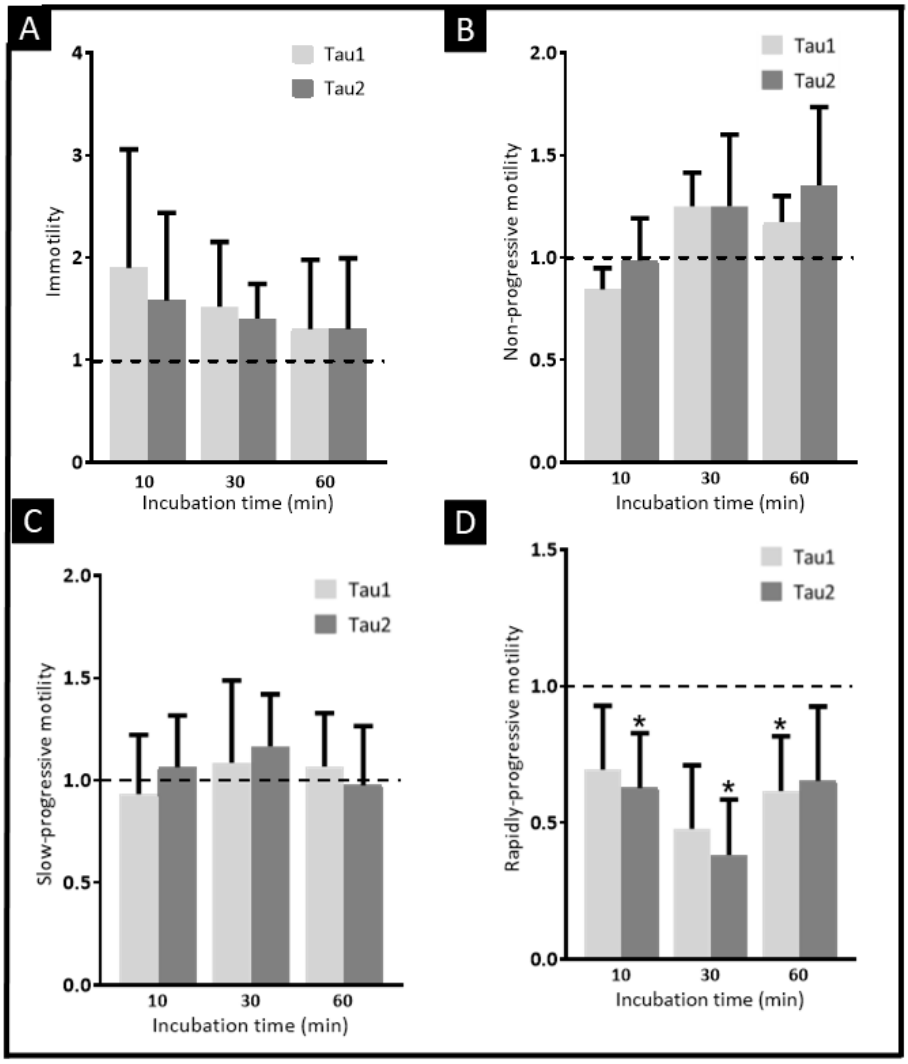

Figure 13. *Impact of TAU incubation in motility parameters of bovine spermatozoa. 7.5 x 10^6 spermatozoa were incubated with 10 or 100 nM (Tau1 and Tau2, respectively) and motility parameters were assessed with Sperm Class Analyzer CASA System, after 10, 30 and 60 min.* ***A.*** *Immotility;* ***B.*** *NP motility;* ***C.*** *SP motility;* ***D.*** *RP motility. Each bar represents the mean of five experiments (n=5), after normalization to the NC1 of the respective timepoint, represented as a line drawn at 1.0. Statistically significant findings are indicated with (*) representing a p-value inferior to 0.05.*

The alternative analysis showed a similar non-statistically significant increase in immotile spermatozoa (**Figure 14A**), while regarding RP cells, they were found increased in Tau1 after 10 and 60 min of incubation (**Figure 14B**). Hyperactivated motility was increased in Tau1 at 10 and 60 min, as well as Tau2 at 60 min. Circular motion was also increased across all conditions and timepoints, except Tau2 after 30 min of incubation (**Figure 14C** and **Figure 14D**).

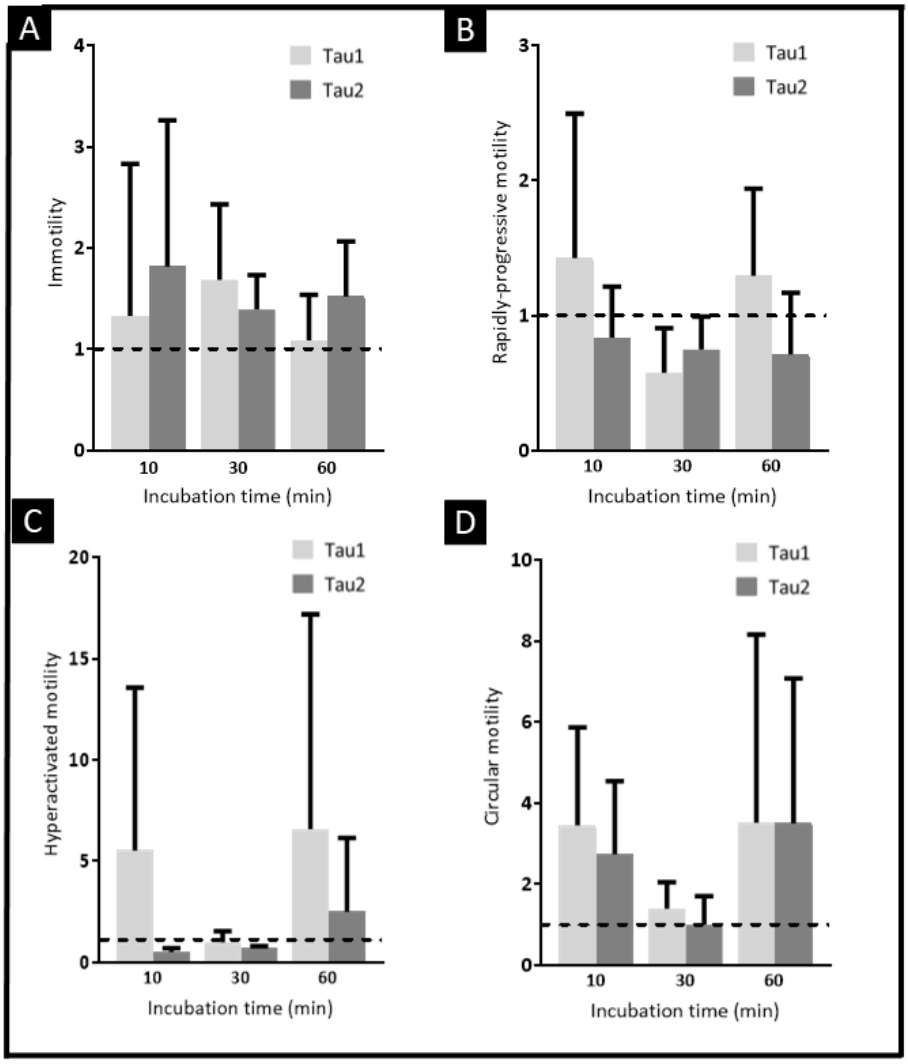

Figure 14. *Impact of TAU incubation in motility parameters of bovine spermatozoa. 7.5 x 10^6 spermatozoa were incubated with 10 or 100 nM (Tau1 and Tau2, respectively) and motility parameters were assessed with machine learning-based analysis (alternative analysis), after 10, 30 and 60 min.* ***A.*** *Immotility;* ***B.*** *RP motility;* ***C.*** *Hyperactivated motility;* ***D.*** *Circular motility. Each bar represents the mean of three experiments (n=3), after normalization to the NC1 of the respective timepoint, represented as a line drawn at 1.0.*

3.2.3. Cypermethrin effect on bovine spermatozoa motility

Immotile spermatozoa were found non-significantly increased with both CYP concentrations at all times of analysis (**Figure 15A**). NP motility was increased across all conditions and timepoints except Cyp1 at 10 min (**Figure 15B**). SP motility was consistently decreased (**Figure 15C**). Concerning RP motility, it was significantly decreased with Cyp1 after 10 and 30 min of incubation, as well as Cyp2 after 30 and 60 min of incubation (**Figure 15D**).

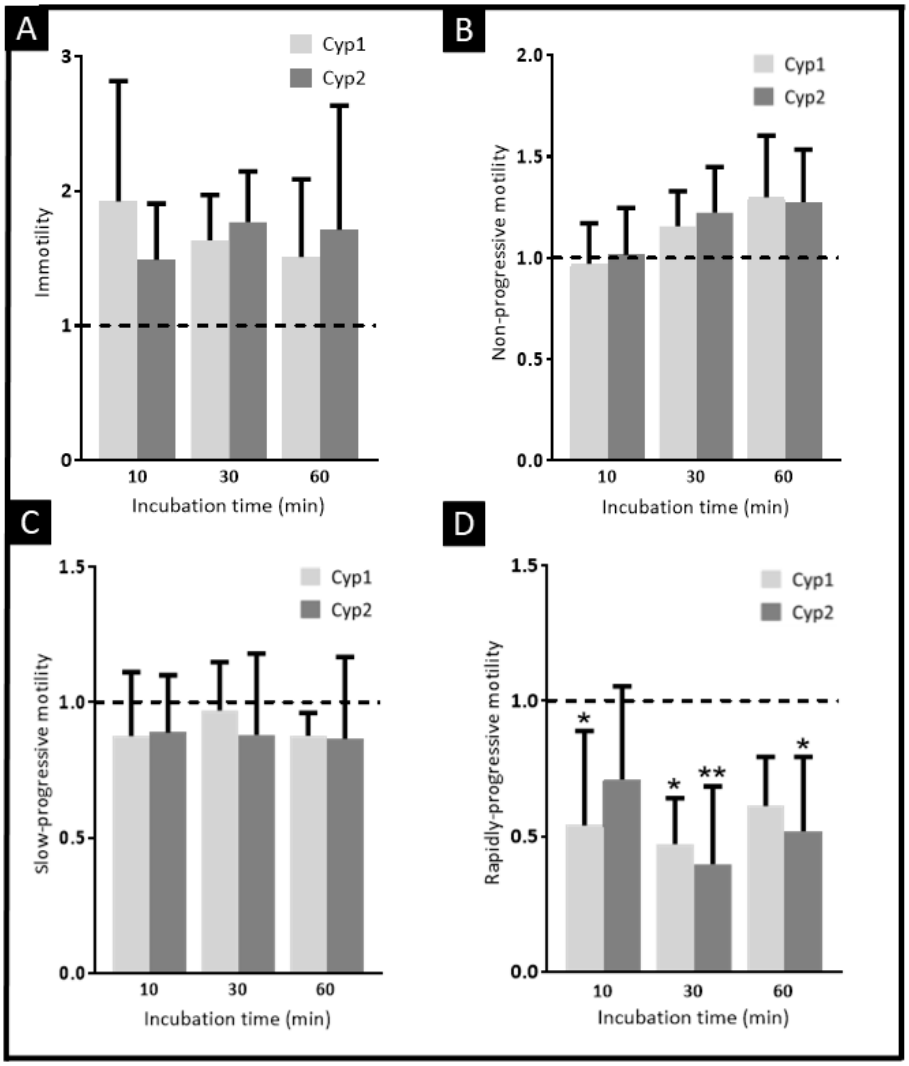

***Figure 15**. Impact of CYP incubation in motility parameters of bovine spermatozoa. 7.5 x 10^6 spermatozoa were incubated with 0.1 or 1 nM (Cyp1 and Cyp2, respectively) and motility parameters were assessed with Sperm Class Analyzer CASA System, after 10, 30 and 60 min **A.** Immotility; **B.** NP motility; **C.** SP motility; **D.** RP motility. Each bar represents the mean of five experiments (n=5), after normalization to the NC1 of the respective timepoint, represented as a line drawn at 1.0. Statistically significant findings are indicated with (*) or (**) if the p-value is inferior to 0.05 and 0.01, respectively.*

The alternative analysis showed a non-statistically significant increase in immotile spermatozoa in Cyp2 at all timepoints and in Cyp1 after 30 min of incubation (**Figure 16A**). RP cells were increased in both conditions after 10 and 60 min of incubation (**Figure 16B**). Hyperactivated and circular motility were increased in all conditions and timepoints (**Figure 16C** and **Figure 16D**).

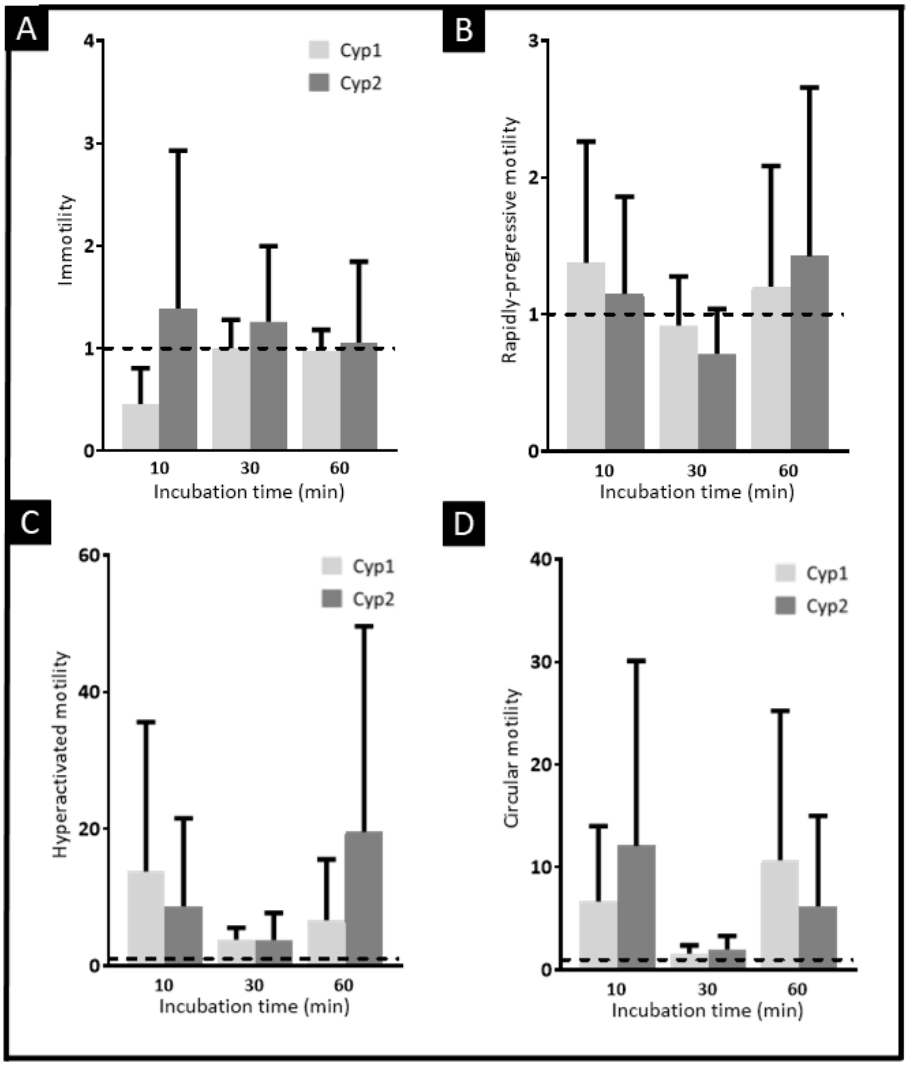

Figure 16. *Impact of CYP incubation in motility parameters of bovine spermatozoa. 7.5 x 10^6 spermatozoa were incubated with 0.1 or 1 nM (Cyp1 and Cyp2, respectively) and motility parameters were assessed with machine learning-based analysis (alternative analysis), after 10, 30 and 60 min.* ***A.*** *Immotility;* ***B.*** *RP motility;* ***C.*** *Hyperactivated motility;* ***D.*** *Circular motility. Each bar represents the mean of three experiments (n=3), after normalization to the NC1 of the respective timepoint, represented as a line drawn at 1.0.*

Comparing CYP conditions with the NC2, the statistically significant differences are shown in **Table 6**.

Table 6. *Statistical comparation between CYP conditions and the NC2 in all motility groups and timepoints (n=5). 7.5 x 10^6 spermatozoa were incubated with 0.1 or 1 nM (Cyp1 and Cyp2, respectively) and motility parameters were assessed with Sperm Class Analyzer CASA System, after 10, 30 and 60 min. Statistically significant findings are highlighted and the p-value for each analysis shown.*

Motility Class	Time	Condition	Statistically Significant	P-value
Immotile	**10**	Cyp1	Yes	*0.0141*
		Cyp2	Ns	*0.0721*

	30	Cyp1	Ns	*0.0721*
		Cyp2	Yes	*0.0141*
	60	Cyp1	Yes	*0.0721*
		Cyp2	Ns	*0.2686*
NP	**10**	Cyp1	Ns	*>0,9999*
		Cyp2	Ns	*0.8491*
	30	Cyp1	Ns	*0.2686*
		Cyp2	Ns	*0.0721*
	60	Cyp1	Ns	*>0,9999*
		Cyp2	Ns	*0.9694*
SP	**10**	Cyp1	Ns	*>0,9999*
		Cyp2	Ns	*0.0918*
	30	Cyp1	Ns	*0.1448*
		Cyp2	Ns	*0.1448*
	60	Cyp1	Ns	*0.0918*
		Cyp2	Ns	*0.2205*
RP	**10**	Cyp1	Ns	*0.2686*
		Cyp2	Ns	*0.7380*
	30	Cyp1	Ns	*0.0562*
		Cyp2	Yes	*0.0189*
	60	Cyp1	Ns	*0.5444*
		Cyp2	Ns	*0.3888*

Comparing the NC1 with the NC2 (**Figure 17**), the only statistically significant difference is a decrease in RP cells after 30 min of incubation (p=0.0286), which suggests that ethanol is generally not affecting the results.

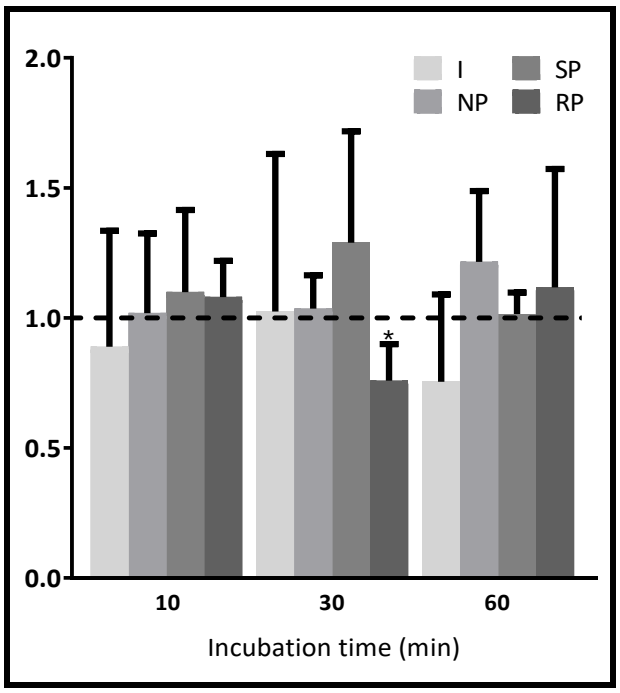

Figure 17. *Differences between the negative controls. 7.5 x 10^6 spermatozoa were incubated with only SPM and ethanol 100%, and motility parameters were assessed with Sperm Class Analyzer CASA System, after 10, 30 and 60 min. Each bar represents the mean of five experiments (n=5), after*

normalization to the NC1 of the respective timepoint, represented as a line drawn at 1.0. Statistically significant findings are indicated with (*) if the p-value is inferior to 0.05.

3.3. Incubation with PP inhibitors impacts bovine spermatozoa kinematic parameters

The kinematic parameters evaluated by the CASA system analysis were VCL, VAP, VSL, LIN, STR, WOB, ALH and BCF. VCL, BCF and ALH are indicators of sperm vigour, whereas VSL, VAP, STR and LIN are related to spermatozoa progression and trajectory. The alternative analysis also retrieved information regarding MAD and DNC. For each condition and timepoint all parameters were assessed in the different sperm motility classes: motile, NP, SP, RP, HYP and CIRC. The motile group is constituted by NP, SP and RP. Non-parametric Kruskall-Wallis tests were performed ($p<0.05$) between the inhibitor conditions and the NC1 (or NC2) for each timepoint, followed by Dunn's correction of the *p-values.*

3.3.1. Effects of cantharidin in the kinematic parameters of spermatozoa

Regarding the CASA system analysis, incubation with CAN resulted in a general decrease in RP spermatozoa's VCL, however only incubation with Can2 for 10 min represented a statistically significant decrease. Regarding both VAP and VSL of RP spermatozoa, Can2 caused a significant decrease after 10 and 60 min of incubation, while Can1 induced a decrease after 60 min. LIN, STR and WOB percentage was decreased in RP spermatozoa after 10 and 60 min of Can2 incubation. ALH and BCF did not present statistically significant alterations following incubation with CAN. Concerning ALH of RP cells, it presents a tendency of increase comparing to the NC1 in all conditions and times of incubations, while BCF was generally decreased (**Figure 18**).

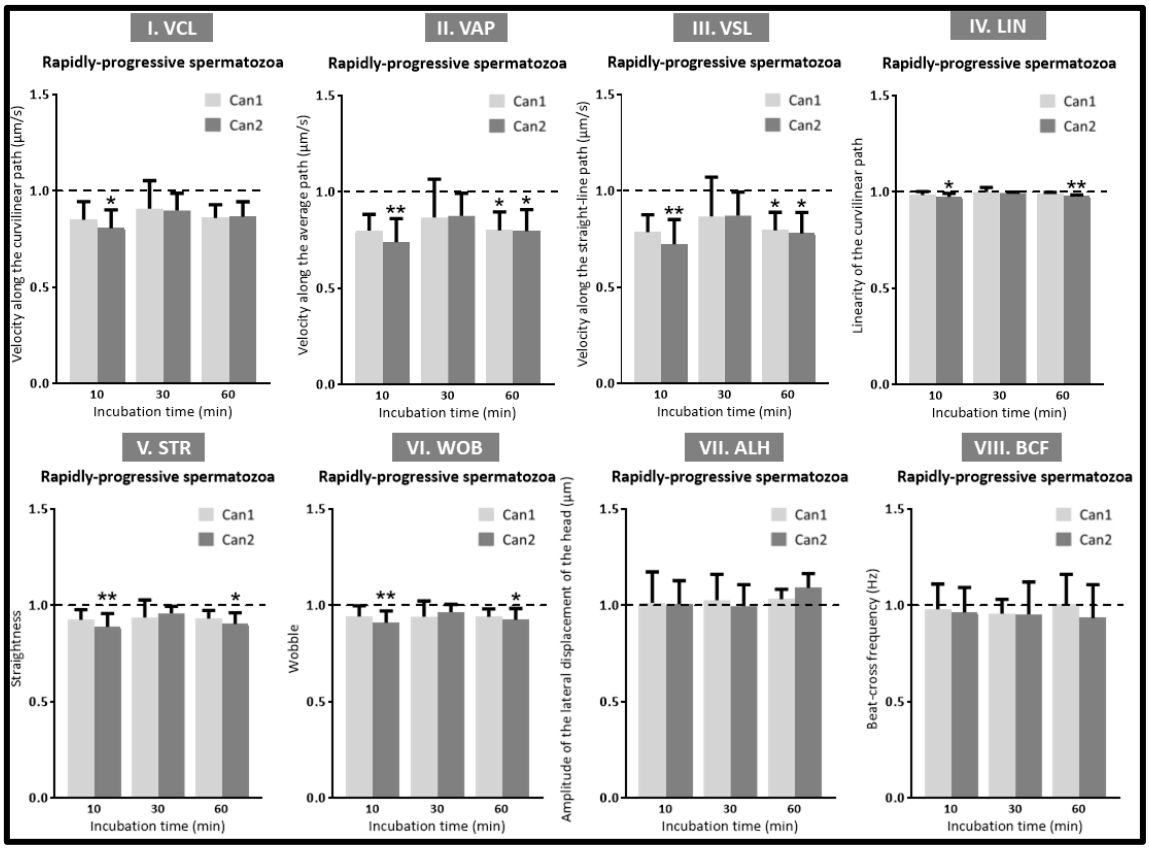

Figure 18. *Impact of CAN incubation in RP bovine spermatozoa. 7.5 x 10^6 spermatozoa were incubated with 100 or 1000 nM (Can1 and Can2, respectively) and kinematic parameters were assessed with Sperm Class Analyzer CASA System, after 10, 30 and, 60 min.* ***I.*** *Velocity along the curvilinear path (VCL);* ***II.*** *Velocity along the average path (VAP);* ***III.*** *Velocity along the straight-line path (VSL);* ***IV.*** *Linearity of the curvilinear path (LIN);* ***V.*** *Straightness (STR);* ***VI****. Wobble (WOB);* ***VII*** *Amplitude of the lateral displacement of the head (ALH);* ***VIII.*** *Beat-cross frequency (BCF). Each bar represents the mean of four experiments (n=5), after normalization to the NC1 of the respective timepoint, represented as a line drawn at 1.0. Statistically significant findings are indicated with (*) or (**) if the p-value is inferior to 0.05 or 0.01, respectively.*

The results of the alternative analysis following incubation with CAN were not statistical significantly different. The results for MAD and DNC are shown in **Figure 19A** and **Figure 19B**, respectively, since those parameters were not retrieved from the CASA analysis. The remaining parameters are shown in **Supplementary Table 1**, available at Supplementary Material.

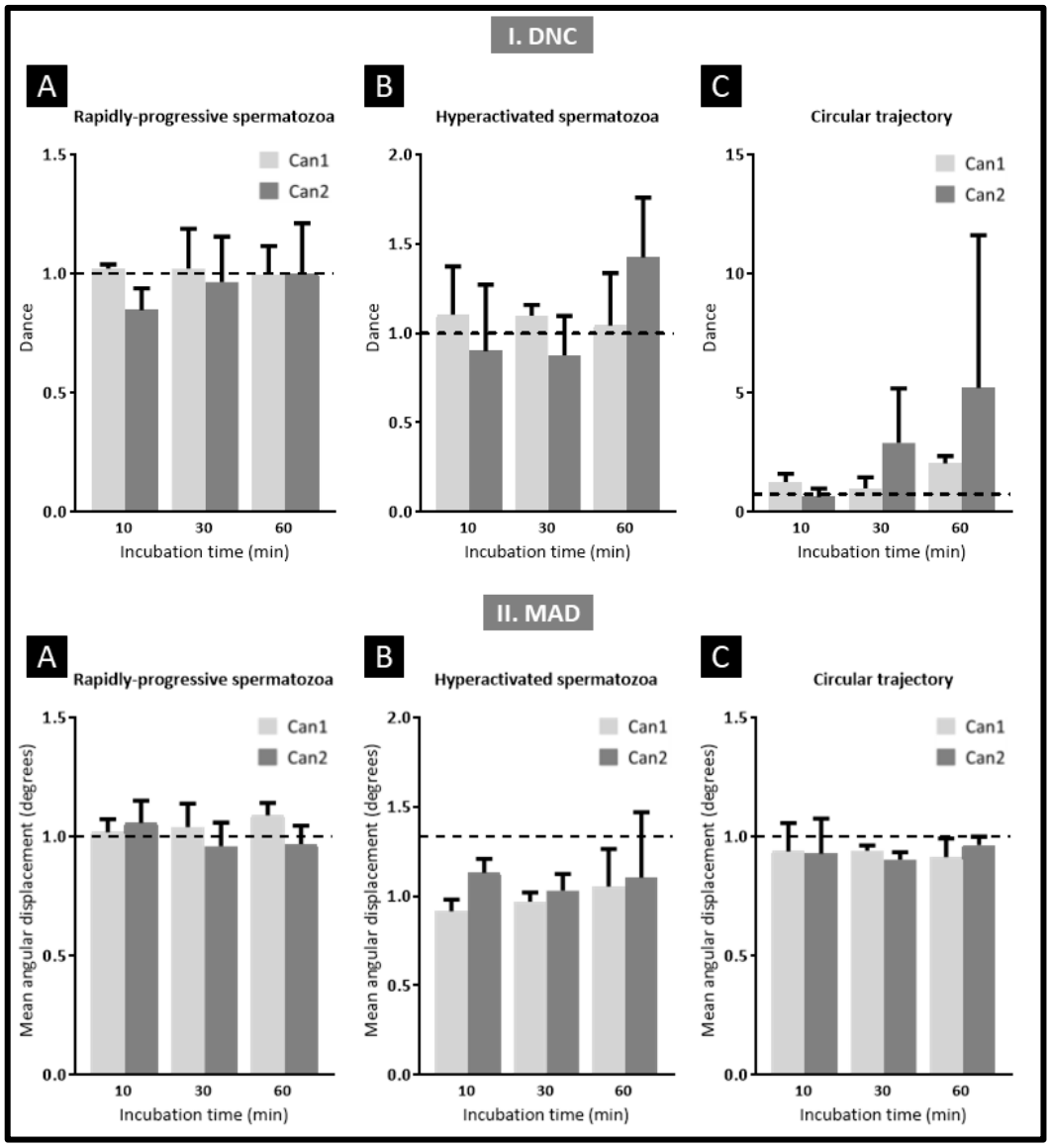

Figure 19. *Impact of CAN incubation in bovine spermatozoa. 7.5 x 10^6 spermatozoa were incubated with 100 or 1000 nM (Can1 and Can2, respectively) and motility parameters were assessed with the machine learning-based analysis (alternative analysis), after 10, 30 and 60 min.* ***I.*** *Dance (DNC):* ***A.*** *RP spermatozoa;* ***B.*** *Hyperactivated spermatozoa;* ***C.*** *Circular trajectory.* ***X.*** *Mean angular displacement (MAD):* ***A****. RP spermatozoa;* ***B.*** *Hyperactivated spermatozoa;* ***C.*** *Circular trajectory. Each bar represents the mean of four experiments (n=3), after normalization to the NC1 of the respective timepoint, represented as a line drawn at 1.0.*

3.3.2. Effects of tautomycin in the kinematic parameters of spermatozoa

Regarding the CASA system analysis, incubation with TAU resulted in a statistically significant decrease in motile and SP spermatozoa's VCL in both concentrations, after 30

min of incubation. Considering VAP, it was significantly decreased in motile cells incubated for 10 min with Tau2, and in SP after 30 min, also with Tau2. Motile spermatozoa's VSL was decreased with Tau2 after 10 and 60 min of incubation, while in SP it was after 30 and 60 for the same concentrations, and after 60 min for Tau1. Both LIN and STR were significantly decreased in motile spermatozoa, with Tau1 after 60 min of incubation. Concerning WOB, in motile spermatozoa it was significantly decreased in all conditions and timepoints, except for Tau1 after 10 and 30 min of incubation. Considering SP sperm, WOB was decreased with Tau2 after 30 and 60 min of incubation (**Figure 20**).

ALH and BCF did not present significant differences following incubation with TAU (**Figure 21**). The results of the alternative analysis upon incubation with TAU were not statistically significant. The results for MAD and DNC are shown in **Figure 21**, since those parameters were not retrieved from the CASA analysis. The remaining parameters are shown in **Supplementary Table 2**, available at Supplementary Material.

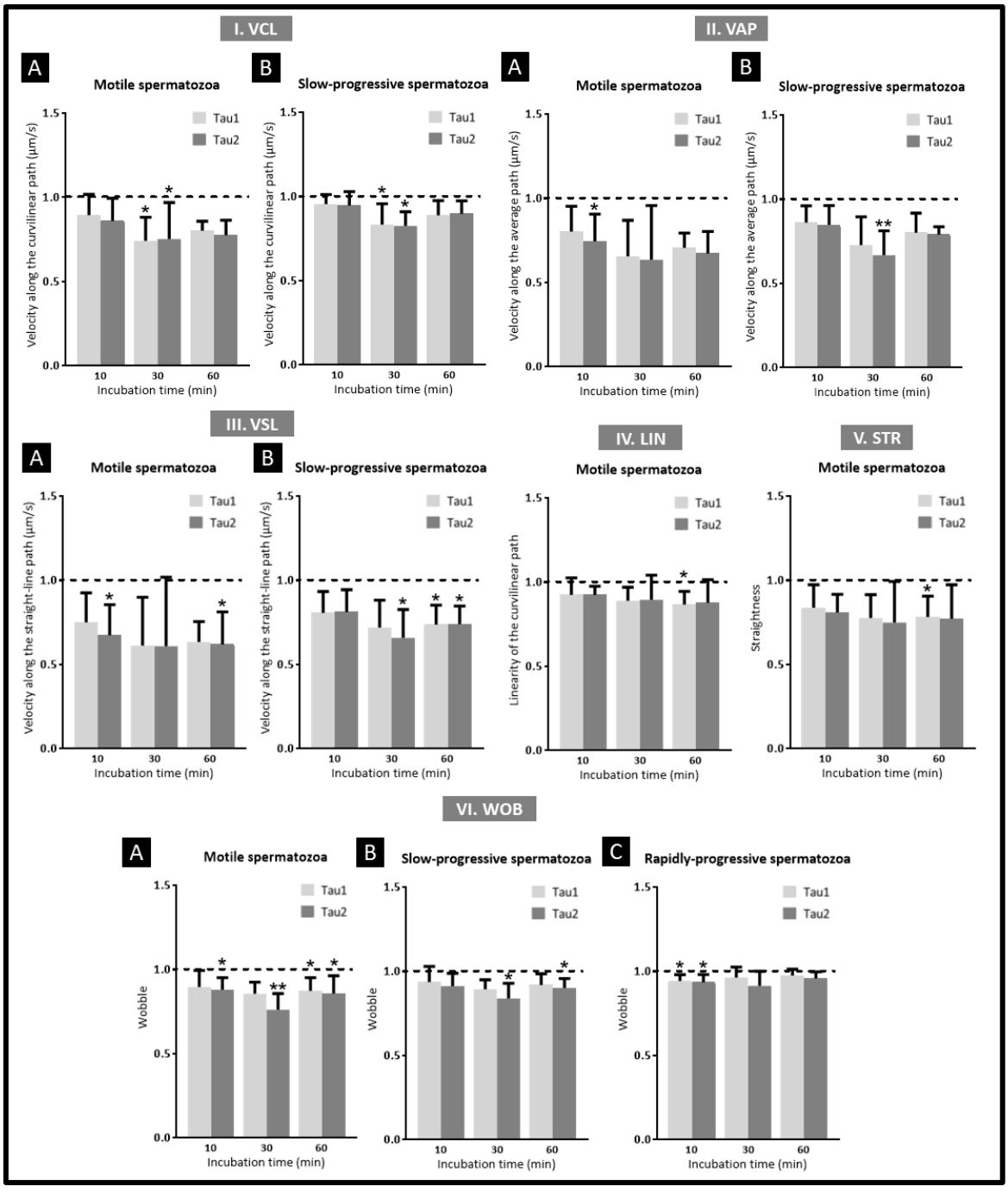

***Figure 20**. Impact of TAU incubation in bovine spermatozoa. 7.5 x10^6 spermatozoa were incubated with 10 or 100 nM (Tau1 and Tau2, respectively) and kinematic parameters were assessed with Sperm Class Analyzer CASA System, after 10, 30 and 60 min. **I.** VCL: **A.** Motile spermatozoa. **B.** SP spermatozoa; **II.** VAP: **A.** Motile spermatozoa. **B**. SP spermatozoa. **III.**VSL: **A**. Motile spermatozoa. **B.** SP spermatozoa **IV.** LIN of motile spermatozoa; **V.** STR of motile spermatozoa; **VI**. WOB: **A.** Motile spermatozoa. **B.** SP spermatozoa. **C.** RP spermatozoa. Each bar represents the mean of four experiments (n=5), after normalization to the NC1 of the respective timepoint, represented as a line*

drawn at 1.0. Statistically significant findings are indicated with (*) or (**) if the p-value is inferior to 0.05 or 0.01, respectively.

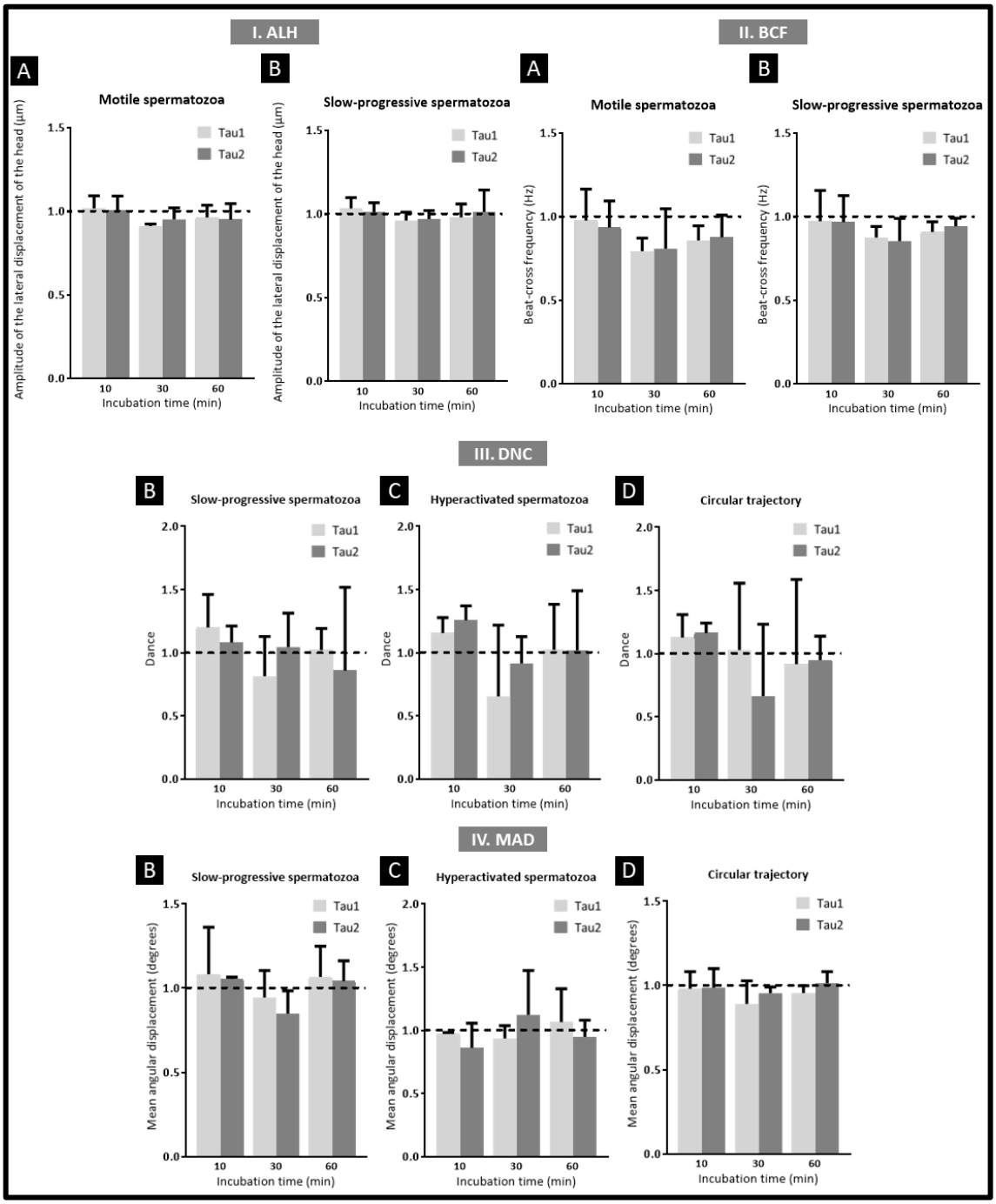

Figure 21. *Impact of TAU incubation in bovine spermatozoa. 7.5 x 10^6 spermatozoa were incubated with 10 or 100 nM (Tau1 and Tau2, respectively) and kinematic parameters were assessed with Sperm Class Analyzer CASA System or machine learning-based analysis (alternative analysis), after 10, 30 and 60 min.* ***I.*** *ALH:* ***A.*** *Motile spermatozoa;* ***B***. *SP spermatozoa.* ***II.*** *BCF:* ***A.*** *Motile spermatozoa;* ***B.*** *SP spermatozoa.* ***III.*** *DNC:* ***B.*** *SP spermatozoa;* ***C.*** *Hyperactivated spermatozoa;* ***D.*** *Circular trajectory.* ***IV.*** *MAD:* ***B.*** *SP spermatozoa;* ***C.*** *Hyperactivated spermatozoa;* ***D.*** *Circular*

trajectory. Each bar represents the mean of three experiments (n=3), after normalization to the NC1 of the respective timepoint, represented as a line drawn at 1.0.

3.3.3. Effects of cypermethrin in the kinematic parameters of spermatozoa

Regarding the CASA system analysis, incubation with CYP resulted in a significant decrease in motile cells VCL with both concentrations (Cyp1 an Cyp2) after all times of analysis. Regarding SP, VCL was significantly decreased with Cyp1 after 30 min of incubation and with both concentrations after 60 min. RP cells VCL was significantly decreased for both concentrations after 10 and 60 min of incubation, as well as Cyp1 after 30. VAP was decreased in motile spermatozoa following incubation with both CYP concentrations after all times of incubation except Cyp2 after 10 min. SP spermatozoa's VAP was significantly decreased with both concentrations after 30 and 60 min of incubation, while in RP it was after 10 and 60 min. This is likewise verified for SP and RP spermatozoa's VSL. Concerning the VSL of motile cells, it was decreased with Cyp1 after 10 and 60 min of incubation and Cyp2 after 30 and 60 (**Figure 22**).

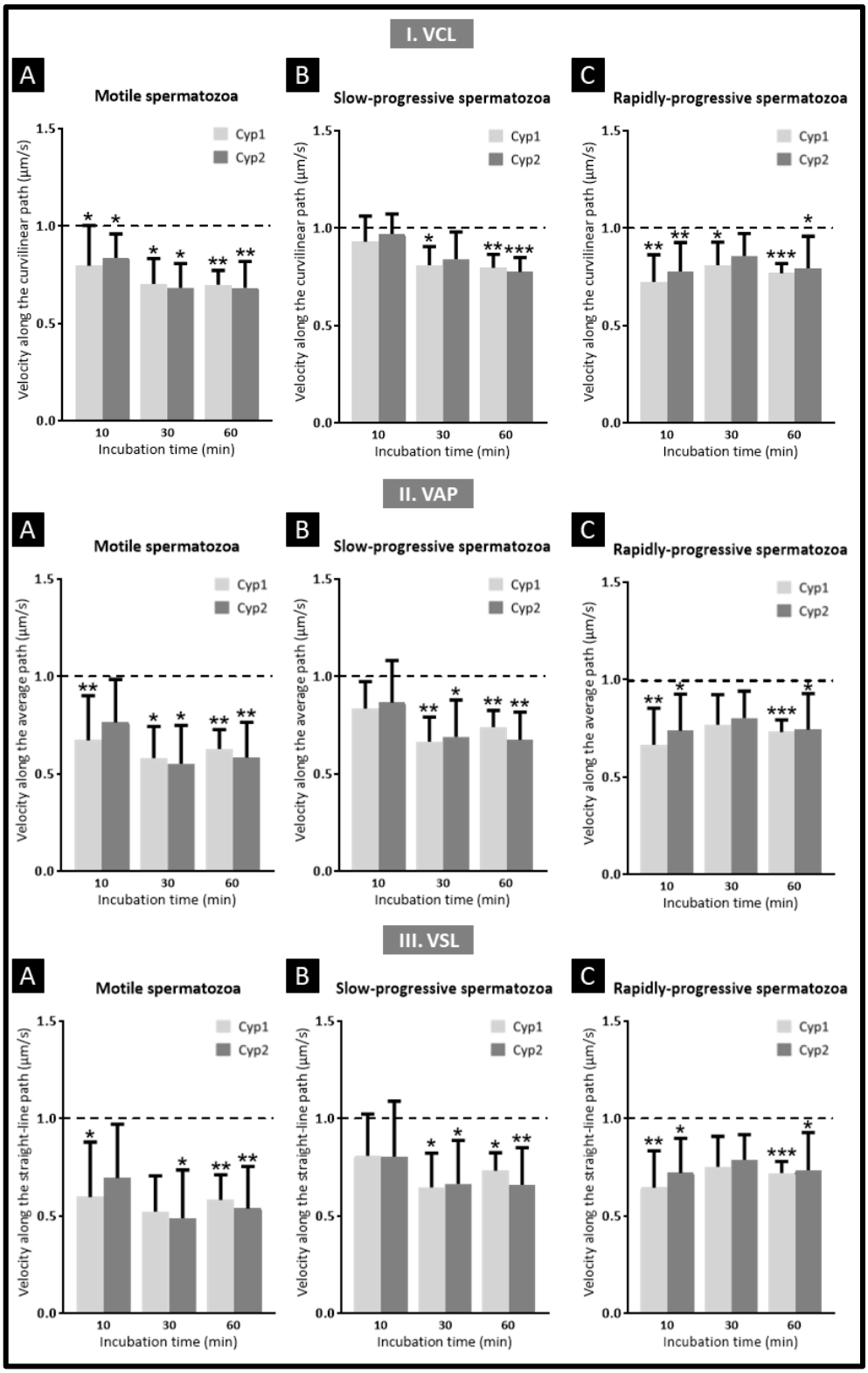

Figure 22. *Impact of CYP incubation in bovine spermatozoa. 7.5 x 10^6 spermatozoa were incubated with 0.1 or 1 nM (Cyp1 and Cyp2, respectively) and kinematic parameters were assessed with Sperm Class Analyzer CASA System, after 10, 30 and 60 min.* ***I.*** *VCL:* ***A.*** *Motile spermatozoa.* ***B.*** *SP spermatozoa.* ***C.*** *RP spermatozoa;* ***II.*** *VAP:* ***A.*** *Motile spermatozoa.* ***B.*** *SP spermatozoa.* ***C.*** *RP spermatozoa;* ***III.*** *VSL* ***A.*** *Motile spermatozoa.* ***B.*** *SP spermatozoa.* ***C.*** *RP spermatozoa. Each bar*

represents the mean of four experiments (n=5), after normalization to the NC1 of the respective timepoint, represented as a line drawn at 1.0. Statistically significant findings are indicated with (*), (**) or (***) if the p-value is inferior to 0.05, 0.01 or 0.001, respectively.

LIN was significantly decreased in RP spermatozoa after 10 min of incubation with Cyp1. STR was significantly decreased in motile spermatozoa following incubation with Cyp1 after 30 and 60 min. WOB motion was significantly decreased in motile spermatozoa with both CYP concentrations across all timepoints, except for Cyp2 after 10 min of incubation and Cyp1 after 60. RP cells WOB was decreased with both CYP concentrations after 30 min of incubation. ALH values of spermatozoa incubated with CYP were not statistically significant. BCF was significantly lower in motile cells for both concentrations 60 min of incubation and for Cyp2 after 30. In SP cells, BCF was significantly decreased with both concentrations after 60 min of incubation (**Figure 23**).

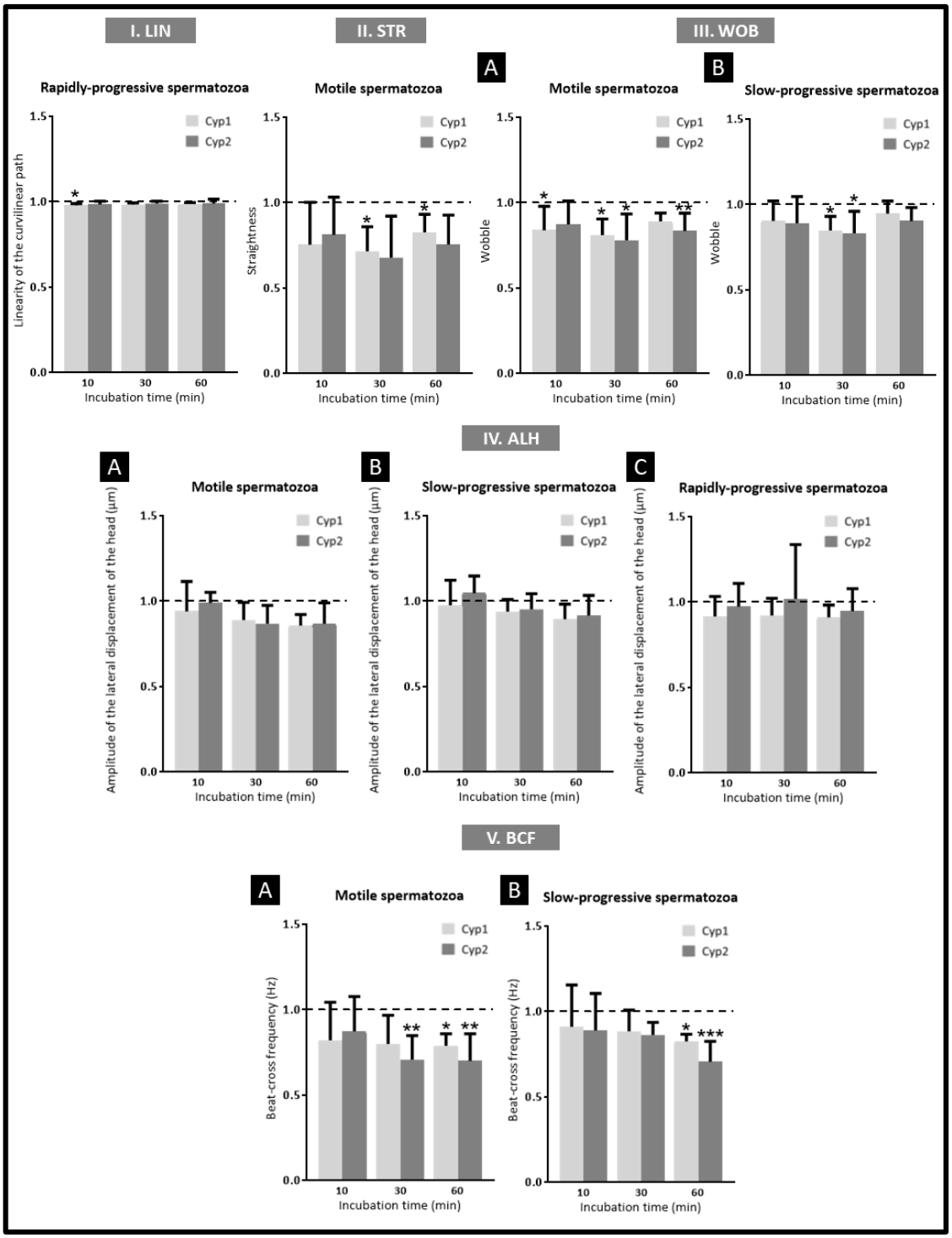

Figure 23. *Impact of CYP incubation in bovine spermatozoa. 7.5 x 10^6 spermatozoa were incubated with 0.1 or 1 nM (Cyp1 and Cyp2, respectively) and kinematic parameters were assessed with Sperm Class Analyzer CASA System or machine learning-based analysis (alternative analysis), after 10, 30 and 60 min.* ***I.*** *LIN path of motile spermatozoa;* ***II.*** *STR of motile spermatozoa;* ***VI****. WOB:* ***A****. Motile spermatozoa.* ***B.*** *SP spermatozoa.* ***III.*** *ALH: A. Motile spermatozoa;* ***B.*** *SP spermatozoa;* ***C.*** *RP spermatozoa* ***VIII.*** *BCF:* ***A****. Motile spermatozoa.* ***B.*** *SP spermatozoa. Each bar represents the mean of four experiments (n=5), after normalization to the NC1 of the respective timepoint, represented*

as a line drawn at 1.0. Statistically significant findings are indicated with (*), (**) or (***) if the p-value is inferior to 0.05, 0.01 or 0.001, respectively.

The results of the alternative analysis following incubation with CYP were not statistically significant. The results for MAD and DNC are shown in **Figure 24** since those parameters were not retrieved from the CASA analysis. The remaining parameters are shown in **Supplementary Table 3**, available at Supplementary Material.

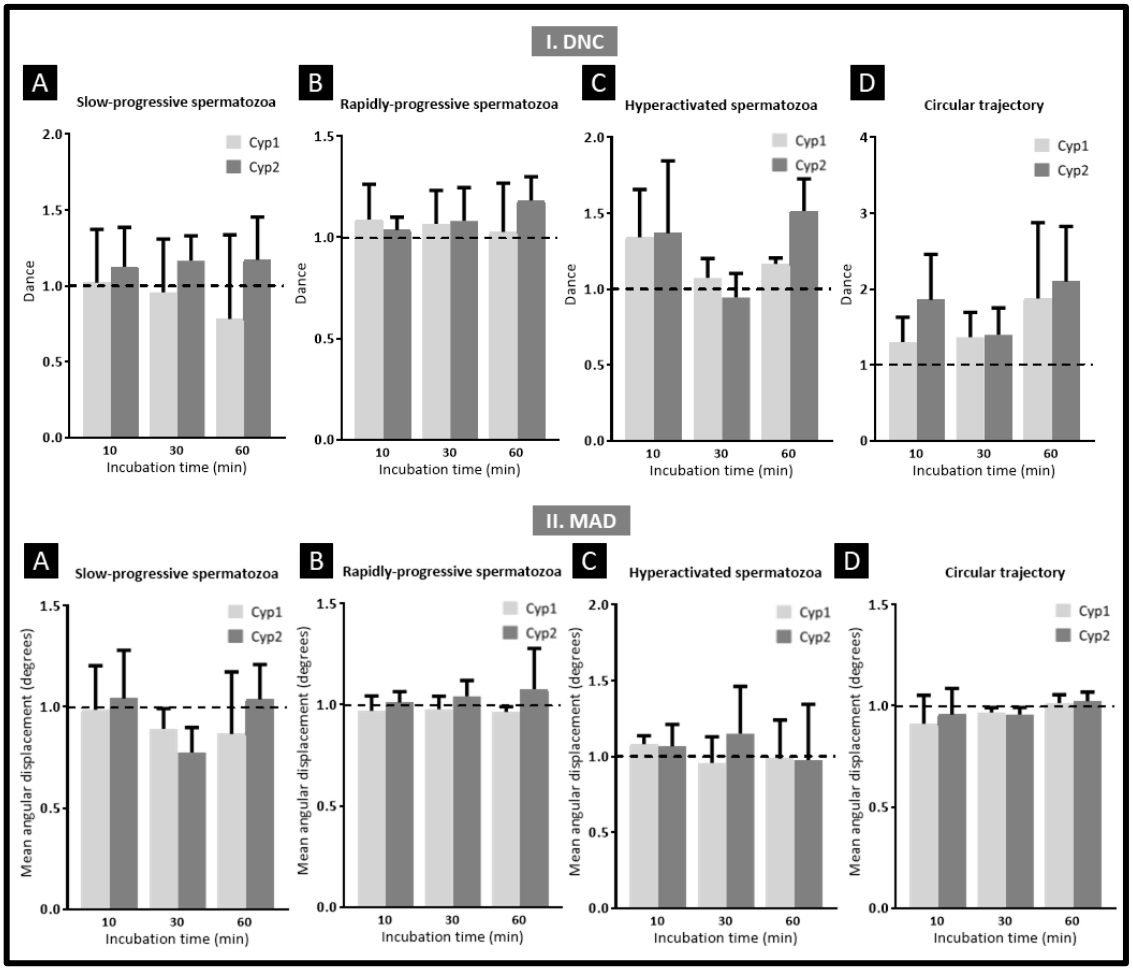

Figure 24. *Impact of CYP incubation in bovine spermatozoa. 7.5 x10^6 spermatozoa were incubated with 0.1 or 1 nM (Cyp1 and Cyp2, respectively) and kinematic parameters were assessed with machine learning-based analysis (alternative analysis), after 10, 30 and 60 min.* ***I.*** *DNC:* ***A.*** *SP spermatozoa;* ***B.*** *RP spermatozoa.* ***C.*** *Hyperactivated spermatozoa;* ***D.*** *Circular trajectory.* ***II.*** *MAD:* ***A.*** *SP spermatozoa;* ***B.*** *RP spermatozoa;* ***C.*** *Hyperactivated spermatozoa;* ***D****. Circular trajectory. Each bar represents the mean of four experiments (n=5), after normalization to the NC1 of the respective timepoint, represented as a line drawn at 1.0.*

3.4. Time-dependent effect of incubation of bovine spermatozoa with PP inhibitors

3.4.1. Impact on motility parameters

Statistically significant findings between times of incubation of each concentration regarding the motility parameters are summarized on **Table 7**, as well as the respective analysis method. The significant results of the multiple comparations between groups are highlighted.

Table 7. *Statistically significant findings regarding the time-dependent effect of the PP inhibitors (CAN, TAU and CYP) on the motility parameters of bovine spermatozoa, upon Kruskall-Wallis analysis. After incubation, kinematic parameters were assessed with Sperm Class Analyzer CASA System or the alternative analysis, after 10, 30 and 60 min. The analysis which showed significant findings on multiple comparations are highlighted.*

Condition	Analysis method	Motility class	*p-value*	Multiple Comparations	*Corrected p-value*
Tau1	CASA Analysis	NP	*0.0111*	10 and 30 min 30 and 60 min	*0.0486* *0.0400*
Tau1	Alternative Analysis	SP	*0.0250*	No	-
Tau2	Alternative Analysis	RP	*0.0500*	No	-
Cyp1	Alternative Analysis	Immotile	*0.0107*	10 and 60 min	*0.0400*

Considering TAU, the results from the CASA analysis showed a time-dependent effect of Tau1 in NP spermatozoa percentage, particularly a difference between NP percentage after 10 and 30 min of incubation, as well as 30 and 60 min (**Figure 25A**). The alternative analysis found a significant difference in the percentage of SP cells, across timepoints in Tau1, while Tau2 significantly decreased RP cells, both without significant differences between specific groups (**Figure 25B** and **Figure 25C**).

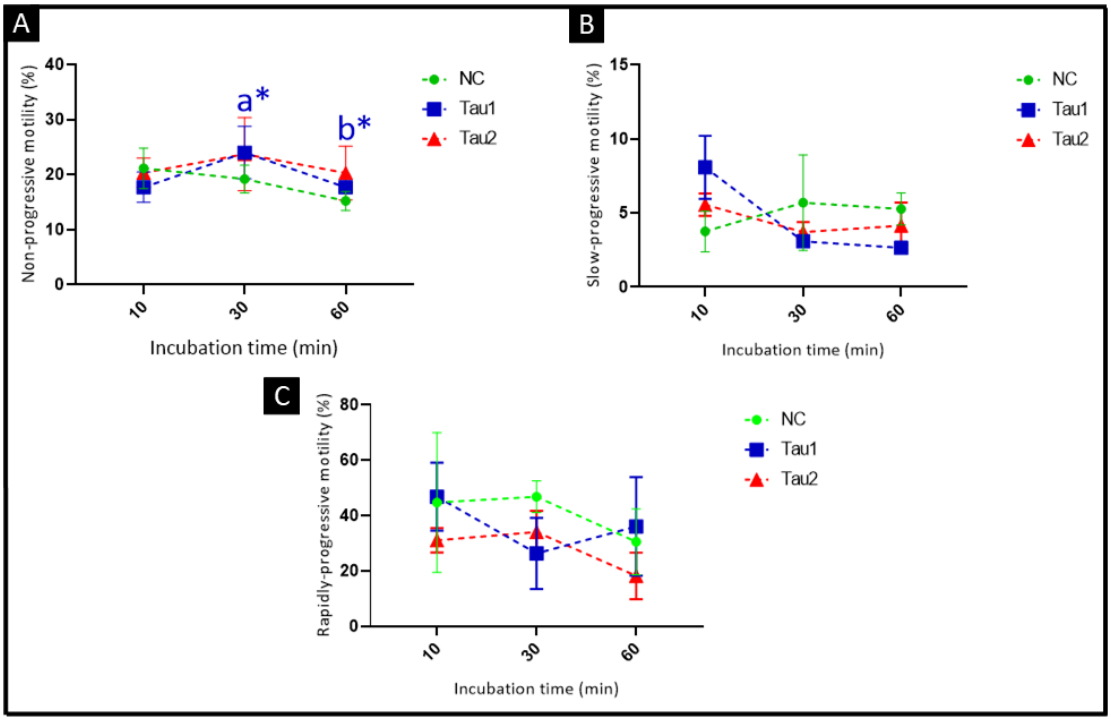

***Figure 25**. Time-dependent effect of TAU incubation in the motility parameters of bovine spermatozoa. 7.5 x 10^6 spermatozoa were incubated with 10 or 100 nM (Tau1 and Tau2, respectively) and motility parameters were assessed after 10, 30 and 60 min. **A.** NP motility, retrieved with Sperm Class Analyzer CASA System analysis; **B**. SP motility, retrieved with the machine learning-based analysis (alternative analysis). **C.** RP motility, retrieved with alternative analysis. Statistically significant findings are indicated with (*) representing a p-value is inferior to 0.05. a* means significant differences between Tau1 after 30 and 10 min of incubation, b* means significant differences between Tau1 after 60 and 30 min of incubation.*

Concerning CYP, the results of the alternative analysis on immotile spermatozoa showed a significant increase throughout time, following incubation with Cyp1, being the difference particularly between 10 and 60 min of incubation (**Figure 26**).

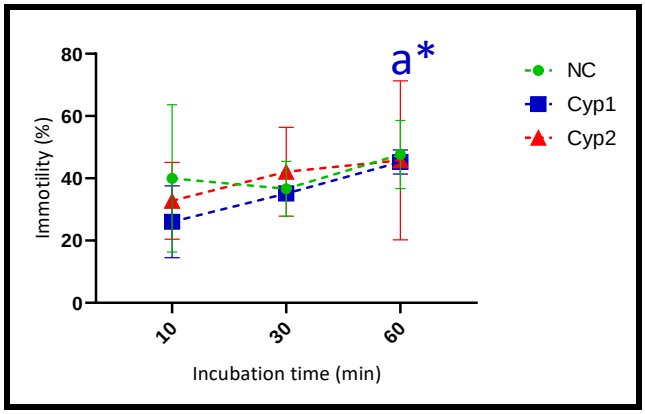

***Figure 26.** Time-dependent effect of Cyp1 incubation in immotile bovine spermatozoa. 7.5 x 10^6 spermatozoa were incubated with 0.1 or 1 nM (Cyp1 and Cyp2, respectively) and motility*

parameters were assessed with the machine learning-based analysis (alternative analysis) after 10, 30 and 60 min. Statistically significant findings are indicated with (*). a represents a difference between Cyp1 after 60 and 10 min of incubation, with a p-value inferior to 0.05*

3.4.2. Kinematic parameters

Statistically significant findings between times of incubation of each concentration regarding the kinematic parameters are summarized on **Table 8**. The significant results of the multiple comparations between groups are highlighted in the table and portrayed on **Figure 27**.

Table 8. *Statistically significant findings regarding the time-dependent effect of the PP inhibitors (CAN, TAU and CYP) on the kinematic parameters of bovine spermatozoa, upon Kruskall-Wallis analysis. After incubation, kinematic parameters were assessed with Sperm Class Analyzer CASA System or the alternative analysis, after 10, 30 and 60 min. The analysis that also showed significant findings on multiple comparations are highlighted.*

Condition	Analysis method	Kinematic parameter	Motility class	*P-value*	Multiple Comparations	*Corrected p-value*
Can1	Alternative Analysis	VSL	SP	*0.0500*	No	-
Can1	Alternative Analysis	VSL	HYP	*0.0286*	No	-
Can1	Alternative Analysis	VAP	SP	*0.0500*	No	-
Can1	Alternative Analysis	LIN	HYP	*0.0250*	30 and 60 min	*0.0171*
Can1	Alternative Analysis	STR	HYP	*0.0107*	30 and 60 min	*0.0338*
Can2	Alternative Analysis	STR	CIRC	*0.0250*	No	-
Can1	Alternative Analysis	WOB	CIRC	*0.0250*	No	-
Can1	Alternative Analysis	ALH	HYP	*0.0250*	No	-

Can2	Alternative Analysis	ALH	CIRC	*0.0500*	No	-
Can1	Alternative Analysis	BCF	HYP	*0.0500*	No	-
Can2	Alternative Analysis	DNC	CIRC	*0.0250*	No	-
Tau1	Alternative Analysis	LIN	SP	*0.0286*	No	-
Tau2	Alternative Analysis	DNC	HYP	*0.0500*	No	-
Cyp1	Alternative Analysis	WOB	SP	*0.0500*	No	-
Cyp1	Alternative Analysis	DNC	HYP	*0.0500*	No	-
Cyp2	CASA analysis	VCL	NP	*0.0488*	10 and 60 min	*0.0486*

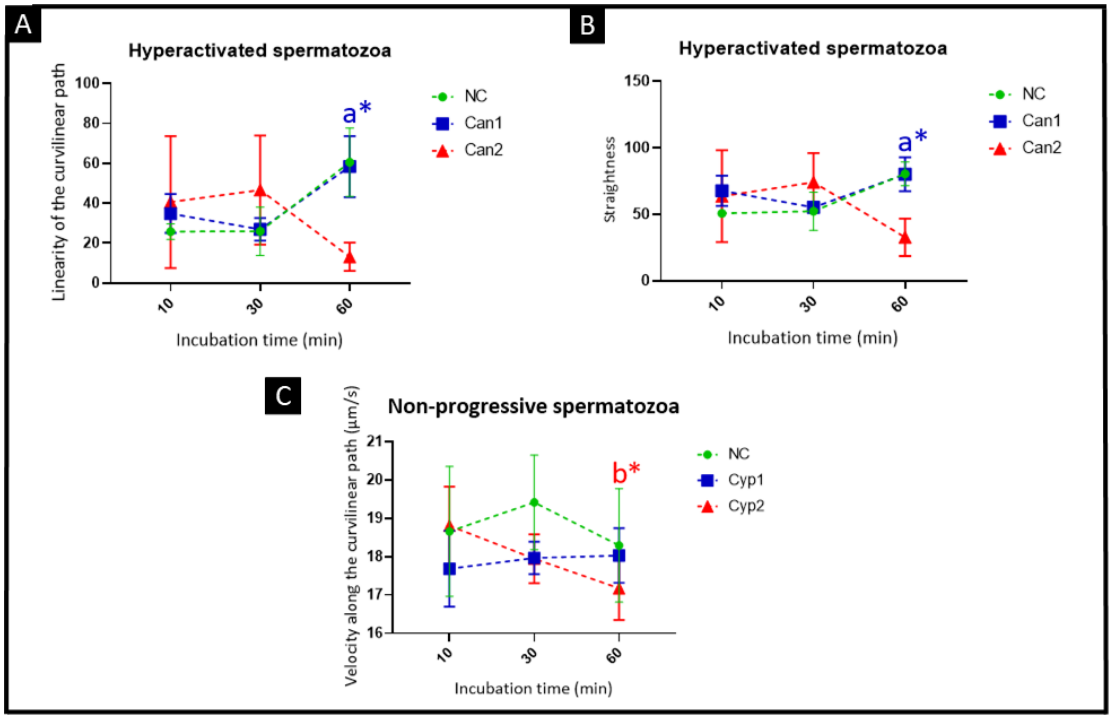

Figure 27. *Time-dependent effect of CAN and CYP incubation in the kinematic parameters of bovine spermatozoa. 7.5 x 10^6 spermatozoa were incubated with 100 or 1000 nM of CAN (Can1 and Can2, respectively), and 0.1 and 1 nM of Cyp (Cyp1 and Cyp2, respectively). Motility parameters were assessed after 10, 30 and 60 min.* ***A.*** *LIN of hyperactivated spermatozoa after incubation with Can1, retrieved with alternative analysis;* ***B****. STR of hyperactivated spermatozoa after incubation with Can1, retrieved with alternative analysis;* ***C.*** *VCL of NP spermatozoa after incubation with Cyp2, retrieved with Sperm Class Analyzer CASA System analysis. Statistically significant findings are*

indicated with (*) representing a p-value is inferior to 0.05. a means significant differences between Can1 after 30 and 60 min of incubation, b* means significant differences between Cyp2 after 10 and 60 min of incubation.*

3.5. Concentration-dependent effect of the incubation with PP inhibitors in bovine sperm motility

3.5.1. Effects of the PP inhibitors are not usually concentration-dependent

To evaluate if the effect on motility and kinematic parameters was concentration-dependent, non-parametric Mann-Whitney tests were performed between the lowest and highest concentration of each inhibitor, for both the CASA and the alternative analysis. The only statistically significant finding is expressed in **Figure 28**. It refers to the CASA analysis and concerns the LIN of RP spermatozoa following incubation with CAN after 60 min.

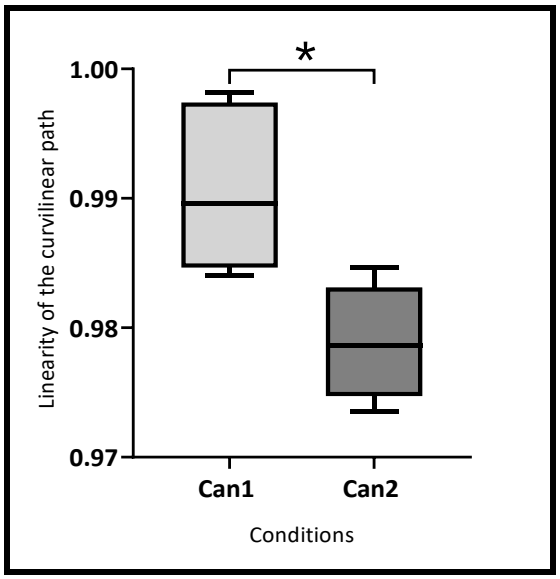

Figure 28. *Concentration-dependent effect of CAN incubation in LIN of RP bovine spermatozoa. 7.5 x10^6 spermatozoa were incubated with 100 or 1000 nM (Can1 and Can2, respectively) and kinematic parameters were assessed with Sperm Class Analyzer CASA System after 10, 30 and 60 min. Statistically significant findings are indicated with (*) representing a p-value inferior to 0.05.*

3.5.2. Comparison between different inhibitors

Comparisons between conditions of different inhibitors were also performed, for the results of the CASA system analysis, particularly between Can1 and Tau1, as well as Can2 and Tau2, using the non-parametric Mann-Whitney test. The comparison between Can1 and Tau1 was performed to assess if there were significant differences between inhibiting only PP2A (Can1) or only PP1 (Tau1), to retrieve information of their individual functions in motility. The comparison between Can2 and Tau2 was to determine if similar effects on motility were verified, following incubation with distinct inhibitors, whose concentrations were chosen to simultaneously inhibit PP1 and PP2A.

Can1 and Tau1 were not statistically different in any parameter or timepoint. Statistically significant results regarding the Can2 and Tau2 comparison are shown in **Table 9** and **Figure 29**.

Table 9. *Statistically significant findings regarding the comparation between kinematic parameters of Can2 and Tau2, in all motility groups and timepoints (n=5). After incubation, kinematic parameters were assessed with Sperm Class Analyzer CASA System, after 10, 30 and 60 min.*

Kinematic parameter	Motility class	Conditions	*P-value*
LIN	RP	Can2 and Tau2	*0.0317*
WOB	SP	Can2 and Tau2	*0.0159*
ALH	RP	Can2 and Tau2	*0.0317*
BCF	RP	Can2 and Tau2	*0.0317*

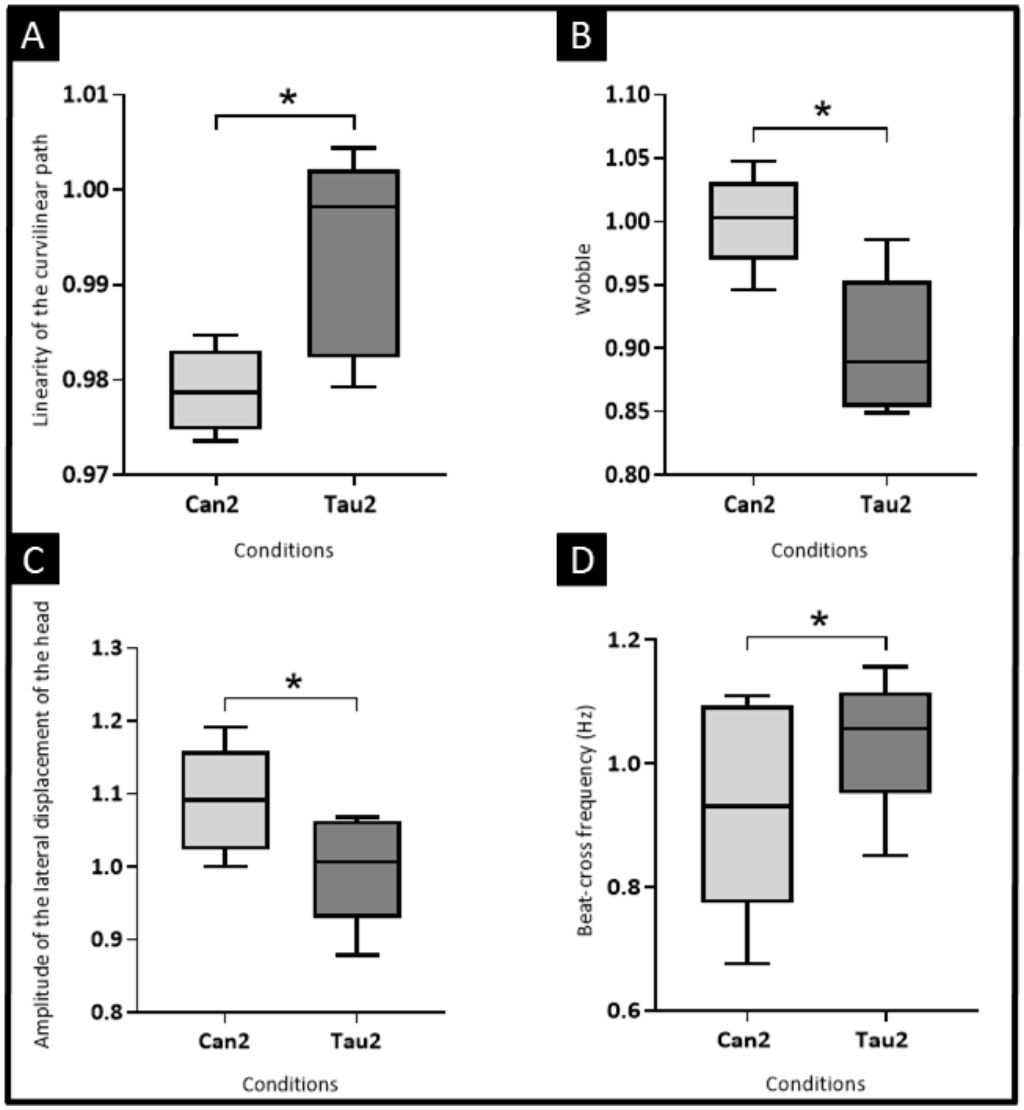

***Figure 29**. Comparison of the effects of Can2 and Tau2 incubation in the kinematic parameters of bovine spermatozoa. 7.5 x10^6 spermatozoa were incubated with 1000 nM and 100 nM (Can2 and Tau2, respectively) and kinematic parameters were assessed with Sperm Class Analyzer CASA System, after 10, 30 and 60 min. **A:** LIN of RP spermatozoa; **B:** WOB of SP spermatozoa; **C.** ALH of RP spermatozoa; **D.** BCF of RP spermatozoa. Statistically significant findings are indicated with (*) representing a p-value is inferior to 0.05.*

3.6. Preliminary results on the incubation of human spermatozoa with tautomycin

Human spermatozoa were incubated with Tau1 and Tau2 and both viability and motility were assessed after 10, 30 and 60 min (n=2). The viability results are shown in **Table 10**. Preliminary results showed that similar to bovine studies, human spermatozoa viability does not seem to be affected by incubation with TAU.

Table 10. *Impact of TAU incubation in the percentage of viable human spermatozoa. 4.0 x10^6 spermatozoa were incubated with 10 or 100 nM (Tau1 and Tau2, respectively) and viability was assessed with Tripan blue solution after 10 and 60 min of incubation. Two experiments were performed (n=2) and the values from each experiment, as well as the mean and SD are expressed for the NC1, Tau1 and Tau2.*

	10 min				60 min			
	1	2	Mean	SD	1	2	Mean	SD
NC1	100	100	100	0	97.73	97.4	97.57	0,23
Tau1	100	98.60	99.30	0,99	95.47	93.85	94.66	1,15
Tau2	96.66	92.77	94.72	2,75	93.60	96.90	95.25	2,33

The information regarding each kinematic parameter is exposed in **Table 11**, **Table 12** and **Table 13**, after 10, 30 and 60 min of incubation, respectively. Due to the low number of samples used (n=2), statistical analysis was not performed. Nevertheless, these results follow the same tendency as the incubation of bovine spermatozoa with TAU, being the mean values of the kinematic parameters generally decreased when comparing to the NC1.

Table 11. *Impact of TAU incubation in the kinematic parameters of human spermatozoa after 10 min of incubation. Two experiments were performed (n=2) and the values from each experiment, as well as the mean and SD are expressed for the NC1, Tau1 and Tau2.*

	NC1				Tau1				Tau2			
	1	2	Mean	SD	1	2	Mean	SD	1	2	Mean	SD
VSL	35,01	15,29	25,15	13,94	20,50	13,72	17,11	4,79	26,94	13,92	20,43	9,20
VCL	69,06	37,06	53,06	22,63	47,82	35,04	41,43	9,04	56,30	35,16	45,73	14,95
VAP	43,90	21,57	32,73	15,79	29,14	20,25	24,69	6,29	36,91	19,69	28,30	12,18
LIN	52,61	33,27	42,94	13,67	36,63	28,94	32,78	5,44	43,99	29,23	36,61	10,43
WOB	65,06	59,87	62,47	3,67	60,38	60,34	60,36	0,03	64,03	57,26	60,64	4,79
STR	78,21	56,98	67,59	15,01	60,03	51,92	55,98	5,73	66,30	53,64	59,97	8,95

ALH	2,25	1,69	1,97	0,40	1,69	1,64	1,67	0,03	1,80	1,69	1,74	0,08
ALHmax	4,26	3,35	3,80	0,65	3,39	3,20	3,29	0,13	3,60	3,26	3,43	0,24
DNC	175,52	93,17	134,34	58,23	106,23	94,85	100,54	8,04	117,53	101,43	109,48	11,39
BCF	26,18	19,89	23,04	4,44	24,89	20,09	22,49	3,39	26,67	19,72	23,20	4,91
MAD	92,05	89,34	90,69	1,91	89,29	88,52	88,90	0,54	90,49	87,71	89,10	1,97
R	941,43	366,16	653,79	406,78	494,25	282,98	388,61	149,39	273,18	164,62	218,90	76,76

Table 12. *Impact of TAU incubation in the kinematic parameters of human spermatozoa after 30 min of incubation. Two experiments were performed (n=2) and the values from each experiment, as well as the mean and SD are expressed for the NC1, Tau1 and Tau2.*

	NC1				**Tau1**				**Tau2**			
	1	**2**	**Mean**	**SD**	**1**	**2**	**Mean**	**SD**	**1**	**2**	**Mean**	**SD**
VSL	19,15	17,48	18,31	1,18	16,62	13,50	15,06	2,21	22,69	14,11	18,40	6,07
VCL	49,22	39,41	44,31	6,94	43,97	35,24	39,61	6,17	49,79	36,48	43,13	9,42
VAP	28,33	22,94	25,64	3,81	24,72	19,73	22,22	3,52	31,19	20,85	26,02	7,31
LIN	34,36	35,83	35,10	1,04	31,75	30,33	31,04	1,00	40,23	30,28	35,25	7,03
WOB	58,01	61,67	59,84	2,59	58,16	56,25	57,20	1,35	64,44	60,93	62,68	2,48
STR	57,75	61,40	59,57	2,58	55,62	54,69	55,16	0,66	63,62	53,97	58,79	6,82
ALH	1,86	1,80	1,83	0,04	1,66	1,67	1,67	0,01	1,72	1,73	1,72	0,01
ALHmax	3,66	3,41	3,54	0,17	3,33	3,39	3,36	0,04	3,38	3,38	3,38	0,00
DNC	121,33	108,99	115,16	8,73	104,15	89,53	96,84	10,34	110,49	97,12	103,80	9,46
BCF	24,47	20,13	22,30	3,07	24,97	20,42	22,70	3,22	25,26	20,10	22,68	3,65
MAD	89,99	89,06	89,52	0,65	87,48	89,59	88,53	1,49	90,09	90,74	90,41	0,46
R	255,44	375,15	315,30	84,65	266,53	293,82	280,17	19,30	1760,94	180,62	970,78	1117,45

Table 13. *Impact of TAU incubation in the kinematic parameters of human spermatozoa after 60 min of incubation. Two experiments were performed (n=2) and the values from each experiment, as well as the mean and SD are expressed for the NC1, Tau1 and Tau2.*

	NC1				**Tau1**				**Tau2**			
	1	**2**	**Mean**	**SD**	**1**	**2**	**Mean**	**SD**	**1**	**2**	**Mean**	**SD**
VSL	20,45	17,80	19,13	1,88	22,85	15,38	19,12	5,29	22,27	14,65	18,46	5,38
VCL	54,15	44,42	49,28	6,88	51,31	36,52	43,91	10,46	52,11	40,63	46,37	8,11
VAP	30,97	23,98	27,48	4,94	31,91	21,74	26,82	7,19	31,49	21,31	26,40	7,19
LIN	34,46	35,42	34,94	0,68	39,19	33,22	36,21	4,22	38,96	30,31	34,63	6,12
WOB	59,16	55,95	57,56	2,27	63,43	61,43	62,43	1,41	60,85	55,17	58,01	4,02
STR	59,20	63,19	61,20	2,82	62,76	57,33	60,04	3,84	64,17	56,15	60,16	5,67
ALH	2,02	2,00	2,01	0,02	1,80	1,66	1,73	0,09	1,87	2,02	1,94	0,11
ALHmax	4,06	3,67	3,87	0,28	3,54	3,21	3,37	0,23	3,75	3,79	3,77	0,03
DNC	138,49	132,55	135,52	4,20	113,63	92,48	103,06	14,95	119,71	130,78	125,24	7,82
BCF	24,37	20,11	22,24	3,01	25,15	20,44	22,79	3,33	24,57	19,55	22,06	3,55
MAD	88,14	89,40	88,77	0,90	90,96	89,92	90,44	0,73	88,36	90,14	89,25	1,26
R	4200,79	327,18	2263,98	2739,06	1183,20	210,70	696,95	687,66	172,70	424,07	298,38	177,75

4. Discussion

According to the literature, an activation of motility was expected after spermatozoa incubation with PP inhibitors[13,25,34,36,60]. Thus, we anticipated a decrease in immotile spermatozoa and an increase in progressively motile (both SP and RP), possibly accompanied by an increase in velocity in the kinematic parameters (VCL, VSL and VAP). Remarkably, the results from the CASA analysis consistently demonstrated a tendency to increased immotile spermatozoa percentage, paired with a generally statistically significant decrease in RP cells percentage, across all conditions and times of incubation (**Figure 11**, **Figure 13** and **Figure 15**). NP and SP motility were the least affected classes since the differences are inconsistent and non-statistically significant. Besides, a decrease in velocity and percentage of all kinematic parameters was also evident (**Figure 18**, **Figure 20** and **Figure 22**).

The concentrations of each inhibitor were selected attending to each PP IC_{50}, however, those had never been tested in spermatozoa. Thereby, their impact on spermatozoa viability and motility was unclear. In the viability assay of this study, there were no significant differences between the inhibitor treatments and the NC1 (**Figure 10**). In fact, higher quantities of formazan were found in the inhibitor treatments, suggesting that spermatozoa remain metabolically active and therefore viable, upon incubation with CAN, TAU and CYP[142,143]. Contrarily, considering the kinematic parameters, the decrease in VCL in all conditions, especially after 30 and 60 min of incubation, paired with diminished BCF and ALH, are indicators of a decrease in cell vigour and viability[109,124]. Therefore, these inhibitor concentrations might not be affecting cell metabolism but somehow interfere with sperm motility. Interestingly, Buranaamnuay *et al.* stated that MTT based assays, as the one used in this study, should be accompanied by other vitality assessments to determine the absolute viability of spermatozoa, since formazan concentration is dependent on parameters other than mitochondrial activity[143]. Additionally, it has been shown that metabolic impairment may increase NAD(P)H Resazurin Oxidoreductase Activity, which disturbs NAD(P)H-Based viability tests[144]. It would be interesting to perform

a viability assay using another methodology and, simultaneously, confirm if there is indeed reductive stress and higher NAD(P)H/NAD(P)$^+$ ratio. Another interesting explanation would be the existence of sperm-free mitochondria. Indeed, recently Dache *et al*. have shown the existence of functional cell-free mitochondria in blood[145]. The authors conjecture that mitochondria could be used to transfer information between cells and even be relevant for early detection and prognosis of various diseases[145]. In the case of the present study, we could hypothesise that spermatozoa release mitochondria (alone or in vesicles) when entering apoptosis, which interferes with the viability test result. To investigate this hypothesis the oxygen consumption of the media should be evaluated.

Regarding the results retrieved with the alternative analysis no statistically significant differences were detected, possibly due to the low number of experiments performed (n=3), which resulted in high values of SD. Nevertheless, a tendency of higher RP was observed, along with increased hyperactivated and circular trajectory spermatozoa percentage, whereas immotile spermatozoa were increased, as occurred with the CASA system analysis (**Figure 12**, **Figure 14** and **Figure 16**). Vitality measurements were not performed prior to the alternative analysis on bovine spermatozoa experiments. However, considering that VCL is frequently used as a measure of cell vitality and vigour, it could be used to inquire about spermatozoa viability. VCL was increased after 10 min of incubation for all conditions and tended to be decreased comparing to the NC1 in the subsequent times of analyse, which could suggest that spermatozoa are losing viability with time. This early increase could also be due to an immediate effect of the PP inhibitors on spermatozoa motility, which then fades. Furthermore, considering the kinematic parameters, in RP spermatozoa it was detected a tendency to achieve higher values of VCL, when compared to both the NC1 and the CASA analysis values. Notably, VCL values from the CASA analysis are consistently lower comparing to the alternative analysis, which might be due to the increased video FR or height of the slides. Concerning the kinematic parameters of the CASA analysis, BCF and ALH are only statistically significantly affected by CYP, especially after 60 min of incubation (**Figure 23**). Along with VCL, these two parameters are indicators of sperm vigor, which further illustrates that after 60 min of incubation, spermatozoa in the inhibitor treatments are losing velocity and viability, comparing to the NC1.

Our results show that CAN affects mostly the kinematic parameters of RP spermatozoa, whereas TAU affects primarily the SP (**Figure 18** and **Figure 20**). For both inhibitors the higher concentration (Can2 and Tau2) exerts more significant effects, which suggests that inhibition of both PP1 and PP2A causes a more pronounced effect on the decrease of the kinematic parameters. In fact, regarding the motility parameters, Can2 and Tau2 also cause the most statistically significant decrease in RP spermatozoa percentage, suggesting that when both PPs are being inhibited, the loss of motility percentage is more emphasized. Other reason for that accentuated decrease could be that higher concentrations of these inhibitors are more toxic for spermatozoa, but this effect was not corroborated by the viability tests. Incubation with CYP affects similarly the kinematic parameters of SP and RP spermatozoa (**Figure 22** and **Figure 23**). Moreover, it causes the most significant decrease in RP percentage, suggesting that PP2B inhibition exerts the most significant role in motility inhibition.

LIN is the least affected trajectory parameter by any inhibitor treatment and particularly by CYP, which might suggest that PPs are less involved with the linear type of movement. Nevertheless, this kinematic parameter is the only one that showed a concentration-dependent effect, following incubation with CAN in RP spermatozoa. This implies that inhibition of both PP1 and PP2A significantly affects RP sperm linearity, when compared to inhibition of PP2A alone. In our study, STR results demonstrated a similar tendency as LIN, despite not always being significantly affected in the same condition and timepoint. Indeed, the alternative analysis showed that both LIN and STR of HYP spermatozoa significantly decreased through time (**Table 8**), which is in accordance with the described pattern of hyperactivated motility, characterized by more curvilinear trajectories. Moreover, LIN values are consistently higher with the CASA analysis when compared to the alternative analysis. This is also verified for WOB. LIN and WOB derive from velocity parameters being a result of VSL/VCL and VAP/VCL, respectively[113]. VCL achieved higher values in the alternative analysis results, which explains why LIN and WOB present lower percentages.

Our results showed that the effects verified after incubation with all PP inhibitors were not generally concentration-dependent. Considering CAN and TAU, similar results

were obtained with both concentrations, which were selected to inhibit solely PP1 or PP2A or both at the same time (**Table 5**). It was expected that the effects of Tau2 and Can2 were the most similar, since they both inhibit the same PPs. Notably, the only statistically significant differences found between conditions of different inhibitors were precisely between Can2 and Tau2 (**Table 9**). Conversely, there were not significant differences between Can1 and Tau1, which were inhibiting only PP2A and PP1, respectively, further implying that the motility alterations are generally not due to a specific PP activity, and they both might play a coordinated role on motility regulation, as previously described in literature. Alternatively, the effects of the lower concentrations could be weaker, and those differences are not evident.

Regarding the alternative analysis results, in all CAN and CYP conditions, as well as in most of TAU conditions, an increased number of hyperactivated spermatozoa was verified, despite the non-capacitating conditions of the experiment. The circular motion was more expressed by spermatozoa in all inhibitor treatments, when compared to the NC1 (videos available at Supplementary Material). It is described in the literature that, when confined between parallel walls, the spermatozoon tends to swim in circles or curvilinear trajectories, which is a resemble of their movement both in the oviduct, close to the epithelial layer, and near the large surface of the egg, being that feature important for fertilization[146]. Recently, it was also observed that spermatozoa movement becomes diffusive and circular, instead of progressive, when the spermatozoon loses the ability to roll[147]. Zaferani *et al.* assessed that rolling control enables spermatozoa to respond to changes in viscosity and viscoelasticity of the FRT mucous during capacitation, transitioning between progressive and circular motion. This functions as a regulatory tool which allows sperm to navigate accordingly to the rheological properties of the FRT[147]. Our results suggest that PP inhibition is influencing sperm rolling and consequently its ability to progressively swim, resulting in the circular motion detected by the alternative analysis and increase in SP spermatozoa in the CASA system. Thereby, we can hypothesize that rolling ability could be regulated by other factors that were not accounted for by Zaferani *et al*, such as phosphorylation-dependent cellular signaling. Alternatively, since the conditions of our experiment were non-capacitating, the lack of other non-PP-related stimuli to reach

the oocyte, provided by the FRT, might also be causing spermatozoa to stop the rolling and consequently the ability to swim progressively.

Concerning CYP, the CASA analysis showed similar results to Zalata and Yuan studies, despite the concentrations used in our study being significantly lower[108,109]. As Yuan described in rat sperm, our results also show a decrease in VCL, VSL, BCF, LIN and STR (**Figure 22** and **Figure 23**). Their results suggest that even at nanomolar concentration, CYP could be toxic for spermatozoa, causing its immobility[109]. Besides, CYP conditions are the ones that present more significant decreases in all kinematic parameters. On the contrary, the alternative analysis reached opposite results, especially in VCL and BCF, as well as an increase in RP cells. In both studies, as well as in most experiments that use this inhibitor, CYP was reconstituted in DMSO, rather than ethanol, which is something to consider when comparing results[108,109]. Notably, upon PP2B inhibition by CYP a huge increase in hyperactivated spermatozoa was observed with the alternative analysis (between 3 and 20 times higher than NC1, non-statistically significant), which is contrary to Dey *et al.* studies and similar to Signorelli *et al.*[34,35]. The first suggested that PP2B presented catalytic activity during capacitation, while the last advocated that PP2B inhibition was required to achieve hyperactivation[34,35]. Dey and colleagues defined hyperactivation by an increase in VAP, VCL and ALH, which was only verified in the HYP class of our study at some of the timepoints of the analysis, so the differences could be due to different criteria of classification[34].

Moreover, a lot of agglutinated spermatozoa were found in CYP conditions (videos available at Supplementary Material). In fact, it was very frequent to witness two spermatozoa swimming vigorously with joined heads even on other inhibitor treatments. When comparing the NC1 with the NC2, there were no statistically significant differences concerning NP spermatozoa, which represents the agglutinated spermatozoa, since they cannot progress in the field but remain with moving tails. When performing both analysis it was evident to the eye that both CYP and NC2 conditions showed larger groups of agglutinated cells; however, the CASA system presented difficulties in recognizing those cells. It is noteworthy that CASA presents analysis limitations, since joined cells were frequently not accounted for. So, despite not having significant differences between NC1 and NC2, ethanol might play a role on CYP effects on NP spermatozoa, independent of PP2B

inhibition. Previously, Dodaran *et al.* tested the impact of sub-lethal concentrations of ethanol on post-thaw bovine spermatozoa motility and viability. Concentrations ranging between 0.03 and 0.15 %(v/v), proved to be beneficial to spermatozoa[148.] These concentrations are however lower than the %(v/v) used in our study (1%). Donnelly and colleagues performed a similar experiment to determine ethanol impact on sperm quality and, by incubating spermatozoa with 0.08 to 0.5% (w/v), a significant decrease in the progressive motility percentage was observed, paired with a decrease in VSL, VCL and ALH[149]. Since the %(w/v) used in this study was 0.79%, a negative impact on sperm motility could be possible, despite the differences between NC1 and NC2 being mostly non-statistically significant.

Previous evidence suggested that an increase in hyperactivation was expected following incubation with TAU, which was not verified by looking at the kinematic parameters of the CASA results. Suzuki and colleagues used 1 and 10 nM and incubated for more than 2 hours, which could explain the disparity of the results. Nevertheless, regarding the alternative analysis, after 60 min of incubation, there was an accentuated statistically non-significant increase in hyperactivated cells, which supports Suzuki's results[106]. In both Suzuki and the alternative analysis, hyperactivated spermatozoa were determined by an initial visual classification, while other studies rely on CASA parameters to classify hyperactivated cells[34,109,129]. Although very valuable, this initial visual classification of the hyperactivated motility pattern can add some bias to the classification, which adds to the disparity between studies that evaluate hyperactivation. Currently, there is not a consensus on how to accurately and objectively define the hyperactivated motility pattern, particularly resorting to the kinematic parameters. Most studies agree that an increase in VCL and ALH is a defining feature of hyperactivated motility pattern. However, this was not verified consistently in the hyperactivated group for any inhibitor treatment and timepoint, and other relevant pattern was also not found. Thus, it contributes to the discussion that hyperactivation is difficult to define and evaluate, as well as to uniform between studies, being hard to compare the role of the PPs in the hyperactivation of spermatozoa[25,34,35,63,129]. **Table 14** shows the kinematic parameters frequently used to describe hyperactivated motility pattern. Green represents the conditions of our study in

which the outcome was in accordance with literature. Only about half of the time, our results show the expected tendency.

***Table 14**. Kinematic parameters frequently used to describe hyperactivated motility pattern. Green represents the conditions in which the outcome of our study was in accordance with the literature*

	CAN						TAU						CYP					
	10		30		60		10		30		60		10		30		60	
	1	2	1	2	1	2	1	2	1	2	1	2	1	2	1	2	1	2
VCL	↑		↓		↓		↑		↓	↑	↓		↑		↓		↓	
LIN	↑		↑		↓		↑		↓		↓		↓		↑		↓	
ALH	↑	↓	↑	↓	↓		↑		↓		↑		↑		↓		↑	
BCF	↓	↑	↓		↓		↑	↓	↑	↓	↓		↑		↓		↑	↓

The results from the experiments performed in human spermatozoa are still preliminary, since only two distinct experiments were performed (n=2). Thereby, a population increase is required to draw reliable conclusions. The vitality measurements showed that most spermatozoa were viable, likewise the bovine experiments. In addition, the kinematic parameters show a similar tendency of decrease (**Table 11**, **Table 12** and **Table 13**).

It is worth noting that the semen samples used in our study were ejaculates from healthy animals. Thereby, sperm epididymal maturation was successfully completed, and the phosphorylation-dependent biochemical mechanisms presumably are functioning, meaning that the PP's activity is inhibited. Thus, by further inhibiting one PP, with CAN, TAU or CYP, it does not mean that the activity of the others is activated. Therefore, for each PP inhibitor condition, the effects cannot be attributed solely to the inhibition of the targeted PP, which makes it even more difficult to distinguish their individual functions. These assumptions could only be made if the spermatozoa were from caput epididymis semen, where the three PPs are still activated, like some authors previously performed[13,60,94,95].

As previously mentioned, the two methodologies of analyse applied in our study frequently achieved dissimilar results, despite the prior experiment being mainly identical. Nonetheless, a distinctive feature of the procedures that preceded the CASA and alternative analysis was the condition of the samples. Semen samples used in the experiments prior to the CASA analysis were acquired shortly after sample collection and

the procedure done after washing the fresh semen sample. The alternative analysis was performed in cryopreserved semen samples, after thawing and washing. Despite the efforts to optimize the cryopreservation procedures, many authors advocate that the freeze and thaw cycle can cause a negative impact on sperm function, particularly a decrease in sperm motility due to mitochondrial damage[150–155]. Nevertheless, recently other authors showed that the impact is not substantial and cryopreserved samples are equally as efficient as fresh semen in terms of the success of fertilization and pregnancy[156,157].

Other important difference between the procedures were the chambers used to load the samples prior to observation. It has been shown that a lower chamber depth might limit natural sperm motility[137,138]. Several authors performed comparisons of different commercially available slides used with CASA systems, in terms of chamber depth and loading method. It was verified that the type of chamber influences the sperm motility parameters obtained[137,140,158,159]. Lenz *et al.* verified that Leja20, the slides used in the CASA system analysis, usually present significantly less progressive percentage and total motility[159]. Soler and colleagues demonstrated significant differences in boar spermatozoa motility patterns when comparing 100 and 10 or 20 µm chambers[120]. The depth of the chambers used was 20 and 200 µm, which could be one explanation why VCL is consistently higher in the results from the alternative analysis.

The use of a very tight FR (100 fps) in the alternative analysis allowed a capture of more detailed videos of spermatozoa, thereby, the motion analysis is more precise, and the parameters retrieved more accurate, specially to evaluate motility patterns characterized by low linearity, such as the hyperactivated[118,119]. This increased FR was also previously shown to retrieve higher VCLs when compared to methods with lower FR[129]. Concerning the classification of the spermatozoa into the motility classes, machine learning-based classification allows a more precise recognition, especially with large amounts of data and permits the researcher to personalize the type of information to acquire, for instance, the desired kinematic parameters and motility groups. This is a feature that the CASA system lacks since the parameters retrieved are pre-defined for each software.

Altogether, the results obtained with the alternative analysis are preliminary and a procedure optimization is still required. Even so, the apparatus and analysis technique revealed to be very promising in the study of sperm motility and morphology. Despite its undeniable advantages, the time of sample analysis is currently longer in comparation to the CASA systems. This brought specific limitations to the experiments performed, because time disparities were required between the analysis of different conditions, which could affect the comparability of the results obtained with both analyses. The alternative analysis is continuously being optimized for either bovine or human samples, which further improves the detail quality of the results retrieved. With further work to improve and adapt the procedures in which usually a CASA system analysis is performed, this technique will become very useful in the study of spermatozoa motility and morphology.

5. Concluding remarks

The main findings of our study are summarized in **Figure 30** as an overview of viability and motility alterations, as well as particular inhibitor effects.

The primary goal of this study was to evaluate the alterations in the motility pattern of spermatozoa, following incubation with three distinct PP inhibitors, CAN, TAU and CYP. Contrarily to what is described in the literature, the CASA system analysis results showed that CAN, TAU and CYP consistently decrease spermatozoa progressive motility, as well as sperm kinematic parameters, without affecting cell viability. Conversely, the results from the alternative analysis showed an increase in progressive motility, particularly RP, hyperactivated and circular trajectory sperm. These contradictive findings underline the complexity of the mechanisms regulating sperm activated and hyperactivated motility, which still presents significant knowledge gaps. Indeed, with the increasing numbers of male infertility, additional investigation on this subject is urgent to better understand, identify, and treat sperm motility-related infertility cases.

Another goal was to compare the results obtained using two methods of semen analysis: the CASA system analysis and machine learning-based analysis (alternative analysis). The contradictions between the results of the two methodologies are likely due to their particular differences, for instance chamber depth, video FR and sample condition. This highlights the importance of the characteristics of the data acquisition and processing methods, which can impact the results and should be carefully evaluated before selection. Further, herein is emphasized that there is still room to improve semen analysis methods and both the investigation and clinical field would greatly benefit from more reliable methodologies.

6. Future Perspectives

Additional research could be done to further explore the properties of CAN, TAU and CYP, as well as to overcome this study limitations. **Figure 30** shows an overview of the possible next steps of this study.

Firstly, an increase in the number of samples analyzed would result in more robust conclusions, specially prior to the alternative analysis, as well as for the human spermatozoa experiments. Besides, there is a need to diversify the methods of measuring viability and/or vitality to overcome the MTT-based assay limitations and corroborate findings regarding this subject.

Performing the same procedures in caput epidydimal spermatozoa, would be valuable to further distinguish PPs role in motility acquisition, since at this stage PPs still present catalytic activity and could be individually inhibited. Studies with PP activators in spermatozoa from ejaculates could also bring new insights on the distinction of PPs individual roles in motility regulation, as well as to compare the motility alterations upon inhibition or activation of these PPs. Furthermore, the concentrations of either PP inhibitors or activators could be diversified.

Lastly, the role of the PPs on hyperactivated motility is still unclear, and studies disagree not only on PP2B state of activity, but also on how to recognize this motility pattern. Therefore, performing these experiments in capacitating conditions with PP activity assessment would allow to a better study of hyperactivation. Concomitantly, rolling control could be further explored, since this is currently a poorly understood component of sperm motility.

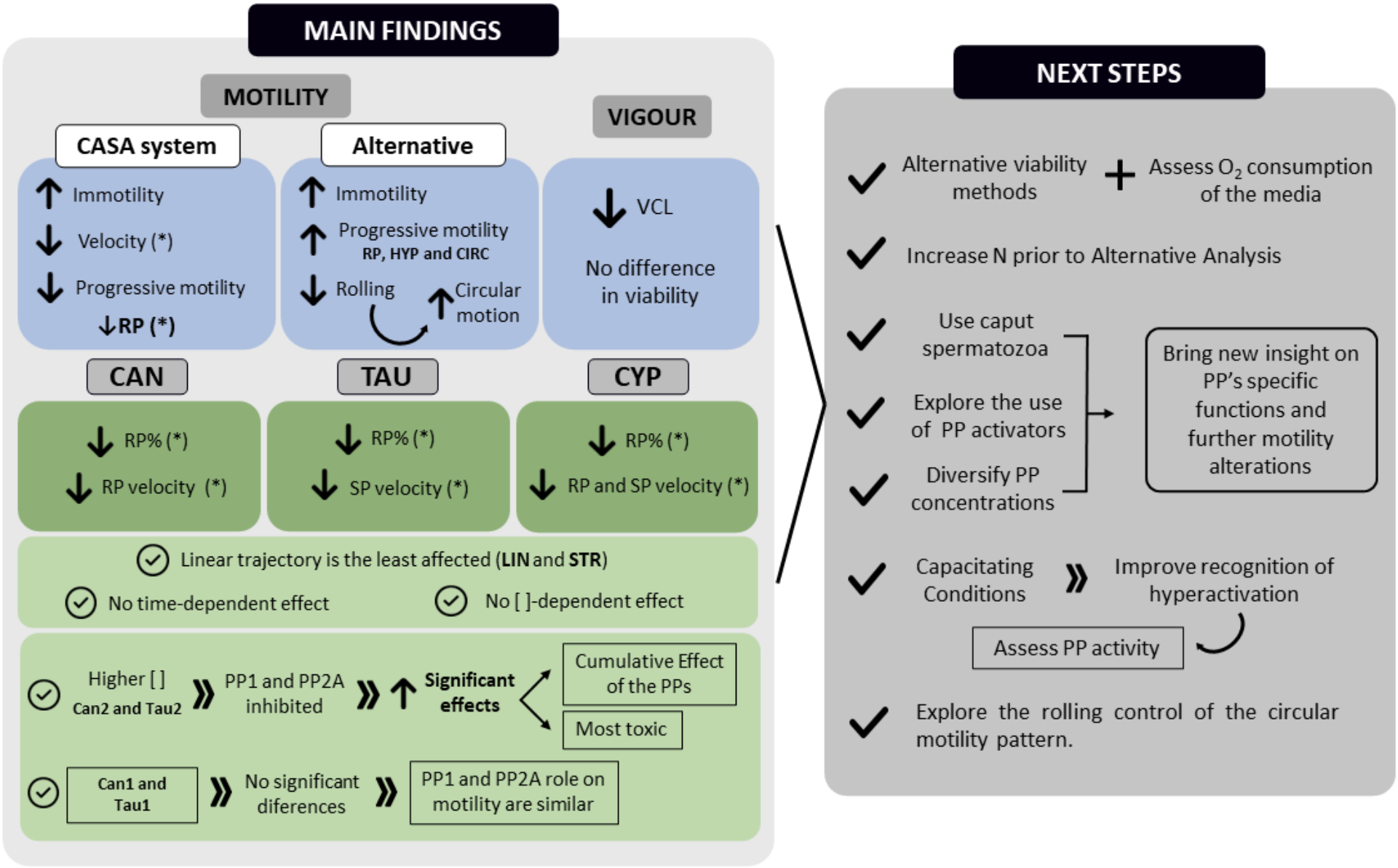

Figure 30. *Main findings of this study, regarding motility, vigour and the effects of CAN, TAU and CYP, as well as potential next steps. Statistically significant findings are indicated with (*).*

7. References

(1) Pesch, S.; Bergmann, M. Structure of Mammalian Spermatozoa in Respect to Viability, Fertility and Cryopreservation. *Micron* **2006**, *37* (7), 597–612. https://doi.org/10.1016/J.MICRON.2006.02.006.

(2) Dcunha, R.; Hussein, R.; Ananda, H.; Kumari, S.; Adiga, S.; Kannan, N.; Zhao, Y.; Kalthur, G. Current Insights and Latest Updates in Sperm Motility and Associated Applications in Assisted Reproduction. *Reprod Sci* **2020**. https://doi.org/10.1007/S43032-020-00408-Y.

(3) Freitas, M. J.; Vijayaraghavan, S.; Fardilha, M. Signaling Mechanisms in Mammalian Sperm Motility. *Biol Reprod* **2017**, *96* (1), 2–12. https://doi.org/10.1095/biolreprod.116.144337.

(4) Fawcett, D. W. The Mammalian Spermatozoon. *Dev Biol* **1975**, *44* (2), 394–436. https://doi.org/10.1016/0012-1606(75)90411-X.

(5) Turner, R. M. Moving to the Beat: A Review of Mammalian Sperm Motility Regulation. *Reprod Fertil Dev* **2006**, *18* (1–2), 25–38. https://doi.org/10.1071/RD05120.

(6) Inaba, K. Molecular Architecture of the Sperm Flagella: Molecules for Motility and Signaling. *Zoolog Sci* **2003**, *20* (9), 1043–1056. https://doi.org/10.2108/ZSJ.20.1043.

(7) Lindemann, C. B.; Lesich, K. A. Flagellar and Ciliary Beating: The Proven and the Possible. *J Cell Sci* **2010**, *123* (4), 519–528. https://doi.org/10.1242/JCS.051326.

(8) Vadnais, M. L.; Aghajanian, H. K.; Lin, A.; Gerton, G. L. Signaling in Sperm: Toward a Molecular Understanding of the Acquisition of Sperm Motility in the Mouse Epididymis. *Biol Reprod* **2013**, *89* (5), 127. https://doi.org/10.1095/BIOLREPROD.113.110163.

(9) Gervasi, M. G.; Visconti, P. E. Molecular Changes and Signaling Events Occurring in Spermatozoa during Epididymal Maturation. *Andrology* **2017**, *5* (2), 204–218. https://doi.org/10.1111/ANDR.12320.

(10) Paoli, D.; Gallo, M.; Rizzo, F.; Baldi, E.; Francavilla, S.; Lenzi, A.; Lombardo, F.; Gandini, L. Mitochondrial Membrane Potential Profile and Its Correlation with Increasing Sperm Motility. *Fertil Steril* **2011**, *95* (7), 2315–2319. https://doi.org/10.1016/J.FERTNSTERT.2011.03.059.

(11) Yanagimachi, R.; Kamiguchi, Y.; Mikamo, K.; Suzuki, F.; Yanagimachi, H. Maturation of Spermatozoa in the Epididymis of the Chinese Hamster. *Am J Anat* **1985**, *172* (4), 317–330. https://doi.org/10.1002/AJA.1001720406.

(12) Dey, S.; Brothag, C.; Vijayaraghavan, S. Signaling Enzymes Required for Sperm Maturation and Fertilization in Mammals. *Front Cell Dev Biol* **2019**, *7* (December), 1–15. https://doi.org/10.3389/fcell.2019.00341.

(13) Vijayaraghavan, S.; Stephens, D.; Trautman, K.; Smith, G.; Khatra, B.; Cruz e Silva, E. F.; Greengard, P. Sperm Motility Development in the Epididymis Is Associated with Decreased Glycogen Synthase Kinase-3 and Protein Phosphatase 1 Activity. *Biol Reprod* **1996**, *54* (3), 709–718. https://doi.org/10.1095/BIOLREPROD54.3.709.

(14) Yanagimachi, R. Fertility of Mammalian Spermatozoa: Its Development and Relativity. *Zygote* **1994**, *2* (4), 371–372. https://doi.org/10.1017/S0967199400002240.

(15) Suarez, S. S.; Pacey, A. A. Sperm Transport in the Female Reproductive Tract. *Hum Reprod Update* **2006**, *12* (1), 23–37. https://doi.org/10.1093/HUMUPD/DMI047.

(16) Molina, L. C. P.; Luque, G. M.; Balestrini, P. A.; Marín-Briggiler, C. I.; Romarowski, A.; Buffone, M. G. Molecular Basis of Human Sperm Capacitation. *Front Cell Dev Biol* **2018**, *6*, 72. https://doi.org/10.3389/FCELL.2018.00072/BIBTEX.

(17) Jin, S. K.; Yang, W. X. Factors and Pathways Involved in Capacitation: How Are They Regulated? *Oncotarget* **2017**, *8* (2), 3600. https://doi.org/10.18632/ONCOTARGET.12274.

(18) Ho, H. C.; Suarez, S. S. Hyperactivation of Mammalian Spermatozoa: Function and Regulation. *Reproduction* **2001**, *122* (4), 519–526. https://doi.org/10.1530/REP.0.1220519.
(19) Cross, N. L.; Razy-Faulkner, P. Control of Human Sperm Intracellular PH by Cholesterol and Its Relationship to the Response of the Acrosome to Progesterone. *Biol Reprod* **1997**, *56* (5), 1169–1174. https://doi.org/10.1095/BIOLREPROD56.5.1169.
(20) López-González, I.; Torres-Rodríguez, P.; Sánchez-Carranza, O.; Solís-López, A.; Santi, C. M.; Darszon, A.; Treviño, C. L. Membrane Hyperpolarization during Human Sperm Capacitation. *Mol Hum Reprod* **2014**, *20* (7), 619–629. https://doi.org/10.1093/MOLEHR/GAU029.
(21) Baldi, E.; Casano, R.; Falsetti, C.; Krausz, C.; Maggi, M.; Forti, G. Intracellular Calcium Accumulation and Responsiveness to Progesterone in Capacitating Human Spermatozoa. *J Androl* **1991**, *12* (5), 323–330. https://doi.org/10.1002/J.1939-4640.1991.TB01610.X.
(22) Nishigaki, T.; José, O.; González-Cota, A. L.; Romero, F.; Treviño, C. L.; Darszon, A. Intracellular PH in Sperm Physiology. *Biochem Biophys Res Commun* **2014**, *450* (3), 1149–1158. https://doi.org/10.1016/J.BBRC.2014.05.100.
(23) Yutaka Tajima; Naomichi Okamura; Yoshiki Sugita. The Activating Effects of Bicarbonate on Sperm Motility and Respiration at Ejaculation. *Biochimica et Biophysica Acta (BBA) - General Subjects* **1987**, *924* (3), 519–529. https://doi.org/10.1016/0304-4165(87)90168-1.
(24) Alvau, A.; Battistone, M. A.; Gervasi, M. G.; Navarrete, F. A.; Xu, X.; Sánchez-Cárdenas, C.; de la Vega-Beltran, J. L.; da Ros, V. G.; Greer, P. A.; Darszon, A.; Krapf, D.; Salicioni, A. M.; Cuasnicu, P. S.; Visconti, P. E. The Tyrosine Kinase FER Is Responsible for the Capacitationassociated Increase in Tyrosine Phosphorylation in Murine Sperm. *Development (Cambridge)* **2016**, *143* (13), 2325–2333. https://doi.org/10.1242/DEV.136499/263999/AM/THE-TYROSINE-KINASE-FER-IS-RESPONSIBLE-FOR-THE.
(25) Battistone, M. A.; da Ros, V. G.; Salicioni, A. M.; Navarrete, F. A.; Krapf, D.; Visconti, P. E.; Cuasnicú, P. S. Functional Human Sperm Capacitation Requires Both Bicarbonate-Dependent PKA Activation and down-Regulation of Ser/Thr Phosphatases by Src Family Kinases. *Mol Hum Reprod* **2013**, *19* (9), 570. https://doi.org/10.1093/MOLEHR/GAT033.
(26) Marquez, B.; Suarez, S. S. Different Signaling Pathways in Bovine Sperm Regulate Capacitation and Hyperactivation. *Biol Reprod* **2004**, *70* (6), 1626–1633. https://doi.org/10.1095/BIOLREPROD.103.026476.
(27) Cohen, P. THE STRUCTURE AND REGULATION OF PROTEIN PHOSPHATASES. *https://doi.org/10.1146/annurev.bi.58.070189.002321* **1989**, *58*, 453–508. https://doi.org/10.1146/ANNUREV.BI.58.070189.002321.
(28) Sontag, E. Protein Phosphatase 2A: The Trojan Horse of Cellular Signaling. *Cell Signal* **2001**, *13* (1), 7–16. https://doi.org/10.1016/S0898-6568(00)00123-6.
(29) Barford, D.; Das, A. K.; Egloff, M. P. THE STRUCTURE AND MECHANISM OF PROTEIN PHOSPHATASES: Insights into Catalysis and Regulation. *http://dx.doi.org/10.1146/annurev.biophys.27.1.133* **1998**, *27*, 133–164. https://doi.org/10.1146/ANNUREV.BIOPHYS.27.1.133.
(30) Fardilha, M.; Esteves, S. L. C.; Korrodi-Gregório, L.; Pelech, S.; da Cruz e Silva, O. A. B.; da Cruz e Silva, E. Protein Phosphatase 1 Complexes Modulate Sperm Motility and Present Novel Targets for Male Infertility. *Mol Hum Reprod* **2011**, *17* (8), 466–477. https://doi.org/10.1093/MOLEHR/GAR004.
(31) Rebelo, S.; Santos, M.; Martins, F.; da Cruz e Silva, E. F.; da Cruz e Silva, O. A. B. Protein Phosphatase 1 Is a Key Player in Nuclear Events. *Cell Signal* **2015**, *27* (12), 2589–2598. https://doi.org/10.1016/J.CELLSIG.2015.08.007.

(32) Cohen, P. The Origins of Protein Phosphorylation. *Nature Cell Biology 2002 4:5* **2002**, *4* (5), E127–E130. https://doi.org/10.1038/ncb0502-e127.
(33) Baldi, E.; Luconi, M.; Bonaccorsi, L.; Forti, G. Signal Transduction Pathways in Human Spermatozoa. *J Reprod Immunol* **2002**, *53* (1–2), 121–131. https://doi.org/10.1016/S0165-0378(01)00089-4.
(34) Dey, S.; Eisa, A.; Kline, D.; Wagner, F. F.; Abeysirigunawardena, S.; Vijayaraghavan, S. Roles of Glycogen Synthase Kinase 3 Alpha and Calcineurin in Regulating the Ability of Sperm to Fertilize Eggs. *The FASEB Journal* **2019**, *34* (1), 1247–1269. https://doi.org/10.1096/FJ.201902163R.
(35) Signorelli, J. R.; Díaz, E. S.; Fara, K.; Barón, L.; Morales, P. Protein Phosphatases Decrease Their Activity during Capacitation: A New Requirement for This Event. *PLoS One* **2013**, *8* (12). https://doi.org/10.1371/journal.pone.0081286.
(36) Smith, G. D.; Wolf, D. P.; Trautman, K.; Cruz e Silva, E. F.; Greengard, P.; Srinivasan, V. Primate Sperm Contain Protein Phosphatase 1, a Biochemical Mediator of Motility. *Biol Reprod* **1996**, *54* (3), 719–727. https://doi.org/10.1095/BIOLREPROD54.3.719.
(37) Fardilha, M.; Esteves, S.; Korrodi-Gregório, L.; Vintém, A.; Domingues, S.; Rebelo, S.; Morrice, N.; Cohen, P.; da Cruz e Silva, O.; da Cruz e Silva, E. Identification of the Human Testis Protein Phosphatase 1 Interactome. *Biochem Pharmacol* **2011**, *82* (10), 1403–1415. https://doi.org/10.1016/J.BCP.2011.02.018.
(38) Lee, J. H.; You, J.; Dobrota, E.; Skalnik, D. G. Identification and Characterization of a Novel Human PP1 Phosphatase Complex. *J Biol Chem* **2010**, *285* (32), 24466. https://doi.org/10.1074/JBC.M110.109801.
(39) Verbinnen, I.; Ferreira, M.; Bollen, M. Biogenesis and Activity Regulation of Protein Phosphatase 1. *Biochem Soc Trans* **2017**, *45* (1), 89–99. https://doi.org/10.1042/BST20160154.
(40) Goldberg, J.; Huang, H. Bin; Kwon, Y. G.; Greengard, P.; Nairn, A. C.; Kuriyan, J. Three-Dimensional Structure of the Catalytic Subunit of Protein Serine/Threonine Phosphatase-1. *Nature 1995 376:6543* **1995**, *376* (6543), 745–753. https://doi.org/10.1038/376745a0.
(41) da Cruz e Silva, E.; Fox, C. A.; Ouimet, C. C.; Gustafson, E.; Watson, S. J.; Greengard, P. Differential Expression of Protein Phosphatase 1 Isoforms in Mammalian Brain. *J Neurosci* **1995**, *15* (5 Pt 1), 3375–3389. https://doi.org/10.1523/JNEUROSCI.15-05-03375.1995.
(42) Berndt, N.; Campbell, D. G.; Caudwell, F. B.; Cohen, P.; Silva, E. F. da C. e; Silva, O. B. da C. e; Cohen, P. T. W. Isolation and Sequence Analysis of a CDNA Clone Encoding a Type-1 Protein Phosphatase Catalytic Subunit: Homology with Protein Phosphatase 2A. *FEBS Lett* **1987**, *223* (2), 340–346. https://doi.org/10.1016/0014-5793(87)80316-2.
(43) Fardilha, M.; L.C. Esteves, S.; Korrodi-Gregorio, L.; A.B. da Cruz e Silva, O.; F. da Cruz e Silva, E. The Physiological Relevance of Protein Phosphatase 1 and Its Interacting Proteins to Health and Disease. *Curr Med Chem* **2010**, *17* (33), 3996–4017. https://doi.org/10.2174/092986710793205363.
(44) Wu, D.; De Wever, V.; Derua, R.; Winkler, C.; Beullens, M.; Van Eynde, A.; Bollen, M. A Substrate-Trapping Strategy for Protein Phosphatase PP1 Holoenzymes Using Hypoactive Subunit Fusions. *J Biol Chem* **2018**, *293* (39), 15152–15162. https://doi.org/10.1074/JBC.RA118.004132.
(45) Alanis-Lobato, G.; Andrade-Navarro, M. A.; Schaefer, M. H. HIPPIE v2.0: Enhancing Meaningfulness and Reliability of Protein-Protein Interaction Networks. *Nucleic Acids Res* **2017**, *45*. https://doi.org/10.1093/nar/gkw985.
(46) Chakrabarti, R.; Cheng, L.; Puri, P.; Soler, D.; Vijayaraghavan, S. Protein Phosphatase PP1 Gamma 2 in Sperm Morphogenesis and Epididymal Initiation of Sperm Motility. *Asian J Androl* **2007**, *9* (4), 445–452. https://doi.org/10.1111/J.1745-7262.2007.00307.X.

(47) Varmuza, S.; Jurisicova, A.; Okano, K.; Hudson, J.; Boekelheide, K.; Shipp, E. B. Spermiogenesis Is Impaired in Mice Bearing a Targeted Mutation in the Protein Phosphatase 1cγ Gene. *Dev Biol* **1999**, *205* (1), 98–110. https://doi.org/10.1006/DBIO.1998.9100.

(48) Chakrabarti, R.; Kline, D.; Lu, J.; Orth, J.; Pilder, S.; Vijayaraghavan, S. Analysis of Ppp1cc-Null Mice Suggests a Role for PP1gamma2 in Sperm Morphogenesis. *Biol Reprod* **2007**, *76* (6), 992–1001. https://doi.org/10.1095/BIOLREPROD.106.058610.

(49) Sinha, N.; Puri, P.; Nairn, A. C.; Vijayaraghavan, S. Selective Ablation of Ppp1cc Gene in Testicular Germ Cells Causes Oligo-Teratozoospermia and Infertility in Mice. *Biol Reprod* **2013**, *89* (5), 1–15. https://doi.org/10.1095/BIOLREPROD.113.110239/2514269.

(50) Sinha, N.; Pilder, S.; Vijayaraghavan, S. Significant Expression Levels of Transgenic PPP1CC2 in Testis and Sperm Are Required to Overcome the Male Infertility Phenotype of Ppp1cc Null Mice. *PLoS One* **2012**, *7* (10), e47623. https://doi.org/10.1371/JOURNAL.PONE.0047623.

(51) Goswami, S.; Korrodi-Gregório, L.; Sinha, N.; Bhutada, S.; Bhattacharjee, R.; Kline, D.; Vijayaraghavan, S. Regulators of the Protein Phosphatase PP1γ2, PPP1R2, PPP1R7, and PPP1R11 Are Involved in Epididymal Sperm Maturation. *J Cell Physiol* **2019**, *234* (3), 3105–3118. https://doi.org/10.1002/JCP.27130.

(52) Mishra, S.; Somanath, P. R.; Huang, Z.; Vijayaraghavan, S. Binding and Inactivation of the Germ Cell-Specific Protein Phosphatase PP1gamma2 by Sds22 during Epididymal Sperm Maturation. *Biol Reprod* **2003**, *69* (5), 1572–1579. https://doi.org/10.1095/BIOLREPROD.103.018739.

(53) Korrodi-Gregório, L.; Ferreira, M.; Vintém, A. P.; Wu, W.; Muller, T.; Marcus, K.; Vijayaraghavan, S.; Brautigan, D. L.; da Cruz e Silva, O. A. B.; Fardilha, M.; da Cruz e Silva, E. F. Identification and Characterization of Two Distinct PPP1R2 Isoforms in Human Spermatozoa. *BMC Cell Biol* **2013**, *14* (1), 1–14. https://doi.org/10.1186/1471-2121-14-15/FIGURES/8.

(54) Schwarz, T.; Prieler, B.; Schmid, J. A.; Grzmil, P.; Neesen, J. Ccdc181 Is a Microtubule-Binding Protein That Interacts with Hook1 in Haploid Male Germ Cells and Localizes to the Sperm Tail and Motile Cilia. *Eur J Cell Biol* **2017**, *96* (3), 276–288. https://doi.org/10.1016/J.EJCB.2017.02.003.

(55) Somanath, P. R.; Jack, S. L.; Vijayaraghavan, S. Changes in Sperm Glycogen Synthase Kinase-3 Serine Phosphorylation and Activity Accompany Motility Initiation and Stimulation. *J Androl* **2004**, *25* (4), 605–617. https://doi.org/10.1002/J.1939-4640.2004.TB02831.X.

(56) Bhattacharjee, R.; Goswami, S.; Dey, S.; Gangoda, M.; Brothag, C.; Eisa, A.; Woodgett, J.; Phiel, C.; Kline, D.; Vijayaraghavan, S. Isoform-Specific Requirement for GSK3α in Sperm for Male Fertility. *Biol Reprod* **2018**, *99* (2), 384–394. https://doi.org/10.1093/BIOLRE/IOY020.

(57) Freitas, M. J.; Silva, J. V.; Brothag, C.; Regadas-Correia, B.; Fardilha, M.; Vijayaraghavan, S. Isoform-Specific GSK3A Activity Is Negatively Correlated with Human Sperm Motility. *Mol Hum Reprod* **2019**, *25* (4), 171–183. https://doi.org/10.1093/molehr/gaz009.

(58) Vijayaraghavan, S.; Mohan, J.; Gray, H.; Khatra, B.; Carr, D. W. A Role for Phosphorylation of Glycogen Synthase Kinase-3alpha in Bovine Sperm Motility Regulation. *Biol Reprod* **2000**, *62* (6), 1647–1654. https://doi.org/10.1095/BIOLREPROD62.6.1647.

(59) Janssens, V.; Goris, J. Protein Phosphatase 2A: A Highly Regulated Family of Serine/Threonine Phosphatases Implicated in Cell Growth and Signalling. *Biochem J* **2001**, *353* (Pt 3), 417–439. https://doi.org/10.1042/0264-6021:3530417.

(60) Dudiki, T.; Kadunganattil, S.; Ferrara, J. K.; Kline, D. W.; Vijayaraghavan, S. Changes in Carboxy Methylation and Tyrosine Phosphorylation of Protein Phosphatase PP2A Are

Associated with Epididymal Sperm Maturation and Motility. *PLoS One* **2015**, *10* (11), 1–18. https://doi.org/10.1371/journal.pone.0141961.

(61) Xing, Y.; Xu, Y.; Chen, Y.; Jeffrey, P. D.; Chao, Y.; Lin, Z.; Li, Z.; Strack, S.; Stock, J. B.; Shi, Y. Structure of Protein Phosphatase 2A Core Enzyme Bound to Tumor-Inducing Toxins. *Cell* **2006**, *127* (2), 341–353. https://doi.org/10.1016/J.CELL.2006.09.025.

(62) Morales, P.; Signorelli, J. R.; Diaz, E. S. Protein Phosphatase-Type 2A (PP2A) Is Involved in the Initial Events of Human Sperm Capacitation. *Biol Reprod* **2010**, *83* (Suppl_1), 172–172. https://doi.org/10.1093/BIOLREPROD/83.S1.172.

(63) Ahmad, K.; Bracho, G. E.; Wolf, D. P.; Tash, J. S. Regulation of Human Sperm Motility and Hyperactivation Components by Calcium, Calmodulin, and Protein Phosphatases. *http://dx.doi.org/10.3109/01485019508987871* **1995**, *35* (3), 187–208. https://doi.org/10.3109/01485019508987871.

(64) Miyata, H.; Satouh, Y.; Mashiko, D.; Muto, M.; Nozawa, K.; Shiba, K.; Fujihara, Y.; Isotani, A.; Inaba, K.; Ikawa, M. Sperm Calcineurin Inhibition Prevents Mouse Fertility with Implications for Male Contraceptive. *Science* **2015**, *350* (6259), 442–445. https://doi.org/10.1126/SCIENCE.AAD0836.

(65) Rusnak, F.; Mertz, P. Calcineurin: Form and Function. *Physiol Rev* **2000**, *80* (4), 1483–1521. https://doi.org/10.1152/PHYSREV.2000.80.4.1483.

(66) Kissinger, C. R.; Parge, H. E.; Knighton, D. R.; Lewis, C. T.; Pelletier, L. A.; Tempczyk, A.; Kalish, V. J.; Tucker, K. D.; Showalter, R. E.; Moomaw, E. W.; Gastinel, L. N.; Habuka, N.; Chen, X.; Maldonado, F.; Barker, J. E.; Bacquet, R.; Villafranca, J. E. Crystal Structures of Human Calcineurin and the Human FKBP12–FK506–Calcineurin Complex. *Nature 1995 378:6557* **1995**, *378* (6557), 641–644. https://doi.org/10.1038/378641a0.

(67) Jin, L.; Harrison, S. C. Crystal Structure of Human Calcineurin Complexed with Cyclosporin A and Human Cyclophilin. *Proceedings of the National Academy of Sciences* **2002**, *99* (21), 13522–13526. https://doi.org/10.1073/PNAS.212504399.

(68) Buffone, M. G.; Wertheimer, E. V.; Visconti, P. E.; Krapf, D. Central Role of Soluble Adenylyl Cyclase and CAMP in Sperm Physiology. *Biochimica et Biophysica Acta (BBA) - Molecular Basis of Disease* **2014**, *1842* (12), 2610–2620. https://doi.org/10.1016/J.BBADIS.2014.07.013.

(69) Sette, C.; Conti, M. Phosphorylation and Activation of a CAMP-Specific Phosphodiesterase by the CAMP-Dependent Protein Kinase: INVOLVEMENT OF SERINE 54 IN THE ENZYME ACTIVATION. *Journal of Biological Chemistry* **1996**, *271* (28), 16526–16534. https://doi.org/10.1074/JBC.271.28.16526.

(70) Dey, S.; Goswami, S.; Eisa, A.; Bhattacharjee, R.; Brothag, C.; Kline, D.; Vijayaraghavan, S. Cyclic AMP and Glycogen Synthase Kinase 3 Form a Regulatory Loop in Spermatozoa. *J Cell Physiol* **2018**, *233* (9), 7239. https://doi.org/10.1002/JCP.26557.

(71) Salvi, F.; Hoermann, B.; del Pino García, J.; Fontanillo, M.; Derua, R.; Beullens, M.; Bollen, M.; Barabas, O.; Köhn, M. Towards Dissecting the Mechanism of Protein Phosphatase-1 Inhibition by Its C-Terminal Phosphorylation. *ChemBioChem* **2021**, *22* (5), 834–838. https://doi.org/10.1002/CBIC.202000669.

(72) Chen, Y.; Cann, M. J.; Litvin, T. N.; Iourgenko, V.; Sinclair, M. L.; Levin, L. R.; Buck, J. Soluble Adenylyl Cyclase as an Evolutionarily Conserved Bicarbonate Sensor. *Science* **2000**, *289* (5479), 625–628. https://doi.org/10.1126/SCIENCE.289.5479.625.

(73) Xie, F.; Garcia, M. A.; Carlson, A. E.; Schuh, S. M.; Babcock, D. F.; Jaiswal, B. S.; Gossen, J. A.; Esposito, G.; van Duin, M.; Conti, M. Soluble Adenylyl Cyclase (SAC) Is Indispensable for Sperm Function and Fertilization. *Dev Biol* **2006**, *296* (2), 353–362. https://doi.org/10.1016/J.YDBIO.2006.05.038.

(74) Pereira, S. R.; Vasconcelos, V. M.; Antunes, A. The Phosphoprotein Phosphatase Family of Ser/Thr Phosphatases as Principal Targets of Naturally Occurring Toxins. *Crit Rev Toxicol* **2011**, *41* (2), 83–110. https://doi.org/10.3109/10408444.2010.515564.

(75) Swingle, M.; Ni, L.; Honkanen, R. E. Small-Molecule Inhibitors of Ser/Thr Protein Phosphatases: Specificity, Use and Common Forms of Abuse. *Methods Mol Biol* **2007**, *365*, 23–38. https://doi.org/10.1385/1-59745-267-X:23.
(76) Honkanen, R.; Golden, T. Regulators of Serine / Threonine Protein Phosphatases at the Dawn of a Clinical Era? *Curr Med Chem* **2002**, *9* (22), 2055–2075. https://doi.org/10.2174/0929867023368836.
(77) Fujiki, H.; Suganuma, M. Tumor Promotion by Inhibitors of ProteinZ Phosphatases 1 and 2A: The Okadaic Acid Class of Compounds. *Adv Cancer Res* **1993**, *61* (C), 143–194. https://doi.org/10.1016/S0065-230X(08)60958-6.
(78) Ishihara, H.; Martin, B. L.; Brautigan, D. L.; Karaki, H.; Ozaki, H.; Kato, Y.; Fusetani, N.; Watabe, S.; Hashimoto, K.; Uemura, D.; Hartshorne, D. J. Calyculin A and Okadaic Acid: Inhibitors of Protein Phosphatase Activity. *Biochem Biophys Res Commun* **1989**, *159* (3), 871–877. https://doi.org/10.1016/0006-291X(89)92189-X.
(79) Fruman, D. A.; Klee, C. B.; Bierer, B. E.; Burakoff, S. J. Calcineurin Phosphatase Activity in T Lymphocytes Is Inhibited by FK 506 and Cyclosporin A. *Proc Natl Acad Sci U S A* **1992**, *89* (9), 3686. https://doi.org/10.1073/PNAS.89.9.3686.
(80) Laidley, C. W.; Cohen, E.; Casida, J. E. Protein Phosphatase in Neuroblastoma Cells: [3H]Cantharidin Binding Site in Relation to Cytotoxicity. *Journal of Pharmacology and Experimental Therapeutics* **1997**, *280* (3).
(81) Enan, E.; Matsumura, F. Specific Inhibition of Calcineurin by Type II Synthetic Pyrethroid Insecticides. *Biochem Pharmacol* **1992**, *43* (8), 1777–1784. https://doi.org/10.1016/0006-2952(92)90710-Z.
(82) MacKintosh, C.; Klumpp, S. Tautomycin from the Bacterium Streptomyces Verticillatus. Another Potent and Specific Inhibitor of Protein Phosphatases 1 and 2A. *FEBS Lett* **1990**, *277* (1–2), 137–140. https://doi.org/10.1016/0014-5793(90)80828-7.
(83) Carmichael, W. W. Cyanobacteria Secondary Metabolites—the Cyanotoxins. *Journal of Applied Bacteriology* **1992**, *72* (6), 445–459. https://doi.org/10.1111/J.1365-2672.1992.TB01858.X.
(84) Swingle, M. R.; Honkanen, R. E. Inhibitors of Serine/Threonine Protein Phosphatases: Biochemical and Structural Studies Provide Insight for Further Development. *Curr Med Chem* **2019**, *26* (15), 2634–2660. https://doi.org/10.2174/0929867325666180508095242.
(85) Woydziak, Z.; Yucel, A.; Chamberlin, A. Tautomycetin Synthetic Analogues: Selective Inhibitors of Protein Phosphatase I. *ChemMedChem* **2021**, *16* (5), 839–850. https://doi.org/10.1002/CMDC.202000801.
(86) Zhang, M.; Yogesha, S. D.; Mayfield, J. E.; Gill, G. N.; Zhang, Y. Viewing Serine/Threonine Protein Phosphatases through the Eyes of Drug Designers. *FEBS J* **2013**, *280* (19), 4739–4760. https://doi.org/10.1111/FEBS.12481.
(87) Ashizawa, K.; Wishart, G. J.; Tomonaga, H.; Nishinakama, K.; Tsuzuki, Y. Presence of Protein Phosphatase Type 1 and Its Involvement in Temperature-Dependent Flagellar Movement of Fowl Spermatozoa. *FEBS Lett* **1994**, *350* (1), 130–134. https://doi.org/10.1016/0014-5793(94)00752-7.
(88) Ashizawa, K.; Magome, A.; Tsuzuki, Y. Stimulation of Motility and Respiration of Intact Fowl Spermatozoa by Calyculin A, a Specific Inhibitor of Protein Phosphatase-1 and -2A, via a Ca2+-Dependent Mechanism. *Reproduction* **1995**, *105* (1), 109–114. https://doi.org/10.1530/JRF.0.1050109.
(89) Ashizawa, K.; Wishart, G. J.; Katayama, S.; Takano, D.; Ranasinghe, A. R. A. H.; Narumi, K.; Tsuzuki, Y. Regulation of Acrosome Reaction of Fowl Spermatozoa: Evidence for the Involvement of Protein Kinase C and Protein Phosphatase-Type 1 and/or -Type 2A. *Reproduction* **2006**, *131* (6), 1017–1024. https://doi.org/10.1530/REP.1.01069.
(90) Goto, N.; Harayama, H. Calyculin A-Sensitive Protein Phosphatases Are Involved in Maintenance of Progressive Movement in Mouse Spermatozoa in Vitro by Suppression

of Autophosphorylation of Protein Kinase A. *J Reprod Dev* **2009**, *55* (3), 327–334. https://doi.org/10.1262/JRD.20170.

(91) Krapf, D.; Arcelay, E.; Wertheimer, E. v.; Sanjay, A.; Pilder, S. H.; Salicioni, A. M.; Visconti, P. E. Inhibition of Ser/Thr Phosphatases Induces Capacitation-Associated Signaling in the Presence of Src Kinase Inhibitors. *Journal of Biological Chemistry* **2010**, *285* (11), 7977–7985. https://doi.org/10.1074/JBC.M109.085845.

(92) Petrunkina, A. M.; Harrison, R. A. P.; Tsolova, M.; Jebe, E.; Töpfer-Petersen, E. Signalling Pathways Involved in the Control of Sperm Cell Volume. *Reproduction* **2007**, *133* (1), 61–73. https://doi.org/10.1530/REP.1.01137.

(93) Harayama, H.; Noda, T.; Ishikawa, S.; Shidara, O. Relationship between Cyclic AMP-Dependent Protein Tyrosine Phosphorylation and Extracellular Calcium during Hyperactivation of Boar Spermatozoa. *Mol Reprod Dev* **2012**, *79* (10), 727–739. https://doi.org/10.1002/MRD.22106.

(94) Huang, Z.; Vijayaraghavan, S. Increased Phosphorylation of a Distinct Subcellular Pool of Protein Phosphatase, PP1γ2, During Epididymal Sperm Maturation. *Biol Reprod* **2004**, *70* (2), 439–447. https://doi.org/10.1095/BIOLREPROD.103.020024.

(95) Smith, G. D.; Wolf, D. P.; Trautman, K. C.; Vijayaraghavan, S. Motility Potential of Macaque Epididymal Sperm: The Role of Protein Phosphatase and Glycogen Synthase Kinase-3 Activities. *J Androl* **1999**, *20* (1), 47–53. https://doi.org/https://doi.org/10.1002/j.1939-4640.1999.tb02495.x.

(96) Leclerc, P.; de Lamirande, E.; Gagnon, C. Cyclic Adenosine 3',5'monophosphate-Dependent Regulation of Protein Tyrosine Phosphorylation in Relation to Human Sperm Capacitation and Motility. *Biol Reprod* **1996**, *55* (3), 684–692. https://doi.org/10.1095/BIOLREPROD55.3.684.

(97) Carrera, A.; Moos, J.; Ning, X. P.; Gerton, G. L.; Tesarik, J.; Kopf, G. S.; Moss, S. B. Regulation of Protein Tyrosine Phosphorylation in Human Sperm by a Calcium/Calmodulin-Dependent Mechanism: Identification of A Kinase Anchor Proteins as Major Substrates for Tyrosine Phosphorylation. *Dev Biol* **1996**, *180* (1), 284–296. https://doi.org/10.1006/DBIO.1996.0301.

(98) Bennett, J. C.; Roggero, C. M.; Mancifesta, F. E.; Mayorga, L. S. Calcineurin-Mediated Dephosphorylation of Synaptotagmin VI Is Necessary for Acrosomal Exocytosis. *J Biol Chem* **2010**, *285* (34), 26269–26278. https://doi.org/10.1074/JBC.M109.095752.

(99) Ashizawa, K.; Wishart, G. J.; Ranasinghe, A. R. A. H.; Katayama, S.; Tsuzuki, Y. Protein Phosphatase-Type 2B Is Involved in the Regulation of the Acrosome Reaction but Not in the Temperature-Dependent Flagellar Movement of Fowl Spermatozoa. *Reproduction* **2004**, *128* (6), 783–787. https://doi.org/10.1530/REP.1.00327.

(100) Bertini, I.; Calderone, V.; Fragai, M.; Luchinat, C.; Talluri, E. Structural Basis of Serine/Threonine Phosphatase Inhibition by the Archetypal Small Molecules Cantharidin and Norcantharidin. *J Med Chem* **2009**, *52* (15), 4838–4843. https://doi.org/10.1021/JM900610K/SUPPL_FILE/JM900610K_SI_001.PDF.

(101) Honkanen, R. E. Cantharidin, Another Natural Toxin That Inhibits the Activity of Serine/Threonine Protein Phosphatases Types 1 and 2A. *FEBS Lett* **1993**, *330* (3), 283–286. https://doi.org/10.1016/0014-5793(93)80889-3.

(102) Li, Y. M.; Mackintosh, C.; Casida, J. E. Protein Phosphatase 2A and Its [3H]Cantharidin/[3H]Endothall Thioanhydride Binding Site. Inhibitor Specificity of Cantharidin and ATP Analogues. *Biochem Pharmacol* **1993**, *46* (8), 1435–1443. https://doi.org/10.1016/0006-2952(93)90109-A.

(103) Neumann, J.; Bokník, P.; Kaspareit, G.; Bartel, S.; Krause, E. G.; Pask, H. T.; Schmitz, W.; Scholz, H. Effects of the Phosphatase Inhibitor Calyculin A on the Phosphorylation of C-Protein in Mammalian Ventricular Cardiomyocytes. *Biochem Pharmacol* **1995**, *49* (11), 1583–1588. https://doi.org/10.1016/0006-2952(95)00101-5.

(104) Kelker, M. S.; Page, R.; Peti, W. Crystal Structures of Protein Phosphatase-1 Bound to Nodularin-R and Tautomycin: A Novel Scaffold for Structure-Based Drug Design of Serine/Threonine Phosphatase Inhibitors. *J Mol Biol* **2009**, *385* (1), 11–21. https://doi.org/10.1016/J.JMB.2008.10.053.

(105) Takai, A.; Sasaki, K.; Nagai, H.; Mieskes, G.; Isobe, M.; Isono, K.; Yasumoto, T. Inhibition of Specific Binding of Okadaic Acid to Protein Phosphatase 2A by Microcystin-LR, Calyculin-A and Tautomycin: Method of Analysis of Interactions of Tight-Binding Ligands with Target Protein. *Biochem J* **1995**, *306 (Pt 3)* (Pt 3), 657–665. https://doi.org/10.1042/BJ3060657.

(106) Suzuki, T.; Fujinoki, M.; Shibahara, H.; Suzuki, M. Regulation of Hyperactivation by PPP2 in Hamster Spermatozoa. *Reproduction* **2010**, *139* (5), 847–856. https://doi.org/10.1530/REP-08-0366.

(107) Ravula, A. R.; Yenugu, S. Pyrethroid Based Pesticides–Chemical and Biological Aspects. *Crit Rev Toxicol* **2021**, *51* (2), 117–140. https://doi.org/10.1080/10408444.2021.1879007.

(108) Zalata, A.; Elhanbly, S.; Abdalla, H.; Serria, M. S.; Aziz, A.; El-Dakrooy, S. A.; El-Bakary, A. A.; Mostafa, T. In Vitro Study of Cypermethrin on Human Spermatozoa and the Possible Protective Role of Vitamins C and E. *Andrologia* **2014**, *46* (10), 1141–1147. https://doi.org/10.1111/AND.12206.

(109) Yuan, C.; Wang, C.; Gao, S. Q.; Kong, T. T.; Chen, L.; Li, X. F.; Song, L.; Wang, Y. B. Effects of Permethrin, Cypermethrin and 3-Phenoxybenzoic Acid on Rat Sperm Motility in Vitro Evaluated with Computer-Assisted Sperm Analysis. *Toxicology in Vitro* **2010**, *24* (2), 382–386. https://doi.org/10.1016/J.TIV.2009.11.001.

(110) Song, L.; Wang, Y. B.; Sun, H.; Yuan, C.; Hong, X.; Qu, J. H.; Zhou, J. W.; Wang, X. R. Effects of Fenvalerate and Cypermethrin on Rat Sperm Motility Patterns In Vitro as Measured by Computer-Assisted Sperm Analysis. *http://dx.doi.org/10.1080/15287390701738517* **2008**, *71* (5), 325–332. https://doi.org/10.1080/15287390701738517.

(111) Zinaman, M. J.; Brown, C. C.; Selevan, S. G.; Clegg, E. D. Semen Quality and Human Fertility: A Prospective Study With Healthy Couples. *J Androl* **2000**, *21* (1), 145–153. https://doi.org/10.1002/J.1939-4640.2000.TB03284.X.

(112) Larsen, L.; Scheike, T.; Jensen, T. K.; Bonde, J. P.; Ernst, E.; Hjollund, N. H. I.; Zhou, Y.; Skakkebæk, N. E.; Giwercman, A.; Bonde, J. P. E.; Henriksen, T. B.; Kolstad, H. A.; Anderson, A. M.; Giwercman, A.; Olsen, J. Computer-Assisted Semen Analysis Parameters as Predictors for Fertility of Men from the General Population. The Danish First Pregnancy Planner Study Team. *Hum Reprod* **2000**, *15* (7), 1562–1567. https://doi.org/10.1093/HUMREP/15.7.1562.

(113) World Health Organization. *WHO Laboratory Manual for the Examination and Processing of Human Semen*, Sixth.; Geneva, 2021; Vol. Edition, V.

(114) Eliasson, R. Semen Analysis with Regard to Sperm Number, Sperm Morphology and Functional Aspects. *Asian J Androl* **2010**, *12* (1), 26–32. https://doi.org/10.1038/AJA.2008.58.

(115) Amann, R. P.; Waberski, D. Computer-Assisted Sperm Analysis (CASA): Capabilities and Potential Developments. *Theriogenology* **2014**, *81* (1), 5-17.e3. https://doi.org/10.1016/J.THERIOGENOLOGY.2013.09.004.

(116) Mortimer, S.; Mortimer, D.; Fraser, L. Guidelines on the Application of CASA Technology in the Analysis of Spermatozoa. *Human Reproduction* **1998**, *13* (1), 142–145. https://doi.org/10.1093/humrep/13.1.142.

(117) Fréour, T.; Jean, M.; Mirallie, S.; Barriere, P. Computer-Assisted Sperm Analysis Parameters in Young Fertile Sperm Donors and Relationship with Age. *http://dx.doi.org/10.3109/19396368.2011.642054* **2012**, *58* (2), 102–106. https://doi.org/10.3109/19396368.2011.642054.

(118) Valverde, A.; Barquero, V.; Soler, C. The Application of Computer-Assisted Semen Analysis (CASA) Technology to Optimise Semen Evaluation. A Review. *J Anim Feed Sci* **2020**, *29* (3), 189–198. https://doi.org/10.22358/JAFS/127691/2020.
(119) Valverde, A.; Madrigal, M.; Caldeira, C.; Bompart, D.; de Murga, J. N.; Arnau, S.; Soler, C. Effect of Frame Rate Capture Frequency on Sperm Kinematic Parameters and Subpopulation Structure Definition in Boars, Analysed with a CASA-Mot System. *Reproduction in Domestic Animals* **2019**, *54* (2), 167–175. https://doi.org/10.1111/RDA.13320.
(120) Soler, C.; Picazo-Bueno, J.; Micó, V.; Valverde, A.; Bompart, D.; Blasco, F. J.; Álvarez, J. G.; García-Molina, A. Effect of Counting Chamber Depth on the Accuracy of Lensless Microscopy for the Assessment of Boar Sperm Motility. *Reprod Fertil Dev* **2018**, *30* (6), 924–934. https://doi.org/10.1071/RD17467.
(121) Muvhali, P. T.; Bonato, M.; Malecki, I. A.; Cloete, S. W. P. Mass Sperm Motility Is Correlated to Sperm Motility as Measured by Computer-Aided Sperm Analysis (CASA) Technology in Farmed Ostriches. *Animals (Basel)* **2022**, *12* (9), 1104. https://doi.org/10.3390/ANI12091104.
(122) Kraemer, M.; Fillion, C.; Martin-Pont, B.; Auger, J. Factors Influencing Human Sperm Kinematic Measurements by the Celltrak Computer-Assisted Sperm Analysis System. *Hum Reprod* **1998**, *13* (3), 611–619. https://doi.org/10.1093/HUMREP/13.3.611.
(123) Yániz, J.; Alquézar-Baeta, C.; Yagüe-Martínez, J.; Alastruey-Benedé, J.; Palacín, I.; Boryshpolets, S.; Kholodnyy, V.; Gadêlha, H.; Pérez-Pe, R. Expanding the Limits of Computer-Assisted Sperm Analysis through the Development of Open Software. *Biology (Basel)* **2020**, *9* (8), 1–16. https://doi.org/10.3390/BIOLOGY9080207.
(124) Duty, S. M.; Calafat, A. M.; Silva, M. J.; Brock, J. W.; Ryan, L.; Chen, Z.; Overstreet, J.; Hauser, R. The Relationship between Environmental Exposure to Phthalates and Computer-Aided Sperm Analysis Motion Parameters. *J Androl* **2004**, *25* (2), 293–302. https://doi.org/10.1002/J.1939-4640.2004.TB02790.X.
(125) Yang, Y.; Zhang, Y.; Ding, J.; Ai, S.; Guo, R.; Bai, X.; Yang, W. Optimal Analysis Conditions for Sperm Motility Parameters with a CASA System in a Passerine Bird, Passer Montanus. *Avian Res* **2019**, *10* (1), 1–10. https://doi.org/10.1186/S40657-019-0174-5/FIGURES/6.
(126) Fabbrocini, A.; Silvestri, F.; Vitiello, V.; Pelosi, S.; Sansone, G.; D'Adamo, R. A Step towards Using the Semen of the Common Pandora Pagellus Erythrinus for Practical Applications of Cryo-Research: The Computer-Assessed Sperm Motility Pattern in Long-Term Cryostored Samples. *Aquaculture* **2020**, *528*. https://doi.org/10.1016/J.AQUACULTURE.2020.735604.
(127) Sloter, E.; Schmid, T. E.; Marchetti, F.; Eskenazi, B.; Nath, J.; Wyrobek, A. J. Quantitative Effects of Male Age on Sperm Motion. *Human Reproduction* **2006**, *21* (11), 2868–2875. https://doi.org/10.1093/HUMREP/DEL250.
(128) Martínez-Pastor, F.; Tizado, E. J.; Garde, J. J.; Anel, L.; de Paz, P. Statistical Series: Opportunities and Challenges of Sperm Motility Subpopulation Analysis. *Theriogenology* **2011**, *75* (5), 783–795. https://doi.org/10.1016/J.THERIOGENOLOGY.2010.11.034.
(129) Mortimer, D.; Mortimer, S. T. Computer-Aided Sperm Analysis (CASA) of Sperm Motility and Hyperactivation. *Methods Mol Biol* **2013**, *927*, 77–87. https://doi.org/10.1007/978-1-62703-038-0_8.
(130) Cancel, A. M.; Lobdell, D.; Mendola, P.; Perreault, S. D. Objective Evaluation of Hyperactivated Motility in Rat Spermatozoa Using Computer-Assisted Sperm Analysis. *Human Reproduction* **2000**, *15* (6), 1322–1328. https://doi.org/10.1093/HUMREP/15.6.1322.
(131) Goodson, S. G.; White, S.; Stevans, A. M.; Bhat, S.; Kao, C. Y.; Jaworski, S.; Marlowe, T. R.; Kohlmeier, M.; McMillan, L.; Zeisel, S. H.; O'Brien, D. A. CASAnova: A Multiclass

Support Vector Machine Model for the Classification of Human Sperm Motility Patterns. *Biol Reprod* **2017**, *97* (5), 698–708. https://doi.org/10.1093/BIOLRE/IOX120.
(132) Ooi, E. H.; Smith, D. J.; Gadêlha, H.; Gaffney, E. A.; Kirkman-Brown, J. The Mechanics of Hyperactivation in Adhered Human Sperm. *R Soc Open Sci* **2014**, *1* (2). https://doi.org/10.1098/RSOS.140230.
(133) Alquézar-Baeta, C.; Gimeno-Martos, S.; Miguel-Jiménez, S.; Santolaria, P.; Yániz, J.; Palacín, I.; Casao, A.; Cebrián-Pérez, J. Á.; Muiño-Blanco, T.; Pérez-Pé, R. OpenCASA: A New Open-Source and Scalable Tool for Sperm Quality Analysis. *PLoS Comput Biol* **2019**, *15* (1), e1006691. https://doi.org/10.1371/JOURNAL.PCBI.1006691.
(134) Hicks, S. A.; Andersen, J. M.; Witczak, O.; Thambawita, V.; Halvorsen, P.; Hammer, H. L.; Haugen, T. B.; Riegler, M. A. Machine Learning-Based Analysis of Sperm Videos and Participant Data for Male Fertility Prediction. *Scientific Reports 2019 9:1* **2019**, *9* (1), 1–10. https://doi.org/10.1038/s41598-019-53217-y.
(135) Barratt, C. L. R.; Wang, C.; Baldi, E.; Toskin, I.; Kiarie, J.; Lamb, D. J. What Advances May the Future Bring to the Diagnosis, Treatment, and Care of Male Sexual and Reproductive Health? *Fertil Steril* **2022**, *117* (2), 258–267. https://doi.org/10.1016/J.FERTNSTERT.2021.12.013.
(136) Ottl, S.; Amiriparian, S.; Gerczuk, M.; Schuller, B. W. MotilitAI: A Machine Learning Framework for Automatic Prediction of Human Sperm Motility. *iScience* **2022**, *25* (8). https://doi.org/10.1016/J.ISCI.2022.104644.
(137) Gloria, A.; Carluccio, A.; Contri, A.; Wegher, L.; Valorz, C.; Robbe, D. The Effect of the Chamber on Kinetic Results in Cryopreserved Bull Spermatozoa. *Andrology* **2013**, *1* (6), 879–885. https://doi.org/10.1111/J.2047-2927.2013.00121.X.
(138) Hoogewijs, M. K.; de Vliegher, S. P.; Govaere, J. L.; de Schauwer, C.; de Kruif, A.; van Soom, A. Influence of Counting Chamber Type on CASA Outcomes of Equine Semen Analysis. *Equine Vet J* **2012**, *44* (5), 542–549. https://doi.org/10.1111/J.2042-3306.2011.00523.X.
(139) Nosrati, R.; Graham, P. J.; Zhang, B.; Riordon, J.; Lagunov, A.; Hannam, T. G.; Escobedo, C.; Jarvi, K.; Sinton, D. Microfluidics for Sperm Analysis and Selection. *Nat Rev Urol* **2017**, *14* (12), 707–730. https://doi.org/10.1038/NRUROL.2017.175.
(140) Dardmeh, F.; Heidari, M.; Alipour, H. Comparison of Commercially Available Chamber Slides for Computer-Aided Analysis of Human Sperm. *https://doi.org/10.1080/19396368.2020.1850907* **2020**, *67* (2), 168–175. https://doi.org/10.1080/19396368.2020.1850907.
(141) Santiago, J.; Silva, J. V.; Fardilha, M. First Insights on the Presence of the Unfolded Protein Response in Human Spermatozoa. *Int J Mol Sci* **2019**, *20* (21). https://doi.org/10.3390/IJMS20215518.
(142) Cory, A. H.; Owen, T. C.; Barltrop, J. A.; Cory, J. G. Use of an Aqueous Soluble Tetrazolium/Formazan Assay for Cell Growth Assays in Culture. *Cancer Commun* **1991**, *3* (7), 207–212. https://doi.org/10.3727/095535491820873191.
(143) Buranaamnuay, K. The MTT Assay Application to Measure the Viability of Spermatozoa: A Variety of the Assay Protocols. *Open Vet J* **2021**, *11* (2), 251. https://doi.org/10.5455/OVJ.2021.V11.I2.9.
(144) Aleshin, V. A.; Artiukhov, A. v.; Oppermann, H.; Kazantsev, A. v.; Lukashev, N. v.; Bunik, V. I. Mitochondrial Impairment May Increase Cellular NAD(P)H: Resazurin Oxidoreductase Activity, Perturbing the NAD(P)H-Based Viability Assays. *Cells 2015, Vol. 4, Pages 427-451* **2015**, *4* (3), 427–451. https://doi.org/10.3390/CELLS4030427.
(145) al Amir Dache, Z.; Otandault, A.; Tanos, R.; Pastor, B.; Meddeb, R.; Sanchez, C.; Arena, G.; Lasorsa, L.; Bennett, A.; Grange, T.; el Messaoudi, S.; Mazard, T.; Prevostel, C.; Thierry, A. R. Blood Contains Circulating Cell-Free Respiratory Competent Mitochondria. *The FASEB Journal* **2020**, *34* (3), 3616–3630. https://doi.org/10.1096/FJ.201901917RR.

(146) Elgeti, J.; Kaupp, U. B.; Gompper, G. Hydrodynamics of Sperm Cells near Surfaces. *Biophys J* **2010**, *99* (4), 1018. https://doi.org/10.1016/J.BPJ.2010.05.015.
(147) Zaferani, M.; Javi, F.; Mokhtare, A.; Li, P.; Abbaspourrad, A. Rolling Controls Sperm Navigation in Response to the Dynamic Rheological Properties of the Environment. *Elife* **2021**, *10*. https://doi.org/10.7554/ELIFE.68693.
(148) Dodaran, H. V.; Zhandi, M.; Sharafi, M.; Nejati-Amiri, E.; Nejati-Javaremi, A.; Mohammadi-Sangcheshmeh, A.; Shehab-El-Deen, M. A. M. M.; Shakeri, M. Effect of Ethanol Induced Mild Stress on Post-Thawed Bull Sperm Quality. *Cryobiology* **2015**, *71* (1), 12–17. https://doi.org/10.1016/J.CRYOBIOL.2015.06.008.
(149) Donnelly, G. P.; McClure, N.; Kennedy, M. S.; Lewis, S. E. M. Direct Effect of Alcohol on the Motility and Morphology of Human Spermatozoa. *Andrologia* **1999**, *31* (1), 43–47. https://doi.org/10.1111/J.1439-0272.1999.TB02841.X.
(150) Oberoi, B.; Kumar, S.; Talwar, P. Study of Human Sperm Motility Post Cryopreservation. *Med J Armed Forces India* **2014**, *70* (4), 349. https://doi.org/10.1016/J.MJAFI.2014.09.006.
(151) Keel, B. A.; Webster, B. W. Semen Cryopreservation Methodology and Results. *Barratt, C L R, Cooke, I D Donor insemination* **1993**.
(152) Palomar Rios, A.; Gascón, A.; Martínez, J. v.; Balasch, S.; Molina Botella, I. Sperm Preparation after Freezing Improves Motile Sperm Count, Motility, and Viability in Frozen-Thawed Sperm Compared with Sperm Preparation before Freezing-Thawing Process. *J Assist Reprod Genet* **2018**, *35* (2), 237. https://doi.org/10.1007/S10815-017-1050-Z.
(153) O'Connell, M.; McClure, N.; Lewis, S. E. M. The Effects of Cryopreservation on Sperm Morphology, Motility and Mitochondrial Function. *Human Reproduction* **2002**, *17* (3), 704–709. https://doi.org/10.1093/HUMREP/17.3.704.
(154) Khalil, W. A.; El-Harairy, M. A.; Zeidan, A. E. B.; Hassan, M. A. E.; Mohey-Elsaeed, O. Evaluation of Bull Spermatozoa during and after Cryopreservation: Structural and Ultrastructural Insights. *Int J Vet Sci Med* **2018**, *6* (Suppl), S49. https://doi.org/10.1016/J.IJVSM.2017.11.001.
(155) Ugur, M. R.; Saber Abdelrahman, A.; Evans, H. C.; Gilmore, A. A.; Hitit, M.; Arifiantini, R. I.; Purwantara, B.; Kaya, A.; Memili, E. Advances in Cryopreservation of Bull Sperm. *Front Vet Sci* **2019**, *6*, 268. https://doi.org/10.3389/FVETS.2019.00268/XML/NLM.
(156) Nagata, M. P. B.; Egashira, J.; Katafuchi, N.; Endo, K.; Ogata, K.; Yamanaka, K.; Yamanouchi, T.; Matsuda, H.; Hashiyada, Y.; Yamashita, K. Bovine Sperm Selection Procedure Prior to Cryopreservation for Improvement of Post-Thawed Semen Quality and Fertility. *J Anim Sci Biotechnol* **2019**, *10* (1), 1–14. https://doi.org/10.1186/S40104-019-0395-9/FIGURES/3.
(157) Cherouveim, P. The Impact of Cryopreserved Sperm on Intrauterine Insemination (IUI) Outcomes: Is Frozen as Good as Fresh?, 2022.
(158) Lannou, D. Le; Griveau, J. F.; Pichon, J. p. L.; Quero, J. C. Effects of Chamber Depth on the Motion Pattern of Human Spermatozoa in Semen or in Capacitating Medium. *Hum Reprod* **1992**, *7* (10), 1417–1421. https://doi.org/10.1093/OXFORDJOURNALS.HUMREP.A137585.
(159) Lenz, R. W.; Kjelland, M. E.; Vonderhaar, K.; Swannack, T. M.; Moreno, J. F. A Comparison of Bovine Seminal Quality Assessments Using Different Viewing Chambers with a Computer-Assisted Semen Analyzer. *J Anim Sci* **2011**, *89* (2), 383–388. https://doi.org/10.2527/JAS.2010-3056.